

# **STUDY OF THE EFFECT OF ELECTRIC FIELDS ON LIQUID-VAPOUR PHASE TRANSITION**

## **THESIS**

**Presented to the Aligarh Muslim University, Aligarh  
in the partial fulfilment of the requirements for the award of  
the Degree of Doctor of Philosophy  
( Ph. D. ) in Physics**

By

DEVENDRA SINGH PARMAR

Supervisor

Dr. A. K. Jalaluddin

DEPARTMENT OF PHYSICS,  
ALIGARH MUSLIM UNIVERSITY,  
ALIGARH (INDIA)



1973



T1412

T1412

## A B S T R A C T

The thesis contains a systematic and quantitative "Study of the effect of electric fields on liquid-vapour phase transition" in three organic liquids, namely, 99% n-Hexane, 95% n-Pentane and 95%iso-Pentane, in the thermodynamically stable and metastable states. The experimental setup essentially consists of a miniature Bubble Chamber and a thin film technique developed to introduce an intense electric field at the chamber-liquid interface. One of the main objects of the work is to predict the boundary of absolute thermodynamic stability of the liquids used on the basis of the results obtained in the present experiment. A brief historical review of the literature available on liquid-vapour phase transition with special reference to the study of the metastable state of liquids is given<sup>in</sup> chapter I of the thesis.

In chapter II, an attempt has been made to review in brief the various theories and concepts which are useful in understanding the occurrence and nature of the metastable states. It mainly deals with the van der Waals and van der Waals - Maxwell theories, the Kinetic theory

of nucleation, the statistical 'hole' theory of Fürth and the rigorous statistical theory of the metastable states developed by Lebowitz and Penrose. The essential difference between the heterogeneous and homogeneous nucleation and the role of external factors, like the presence of impurities, suspended particles, irregularities at the interface, incidence of ionizing radiation and application of electric fields on nucleation in liquids has also been discussed in this chapter.

The principle and construction of the miniature bubble chamber used in the present study have been described in detail in chapter III. The details of other accessories, e.g. the high voltage (0-5KV, both alternating and unidirectional) power unit, the dynamic expansion mechanism, the electromagnetic and mechanical valves used in the expansion of the chamber, the static and dynamic pressure gauges, the electronic as well as electrical circuits used in the simultaneous measurement of static and dynamic pressures in the chamber and detection of the initiation of boiling in the liquid have been given. The mechanism of introduction of intense electric stress in the liquid at the liquid-glass interface



through a thin, transparent and highly conducting layer ( $\approx 10^{-5}$  cm) of tin oxide deposited on the inner surface of the thick-walled capillary glass chamber has been described. The instantaneous pressure, the instant of application of the electric field at a given pressure and the initiation of boiling in the liquid detected optically have been recorded using a dual beam oscilloscope.

Chapter IV of the thesis deals with the experimental observations. The critical voltage  $V_c$  required for inducing nucleation at a given temperature  $T$  and pressure  $P_L$  have been plotted against the degree of superheat. The degree of superheat has been defined as  $\Delta p (= P_S - P_L)$ ,  $P_S$  being the saturated vapour pressure at  $T$ ) or as  $\Delta T (= T - T_S)$ ,  $T_S$  being the boiling point at a given pressure  $P$ ). The general pattern of the  $\Delta p$  versus  $V_c$  or  $\Delta T$  versus  $V_c$  curves is similar.

Analysis and interpretation of the experimental results are given in chapter V. The main reason for the formation of bubbles at the tin oxide boundary seems to be due to the direct effects of the field. A model has been proposed for the determination of the electric field intensity at the tin oxide edge and an expression for the

electric field intensity has been derived under the given electrode geometry, considering the electrode system used as a cylindrical capacitor and the medium between them as a composite dielectric consisting of liquid and glass dielectrics. The electric field thus calculated at the edge is found to be  $\approx 10^6$  volts/cm for the applied voltages of about 1 KV at the tin oxide layer.

The various electro-hydrodynamic effects, namely the dielectrophoretic creeping of the liquids, dielectrophoretic forces on air bubbles in the dielectric liquids and dielectrophoretic change in surface tension observed in a series of control experiments have been reported. These experiments confirm the presence of an intense field at the edge of the tin oxide layer.

The possible reasons for the initiation of nucleation due to an electric field of suitable intensity have been analysed in the present thesis on the basis of a study of the electrical forces on a conductor. A quantitative estimation of the effect of electric field has been made by calculating:

(1) the energy contributed per unit volume by the external electric field to the dielectric test liquid from the

equation  $\epsilon(T) E^2/8\pi$ , where  $\epsilon(T)$  is the dielectric constant of the liquid expressed as a function of the temperature and  $E$  is the intensity of the electric field;

(2) the force due to electric field per unit area.

It has been reported that the energy,  $W_e^*$ , contributed by the electric field over the volume of a critical bubble of radius  $r_c$  is in good agreement with the value of the thermal energy calculated on the basis of the following well known equation for the formation of a critical nucleus of the same size:

$$W_m^* = \frac{16\pi\sigma(T)^3}{3 \Delta p^2}$$

Where  $\sigma(T)$  is the surface tension of the liquid as a function of temperature.

The limiting negative pressures due to the applied electrical forces at the interface corresponding to various critical voltages and temperatures are found to be higher than those obtained theoretically from the kinetic theory. But these values happen to be somewhat lower than the theoretical values obtained from Fürth's "hole" theory.

The experimental  $P$ ,  $T$ ,  $V_c$  data have been found to fit in equations of the form

$$V_c = A (T_m - T)^a + B (T_m - T)^b$$

where  $A$  and  $B$  are constants and the powers ' $a$ ' and ' $b$ ' vary in the range  $a = 0.5 \pm 0.5$ ,  $b = 2.5 \pm 1.5$ .  $T_m$  in the above equation has the significance of the limit of stability of the liquid at a given  $P$ .

An extrapolation of  $V_c - T$  relation to fulfil the boundary condition  $V_c = 0$  at  $T = T_m$  gives the limiting value of the superheat temperature at a given pressure. The locus of these limiting values in the  $P$ - $T$  plane, terminating at the critical point, happens to be the boundary of absolute thermodynamic stability of liquid (spinodal).

The present work demonstrates for the first time the role of intense electric field at the edges of thin films in producing liquid-vapour phase transition. It also offers a practical method for the determination of the boundary of absolute thermodynamic stability of liquids, a fundamental quantity from the point of view of understanding the structure of the liquid state.

Certified that the work presented in the thesis, entitled "Study of the Effect of Electric Fields on Liquid - Vapour Phase Transition", is the original work of Mr. D.S. Parmar done under my supervision.

*A. K. Jalaaluddin*  
(A.K. JALAUDDIN)

## A C K N O W L E D G E M E N T S

It is a great pleasure to me to express my deepest feelings of gratitude to Dr. A.K. Jalaluddin, my guide, for his sincere supervision, sustained interest, and stimulating encouragement throughout the course of the study. It would not be exaggerating, if I add that without his efforts the work would not have had the present features, values, and dimensions.

To Professor Reis Ahmed, Head of the Department of Physics, A.M.U., Aligarh, I owe my sincere thanks for his keen interest, continued inspirations, and full extension of facilities in the department to carry out the project.

I wish to express my deep sense of gratitude to Dr. N.K. Ganguly, VEC Project, BARC, Bombay for many helpful, thought provoking, and constructive suggestions, and the keen interest shown by him in the work during his frequent visits to Aligarh.

I take the opportunity to extend thanks to Dr. G.S. Gupta, Department of Chemistry, A.M.U., Professor J.K.Ghosh, St. John's College, Agra, Drs. R.J. Singh and K. Ramma Reddy, Department of Physics, A.M.U., for many useful discussions, and Professor J.H. Calderwood and Dr. C.J. Smith, Department of Electronics and Electrical Engineering, University of Salford, England for their helpful criticism and suggestions.

Thanks are further extended to the faculty members and my colleagues at the Department of Physics, A.M.U., with special mention to Mr. Hashmat Husain, for their cooperation during the work.

I shall miss the bus if I don't mention my thanks to staff of the Mechanical and Electrical Workshop, Department of Physics, and the Computer Centre who were always very cooperative, and extended valuable assistance whenever asked for, and Mr. Mukhtar Husain for neat and clean typing of the thesis.

The financial assistance given by C.S.I.R. is, further, gratefully acknowledged.

Finally, I wish to mention my warm thanks to all my friends and well wishers, specially my wife Mamata, who were all encouragement to me during the course of the study.

(DEVENDRA SINGH PARMAR)

## C O N T E N T S

	Page
<b>I. I N T R O D U C T I O N</b> ... ..	1
A. General ... ..	2
B. Historical ... ..	5
C. Limitations of Different Methods ... ..	9
D. Present Method ... ..	10
<b>R E F E R E N C E S</b> ... ..	12
<b>II. S O M E T H E O R E T I C A L C O N S I D E R A T I O N S</b> ... ..	14
1. Metastable States ... ..	15
2. Limit of absolute thermodynamic boundary of stability of liquids ... ..	15
(a) Equation of State approach ... ..	17
(b) Statistical mechanical theories ... ..	19
1) Fürth's hole theory ... ..	19
ii) Van der Waals-Maxwell theory. ... ..	21
iii) Rigorous treatment of metastable states in the van der Waals-Maxwell theory. ... ..	23
(c) Kinetic theory ... ..	26
Limitations of Kinetic theory ... ..	31
3. Homogeneous nucleation and hetero- geneous nucleation. ... ..	34
4. Factors affecting the phase transition ... ..	36
5. Effects of ionizing radiation and electric field. ... ..	37
6. Aims and scope of present study ... ..	42
<b>R E F E R E N C E S</b> ... ..	44
<b>III. E X P E R I M E N T A L S E T U P A N D W O R K I N G P R I N C I P L E</b> ... ..	47
3.1. Principle of Bubble Chamber Technique ... ..	48



			Page
3.2. Experimental set-up	...	...	50
3.3 The Chamber	...	...	52
(a) The Experimental Liquid Chamber	...		52
(b) The Buffer Chamber	...	...	54
(c) The Pressure Generator	...	...	55
(d) The Volume Control System	...	...	55
(e) The Temperature Control System	...	...	56
(f) The Electromagnetic Valve	...	...	57
(g) The Optical Indicator of Boiling	...	...	58
1) The High Voltage Unit	...	...	59
ii) The Electrical Connections	...		60
3.4. Cleaning and Filling of the High Pressure Chamber	...	...	61
3.5. Mechanism of the expansion of the Chamber	...	...	65
3.6. Dynamic measurement of pressure	...	...	65
3.7. Procedure	...	...	69
3.8. Control mechanism	...	...	71
REFERENCES	...	...	77
IV. EXPERIMENTAL RESULTS	...	...	78
V. DISCUSSIONS AND CONCLUSIONS	...	...	116
5.1. The nature of interface	...	...	119
5.2. Calculation of electric field	...	...	120
5.3. Experiments	...	...	127
(a) Dielectrophoretic Creeping of the liquids.	...	...	128
(b) Control experiment on the effect of dielectrophoretic forces on air bubble in the liquid.	...	...	133

	Page
(c) Control experiment on dielectrophoretic change in surface tension.	... 135
5.4. The forces on a conductor	... 138
5.5. Consequences of the forces at the interface.	... 139
5.6. Change in surface tension due to external electric field.	... 140
5.7. Force due to external electric field	... 142
5.8. Energy contributed by the electric field.	... 145
5.9. Determination of the limit of stability of liquids.	... 152
REFERENCES	... 162
PUBLICATIONS	

\*\*\*\*\*

## INTRODUCTION

### A. GENERAL:

Phase transitions occur in almost every liquid of interest to man and even in man itself. The ubiquitous occurrence of phase transitions in liquids causes a wide spread concern over the need of a better understanding of the phenomenon among scientists and those in scientifically based professions. Study of the mechanism of phase transition has, therefore, attracted attention of physicists, engineers, mathematicians and biologists alike. But an exact knowledge of phase transition still remains an unsolved problem in statistical mechanics. Description of various phase transitions is based on phenomenological thermodynamical theories of equilibrium states. However, it is our common experience that many of the phase transitions occur under metastable condition of the mother phase. For example, study of the nucleation in liquids have revealed that a liquid is often found to remain heated at temperatures much above its thermodynamical boiling point (corresponding to the external pressure) without actually giving rise to ebullition, in which case the liquid is said to be superheated.

Nature provides many examples of metastable states;<sup>1</sup> they include supercooled vapours and liquids, supersaturated solutions, and ferromagnets in the part of the hysteresis loop where the magnetisation and the applied magnetic field are in opposite directions. They arise when some thermodynamic parameter of the system, such as the temperature or the magnetic field, is changed from a value for which the stable equilibrium state has a single thermodynamic phase, to one for which it has at least part of the system in some new thermodynamic phase. Instead of making the appropriate phase transition, however, the system may go over continuously into a one-phase state, called a metastable state, which appears, while it lasts to be stationary in time in the same manner as a stable equilibrium state.

The superheating of liquids and the phenomenon of "stretching of liquids" are intimately related; the maximum negative pressure that a given liquid can withstand being a measure of the superheat temperature to which the liquid could be raised. There is no word, such as "superheat" to express this condition, but it is

clear that the transgression of the phase boundary has occurred. A study of these properties of liquids provides means for elucidating these kinetics of phase transition of liquids. An investigation of the problem of superheating is also of interest for investigating phenomena like that of heat transfer to boiling liquids either with a view to exploring the mechanism of formation and growth of vapour bubbles, or evolving means for curing\transfer systems, like boilers, heat exchangers, atomic reactors, etc. of superheat. Cavitation or spontaneous formation of vapour in a stressed liquid, is also of interest to engineers who wish to avoid it in the operation of underwater sound generators, ship-propellers and other underwater equipments. The superheated state of liquids also have importance from the more fundamental stand point of studying the structure of the liquid state and also in determining the boundary of stability of liquids, at which the liquid can no longer remain in the liquid state.

Inspite of the importance of the phenomenon of superheating of liquids, very little work has yet been done in this field. This is mainly due to the formidable

difficulties encountered in maintaining a liquid of considerable volume at a fairly high degree of superheat for considerable period of time for experimental observation. Presence of suspended microscopic solid particles and dissolved gases in a liquid, non-uniformity of the surface of the container or incidence of an ionizing particle on the test liquid might give rise to sudden growth of vapour nuclei in a superheated liquid thus making any experiment with superheated liquid a very difficult task.

#### B. HISTORICAL

Wisner and his coworkers<sup>2</sup> in 1922, made the first attempts to reach the limiting value of superheat of liquids by two methods of investigation, (a) suddenly heating the liquid in open capillaries at atmospheric pressure, and (b) reducing the pressure on the liquid in closed tubes at fixed temperatures. With these methods they were able to superheat water upto a temperature of 270°C. The maximum superheat of other organic liquids was reproducible within a narrow range. But the results obtained with different samples differed considerably, and Wisner et al accounted for such difference in the

behaviour of different samples as due to notes which are present in all ordinary liquids. They investigated about twelve organic liquids and water and the limit of superheat reached in these liquids agreed fairly well with the values obtained indirectly from the van der Waals equation.

Harvey, Whiteley, Mc Elory and Barnes<sup>3</sup> in 1944 found that water could be superheated to 202-206°C at atmospheric pressure provided it was first subjected to a hydrostatic pressure of 1000 atm., or more for 15-30 minutes, in order to force the dissolved gas nuclei into solution. In another experiment Harvey, Mc Elory and Whiteley<sup>4</sup> in 1947 used the method of pressure pulse to produce the fracture of liquids. They stocked the test tube containing the liquid with a rubber hammer with increasing pressure until the liquid cavitated on the inner surface of the test tube.

The experimental technique of Briggs<sup>5</sup> developed in 1951 consisted of spinning a horizontal glass tube (scrupulously cleaned) about a vertical axis along the center of the tube. The tube contained the liquid and was open at both ends. The centrifugal force needed to break the liquid column was observed.



Thus Briggs was able to subject water to a negative pressure of nearly 270 atmospheres at room temperature.

The values of negative pressure obtained in these methods differed amongst themselves and also from those deduced from the van der Waals equation. This is mostly due to the variation of the nature of the interface and also the experimental technique employed in the different methods. Their deviation from the theoretical prediction of the van der Waals equation should partially be due to the approximations inherent in the equation itself. In the case of water the divergence between the different values is very wide and this is ascribed also to the presence of large quantity of dissolved gases and formation of aggregate.<sup>6</sup>

Trefethen<sup>7</sup> in 1957 first pointed out that high and reproducible value of superheat of liquids could be expected if the experimental liquid were heated by means of another liquid. Wakeshima and Takata<sup>18</sup> performed an experiment in which droplets of the test liquid were introduced into a vertical column of denser immiscible liquid, possessing an upwardly increasing steady temperature gradient, in order to find at which temperature level the liquid drop exploded during its ascent.

Jalaluddin and Sinha<sup>8</sup> in 1961 devised a method for measuring the maximum superheat temperatures of liquids which offered a practical method for studying the effect of varying the nature of the interface on the superheat of liquids. The results obtained from these experiments were found fairly in agreement with the values obtained by Kenrick, Gilbert and Wismer<sup>9</sup> as well as with those deduced from van der Waals equation. Skripov and Ermakov<sup>10</sup> obtained better results by improving the experiments of Wakoshima and Takata.

With the development of bubble chambers it has been found possible to superheat liquids within a fraction of a second and as a result of which a higher degree of superheat of liquids could be attained. Jalaluddin and Zamkov<sup>11</sup> investigated the nucleation kinetics in superheated liquids by light scattering method using a bubble chamber and derived an empirical equation of state<sup>12</sup> which could explain the boundary of stability of liquids through their compressibility.

Apfel<sup>13</sup> very recently designed an experiment using an standing acoustic wave field in a column of a liquid in which an immiscible droplet of another liquid was trapped. In this experiment, a filtered ether

droplet suspended in filtered glycerine was superheated and acoustically stressed until the combination produced an explosive liquid-to-vapour phase transition. The results are in very good agreement with the predictions of homogeneous nucleation theory.

#### C. LIMITATIONS OF DIFFERENT METHODS.

Although all the above experiments present fairly an accurate estimate of the maximum attainable degree of superheat of various liquids, the results obtained from them do not necessarily correspond to the actual theoretical limiting value of the superheat of liquids. Since the initiation of nucleation at any particular microscopic volume of the liquid rapidly spreads over the entire volume of the test liquid at higher degrees of superheat, even a very low rate of nucleation such as  $10^2$  bubbles per unit volume per unit time may correspond to the phenomenon of homogeneous nucleation in a liquid under a given condition of the experiment. But the physical significance of the boundary of stability of a liquid lies in the fact that if such a condition is ever realised in any experiment, nucleation should start simultaneously at all microscopic volume elements of the sample whose size is comparable to the

embryonic bubble of vapour. This would mean a very high order of rate of nucleation in the liquid. According to Skripov<sup>19</sup> this would mean a factor of about  $10^{20}$  difference in the order of magnitude between the observable rate of nucleation and the expected rate of nucleation at the boundary of stability of the liquid.

#### D. PRESENT METHOD.

The problem of experimentally determining the limit of stability of liquids could be attacked in a better fashion by using an external perturbation of known magnitude for producing nucleation in a superheated liquid. Once the critical magnitude of the external perturbation inducing nucleation and its change with the fundamental thermodynamic parameters e.g., pressure and temperature of the liquid are known, it becomes much easier to determine the limit of stability of liquids by extrapolating the results upto those values of pressure and temperature of the liquid which correspond to the zero value of the external perturbation. In the present work electric field has been used as the external perturbation.

This idea is based on the earlier experimental observations of electric field induced nucleation in superheated liquids.<sup>14</sup> The method devised for the present investigation essentially consists of a miniature bubble chamber.<sup>15</sup> Nucleation in the chamber liquid is induced with the help of an external electric field applied through a thin and transparent metallic film of tin oxide deposited on the inner surface of the glass chamber.<sup>16</sup> The electrostatic field is applied in the liquid in such a way that it does not produce any heating in the liquid. With the help of this device it has been found possible to formulate a relationship between the attainable degree of superheat of the liquid and the voltage applied. Apart from some practical importance of the device itself, the relation mentioned above enables one to determine the limit of stability of liquids as a result of extrapolation.<sup>17</sup>

# REFERENCES

1. Frenkel, J., "Kinetic Theory of Liquids," (Dover Publications, N.Y., 1955) Ch.7.
2. Wisner, K.L., J.Chem.Phys., 26, 301 (1922).
3. Harvey E.H., McElroy D.M. and Whiteley H., J. Appl. Phys., 18, 162 (1947).
4. Harvey E.H., Whiteley H., McElroy D.M., Pease D.C. and Barnes D.K., J.Coll. Compds. Phys. 24, 25 (1944).
- 5.(a) Briggs L.J., J. Chem. Phys., 19, 970 (1951).  
(b) Briggs L.J., J. Appl. Phys., 24, 488 (1953).
6. Dixon, Sci. Proc. R., Dublin Soc., 12 (1909).
7. Trefethan, L., J.Appl.Phys., 28, 923 (1957).
- 8.(a) Sinha, D.B. and Jalaluddin, A.K., Ind. J. Phys., 35, 6 (1961).  
(b) Jalaluddin A.K., "On the superheat of liquids," Ph.D. thesis, Calcutta Univ., 1962.
9. Kenrick F.D., Gilbert C.S. and Wisner K.L., J. Chem. Phys., 28, 1297 (1924).
10. Skripov V.P. and Ermakov G.V., Zur. Fisi.Khim, 38, (1964) - In Russian.
11. Jalaluddin A.K. and Zamkov V.A., Ukra. Fisi. Zur., 12, 1 (1967) - In Russian.
12. Jalaluddin A.K., " A study of the superheated state of liquids by light scattering methods", Ph.D. Dissertation, Moscow State University, 1967 - In Russian.

13. (a) Apfel R.E., J. Acous. Soc. Amer., 49, 1, pt. 2, 145 (1971).  
 (b) Apfel R.E., J. Acous. Soc. Amer., 48, 1179 (1970).  
 (c) Apfel R.E., J. Chem. Phys., 54, 62 (1971).  
 (d) Apfel R.E., Nature Physical Sciences, 233, 119 (1971).
14. Jalaluddin A.K. and Sinha D.B., Nuovo Cimento Suppl., Ser X, 26, 234 (1962).
15. Delone N.B., Puzirkovie Kamori, Moscow (1963).
16. Parmar D.S. and Jalaluddin A.K., Phys. Lett., 42A, 497 (1973).
17. Parmar D.S. and Jalaluddin A.K., J. Phys. D., Appl. Phys., 6, (1973).
18. Wakeshima H. and Takata K., J. Phys. Soc. Jap., 13, 1398 (1958).
19. Skripov V.P., Ukra. Fisi. Zur., 2, 4, 393 (1964).

\*\*\*\*\*

SOME THEORETICAL CONSIDERATIONS



### 1. Metastable states:

The metastable states appear to be completely determined by the values of the thermodynamic parameters, in just the same way as the equilibrium stable states. The distinguishing feature of the metastable state is that, eventually, either through some external disturbances or a spontaneous fluctuation which nucleates the missing phase in some small part of the system, the system undergoes an irreversible process which leads it inexorably to the corresponding stable equilibrium state. Thermodynamically, the irreversibility of this transition corresponds to a decrease in free energy or an increase in entropy.

The metastable thermodynamic states are characterised by the following properties:

- (a) Only one thermodynamic phase is present,
- (b) a system that starts in this state is likely to take a long time to get out,
- (c) Once the system has gotten out, it is unlikely to return.

### 2. Limit of absolute thermodynamic boundary of stability of liquids.

The thermodynamic boundary of stability of liquid-vapour system is defined by the equation:

$$\left(\frac{\partial P}{\partial V}\right)_T = 0 \quad , \quad \left(\frac{\partial T}{\partial S}\right)_P = 0 \quad \dots\dots (2.1)$$

These conditions correspond to the limit of stability of the homogeneous state of the substance with respect to continuous phase changes. Eq 2.1 is a fundamental curve of the liquid - vapour system, called the spinodal. When the chemical potentials of the liquid and vapour phases are equal, the liquid and vapour are said to be in equilibrium and the curve which corresponds to this is defined as binodal. The homogeneous mass existing at a thermodynamic state between the binodal and spinodal is metastable since this is not mechanically and thermodynamically stable. According to Gibbs<sup>1</sup>, the thermodynamic phase stability boundary is obtained as a consequence of the stability determinant. The stability determinant is made up of second derivatives of the internal energy with respect to the entropy, and it is equal to zero at the thermodynamic boundary of stability of phases.

The metastable superheated state of liquids is simply the analytic continuation of the pressure as a function of density. In any equation for liquids there is no indication of the existence of the phase transition point i.e. the limit of superheat of liquids. It is still not clearly known whether the intermolecular potential in

the liquid is an infinite range potential needed to obtain a van der Waals type equation of state, or whether this is essentially a short range potential. Lebowitz<sup>2</sup> has shown that a realistic model for the intermolecular potential in liquids, of the Kac<sup>3</sup> form, do, in fact, predict a metastable superheated region. The thermodynamic boundary of stability of liquids can be defined as a singularity in the pressure - density curve of the liquid at a specified temperature. Fisher<sup>4</sup> argued for the existence of the essential singularity at a density value corresponding to the liquid-vapour transition. Langer<sup>5</sup> using a very ingenious analysis of a model system partition function also argued for the existence of essential singularity at the liquid-vapour transition point. In view of lack of our knowledge regarding real physical systems any information pertaining to their boundary of stability has much theoretical importance.

#### Theoretical approaches towards the limit of superheat:

##### (a) Equation of state approach:

The van der Waals equation of state,

$$\left(P + \frac{a}{v^2}\right)(v-b) = RT, \quad \dots\dots\dots (2.2)$$

predicts a discontinuous change of state if there is any region for which  $(\partial P / \partial V)_T$  is positive, such as the portion AB in Fig.2.1. Obviously this portion of the curve is not realizable in practice. The pressure at which the change of state from liquid to vapour in equilibrium with it takes place is determined by the well known rule of equal areas (dotted lines in Fig.2.1) which is the consequence of the fact that at equilibrium, the thermodynamic potentials of the liquid and the vapour must be equal and of the thermodynamic relation,  $(\partial G / \partial P)_T = V$  (where  $G$  = Gibbs free energy). Below this equilibrium vapour pressure, the liquid should be capable of existing in the metastable state, provided that  $(\partial P / \partial V)_T$  is still negative. The limit of metastable region will be reached when  $(\partial P / \partial V)_T$  vanishes, i.e. at points, such as A, C and D in Fig. 2.1.

Temperley<sup>6</sup> deduced from eq.2.2 the maximum temperature to which the liquid can be superheated at zero pressure (point C in Fig. 2.1). According to him the maximum superheat temperature is given by

$$T_m = \frac{27}{32} T_c \quad \dots\dots\dots (2.3)$$

where  $T_c$  is the critical temperature. Below this temperature the region of metastability should extend to

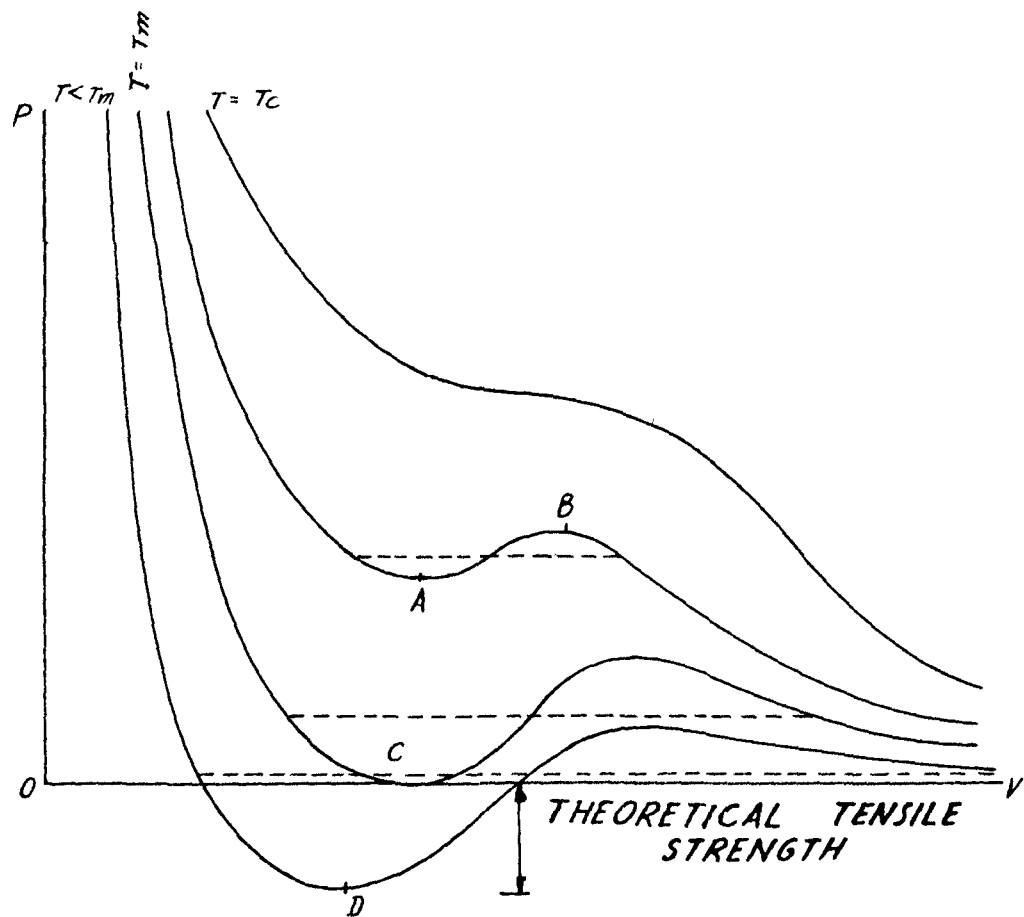


FIG. 2-1 ISOTHERMALS OF A VANDER WAALS GAS. DOTTED LINES INDICATE EQUILLIBRIUM PRESSURE.

negative pressures and the liquid should accordingly be capable of withstanding tensions (point D in Fig.2.1).

(b) Statistical mechanical theories:

(1) F $\ddot{u}$ rth's hole theory: F $\ddot{u}$ rth<sup>7</sup> employed the 'hole' theory of liquids for the prediction of the limit of superheat of liquids. The idea of 'holes' was suggested by the fact that even in perfect crystals a certain number of sites in the lattice are unoccupied, and that the atoms can change their positions by jumping from one place to a neighbouring unoccupied place or hole. It seemed to F $\ddot{u}$ rth, therefore, plausible to assume that the most significant feature of a liquid, namely, its 'fluidity', is due to a very large number of such holes in its structure. The holes are considered as the counterparts of the clusters in a dense gas or vapour. They are formed by the action of the irregular thermal movement (or by the statistical fluctuation) and are destroyed again by the same process; they interact with each other, and they perform a kind of Brownian motion. The sizes of the holes obey a certain statistical distribution law, the frequency of larger holes increasing more and more as the temperature is increased or the

pressure diminishes. Evaporation consists in the complete destruction of the structure of the system by the holes so that it breaks into pieces which are not connected with each other. In order to simplify the statistical treatment of the fluctuation phenomenon which is responsible for the creation of the holes, it is assumed in this theory that the matter outside the holes is a continuum with the normal surface tension of the liquid, and that the holes are filled with saturated vapour corresponding to the given temperature.

Following the method of classical statistical mechanics, F  rth expressed the average volume,  $\bar{V}$ , of a hole and its average surface area,  $\bar{F}$ , by the equation

$$3(P_L - P_S) \bar{V} + 2\sigma \bar{F} - 7 kT = 0 \quad \dots\dots (2.4)$$

where  $P_S$  and  $P_L$  are respectively the saturated vapour pressure and the external pressure on the liquid at temperature  $T$ , and  $\sigma$  is the surface tension at the same temperature. Eliminating  $\sigma$  and  $\bar{F}$  in terms of  $\bar{V}$ , the above equation reduces to the form

$$\frac{3(P_L - P_S)}{7 kT} = \frac{1}{\bar{V}} \left[ 1 - \left( \frac{\bar{V}}{\bar{V}_S} \right)^{\frac{8}{3}} \right] \quad \dots\dots (2.5)$$

against

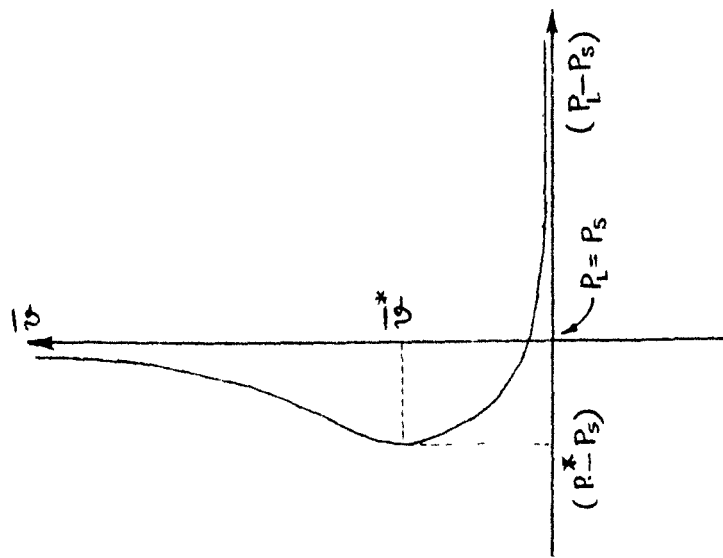
where  $v_g$  is a constant.  $\bar{v}$  is plotted  $\lambda^3(P_L - P_g)/7KT$  in Fig.2.2. The average volume of a hole over the region on the left hand side of  $\bar{v}$  axis is infinite, corresponding to the phenomenon of boiling. Values of  $\bar{v}$  between  $v_0$  and  $v^*$  represent a metastable superheated state, since  $(\partial \bar{v} / \partial P_L)_T$  is negative and finite, the point  $\bar{v} = \bar{v}^*$ ,  $(\partial \bar{v} / \partial P_L)_T$  becomes infinite, and the liquid is completely unstable. Thus we get after some substitution for the pressure  $p^*$  corresponding to  $\bar{v}^*$ ,

$$(P_g - P^*) = 1.3 \sigma^{-3/2} (KT)^{1/2} \dots\dots\dots (2.6)$$

This enables us to calculate the limiting lower value of the hydrostatic pressure  $P^*$ , corresponding to a given temperature upto which the liquid could be expanded before spontaneously breaking down to the vapour phase. The  $P^* - T$  curve thus actually represents the spinodal in the  $P-T$  plane.

(11) van der Waals - Maxwell theory: In statistical mechanics, there are several approximate theories giving metastable equilibrium states instead of, or in addition to, the stable ones. One of these is the van der Waals-Maxwell theory of the liquid-vapour transition. Seeing





CONDITION OF INSTABILITY OF VAPOUR BUBBLE

FIG. 2.2

the interaction between the molecules of a classical fluid as a competition between the two distinct parts of the molecular force, a short range repulsive part and a long range attractive part, van der Waals<sup>8</sup> arrived at the equation of state

$$p = kT \rho / (1 - \rho b) - \frac{1}{2} \alpha \rho^2 \equiv p_{\text{vdw}}(\rho, T) \dots\dots (2.7)$$

where  $p$  is the pressure,  $k$ , Boltzman constant,  $T$  the temperature,  $\rho$  the number density and  $\alpha$  and  $b$  are positive constants characterising the long and short range part of the potential, respectively. When  $T$  exceeds the critical temperature  $T_c \equiv -4\alpha/27bk$ , the van der Waals equation gives a good qualitative representation of the isotherms of a real fluid; for  $T < T_c$ , however, each isotherm includes a section where the compressibility is negative, in violation of the thermodynamic stability principle. The reason for this failure is that the agreement leading to eq.2.7 assumes a single phase system; it does not allow for the possibility of co-existing liquid and vapour phases.

Maxwell<sup>9</sup> showed that the co-existence region could be included in the theory by using van der Waals

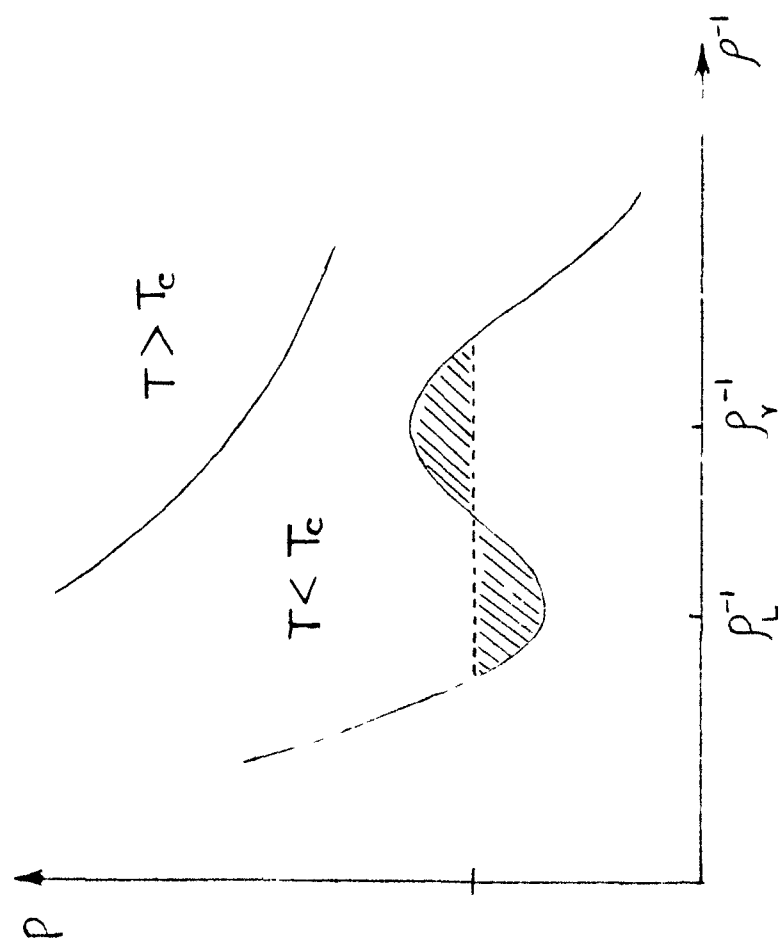
equation of state for both liquid and vapour phases and using the thermodynamic equilibrium condition that the two phases must have equal pressures and chemical potentials. This leads to the following modification of eq 2.7 for  $T < T_c$ :

$$p = \begin{cases} p_{vdw}(p, T) & \text{if } p < p_v(T) \text{ or } p > p_L(T) \\ p_{sat}(T) & \text{if } p_v(T) < p < p_L(T) \end{cases} \dots \quad (2.8)$$

where  $p_v(T)$ ,  $p_L(T)$ ,  $p_{sat}(T)$  may be determined by the graphical construction shown in Fig. 2.3, which shows typical isotherms for the van der Waals equation of state (solid lines) and Maxwell modification (dotted lines). The shaded areas are equal.

(iii) Rigorous treatment of metastable states in the van der Waals-Maxwell theory:

O. Penrose and J.L. Lebowitz<sup>10</sup> investigated a general method for describing metastable states in statistical mechanics and applied it rigorously to the generalised van der Waals system. They considered a classical system, in a  $\mathcal{V}$ -dimensional cube  $\mathcal{Q}$ , with



TYPICAL ISOTHERMS FOR THE VAN DER WAALS EQUATION OF STATE (SOLID LINES) AND MAXWELL'S MODIFICATION (DOTTED LINE). THE SHADED AREAS ARE EQUAL.

FIG. 2.3

pair potential of the form

$$V(\gamma) = q(\gamma) + \mathcal{V}^\gamma \phi(\mathcal{V}\gamma)$$

where  $\gamma$  represents the separation of the pair of the particles,  $q(\gamma)$  is a short range potential and  $\mathcal{V}^\gamma \phi(\mathcal{V}\gamma)$

is a potential (Kac<sup>3</sup> potential) whose range is proportional to the reciprocal of the parameter  $\mathcal{V}$ .

Deviding  $\Omega$  into a net work of cells  $w_1, w_2, \dots$ , they regarded the system as in a metastable state if the mean density of the particles in each cell lies in a suitable neighbourhood of the over all density  $\rho$ , with  $\rho$  and temperature satisfying,

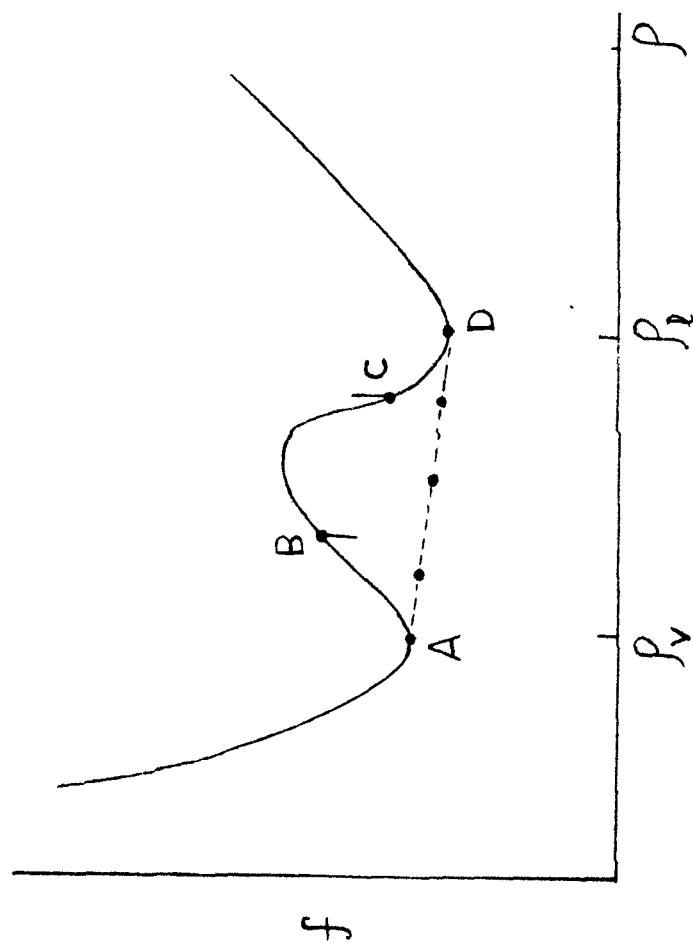
$$f_0(\rho) + \frac{1}{2} \alpha \rho^2 > f(\rho, 0) +$$

and 
$$f_0''(\rho) + 2\alpha > 0$$

where  $f(\rho, +0)$  is the Helmholtz free energy density for the case  $\mathcal{V} \rightarrow 0$ ;  $\alpha = \int \phi(\gamma) d\gamma^2$ ; and  $f_0(\rho)$  is the Helmholtz free energy density for the case  $\phi = 0$ . The relationship between,  $f$ , the Helmholtz free energy per unit volume, and  $\rho$ , the density, has the general form

shown in Fig. 2.4. The points A and D on this line correspond to two phase states, one phase (the vapour) having density  $\rho_v$ , the other (the liquid) having density  $\rho_L$ . Maxwell<sup>9</sup> saw that for densities between  $\rho_v$  and  $\rho_L$  the stable equilibrium states would be the two phase states, but thought that, by careful experimentation, it should also be possible to realize experimentally the parts of the curve labeled AB and CD; these describe the one phase metastable states.

Although van der Waals equation gives the metastable states easily, it is more difficult to see how they could arise in an exact theory; for it follows from the general principles of statistical mechanics<sup>11</sup> that in the thermodynamic limit, the exact free energy density, calculated from the partition function, is a convex function of  $\rho$  and therefore can not give arcs such as AB and CD, which do not lie on a convex curve. To obtain the metastable states, Penrose and Lebowitz<sup>10</sup> used a restricted grand canonical ensemble, that is, one constructed by selecting from a grand canonical ensemble those systems whose configuration is in region R. The chemical potential of this grand canonical ensemble is



HELMHOLTZ FREE ENERGY DENSITY IN THE VAN DER WAALS -  
MAXWELL THEORY

FIG. 2.4

related to  $\rho$  by the analog of the formula

$$\begin{aligned} \mu &= (\partial f / \partial \rho)_T \quad \text{i.e. by} \\ \mu &= d[f_0(\rho) + \frac{1}{2} \alpha \rho^2] / d\rho \\ &= f'_0(\rho) + \alpha \rho \end{aligned} \quad \text{..... (2.9)}$$

For periodic boundary conditions, the conditional probability for a system in the grand canonical ensemble to violate the constraints at time  $t > 0$  is at most  $\lambda t$ , where  $\lambda$  is a quantity going to zero in the limit

$$|\Delta\Omega| \gg \bar{x}^\gamma \gg |\omega| \gg r_0 \log |\Delta\Omega| \quad \text{..... (2.10)}$$

Here  $r_0$  is a length characterizing the potential  $q$ , and  $x \gg y$  means  $x/y \rightarrow +\infty$ . Penrose and Lebowitz have argued that a system started in the metastable state will behave (over times  $\ll \bar{\lambda}^{-1}$ ) like a uniform thermodynamic phase with Helmholtz free energy density

$$f_0(\rho) + \frac{1}{2} \alpha \rho^2 \quad \text{..... (2.11)}$$

but that having once left this metastable state, the system is unlikely to return.

(c) Kinetic theory: Apart from considering the problem of defining the limit of thermodynamic stability of liquids from the point of view of equilibrium states



(as it was done in the above theories) it is equally possible to attack the problem by studying the kinetics of phase transition. In fact, the kinetic theory of nucleation has led to a better understanding of the metastable states themselves.

The various stages of kinetics of liquid-vapour phase change may be conveniently classified as :

- (i) The development of the metastable states, which may be due to a change in temperature, pressure, tension or other chemical or physical conditions.
- (ii) The generation of the first minute specks or nuclei of the new phase. Such nuclei may form homogeneously in the interior of the parent phase or may form heterogeneously around ions, impurity molecules or on dust particles, on surfaces or at structural singularities such as dislocations and other imperfections.
- (iii) The growth of nuclei to a critical size.
- (iv) Spontaneous growth of critical nuclei into macroscopic bubbles.

The kinetic theory of nucleation was mainly developed by Volmer,<sup>13</sup> Bernath,<sup>14</sup> Fisher,<sup>15</sup> Frankel,<sup>16</sup> Döring and others.<sup>17</sup> Apfel<sup>18</sup> have refined Döring's work. A detailed summary

and the general review of the above theories have been given by West-water,<sup>19</sup> Wakeshima,<sup>20</sup> Henderson<sup>21</sup> and recently by Hesse and Widom.<sup>22</sup>

Smoluchowski<sup>23</sup> first realised in his work that local fluctuations of density and temperature always occur in apparently homogeneous liquids. The fluctuation of density and temperature always grow larger with the increase in metastability of liquids and in that case one can consider such a liquid as an emulsion within which bubbles of all sizes are dispersed according to a statistical distribution.

Volmer, who first approached the kinetics of phase transition, considered only those bubbles which contain a certain number of molecules and are capable of growing without further addition of energy and, therefore, have the greatest chance for contributing to the process of boiling. We call these bubbles as nuclei. According to statistical mechanics, this number can be represented by

$$n_x = N \exp \left( - \frac{W_x}{RT} \right) \dots\dots (2.12)$$

where  $n_x$  is the number of clusters containing  $x$  monomers,  $N$  is the total number of molecules (a cluster can also be

treated as a single molecule),  $W_x$  is the work necessary to create a cluster of size  $x$ . The product  $kT$  is the translational energy of an average liquid molecule.

Assuming the cluster to be spherical and the boundary between liquid and vapour as distinct, the work  $W$  is given by

$$W = -VdP + \sigma A \quad \dots\dots (2.13)$$

The first term on the righthand side of this equation represents the work for the creation of a volume  $V$  and the second for the formation of a surface of area  $A$ . The pressure - volume work is

$$VdP = V(P_S - P_L) \quad \dots\dots (2.14)$$

where  $P_S$  and  $P_L$  are respectively the pressure inside the bubble and the external pressure on the bubble. If  $R$  is the radius of the bubble, then  $V = 4\pi R^3/3$ , and  $A = 4\pi R^2$ , then from eq. 2.13,

$$W = \frac{16\pi\sigma^3}{3(P_S - P_L)^2} \quad \dots\dots (2.15)$$

where we have used the Laplace's equation

$$\Delta p = P_S - P_L = \frac{2\sigma}{R} \quad \dots\dots (2.16)$$

$\sigma$  being the surface tension.

This equation of work function for the formation of a vapour nucleus of radius  $R$  does not give any information about the critical radius of the nucleus. However such information might be obtained from the consideration of a vapour-liquid system from the thermodynamic point of view. The relation may be expressed as

$$\Delta F = 4\pi\sigma(R^2 - \frac{2R^3}{3R_0}) \quad \dots\dots (2.17)$$

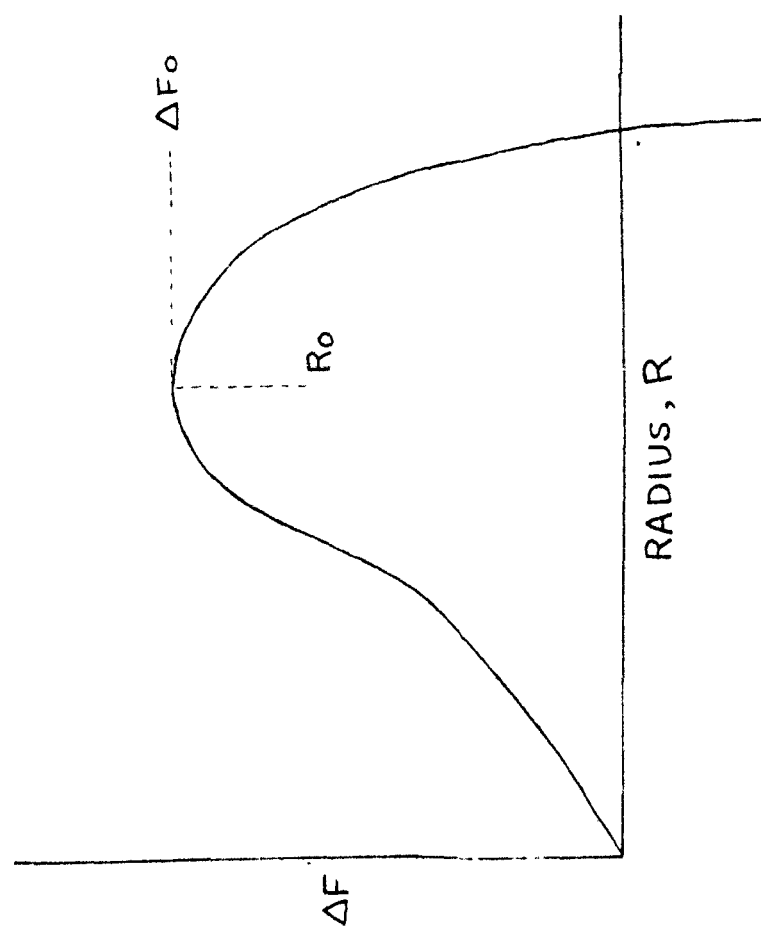
where  $\Delta F = F_2 - F_1$

$F_1$  = total free energy of the superheated liquid,

$F_2$  = total free energy of the liquid + one vapour nucleus,

$R_0$  = radius of a nucleus of the particular size corresponding to a definite value of  $\Delta F$  for stability.

The relationship between the thermodynamic work function and the radius of a vapour nucleus is shown in Fig.2.5. The curve has a maximum which means that for a superheated liquid at a stated temperature and pressure, one and only one nuclear size is capable of further growth and development.



CHANGE IN FREE ENERGY FOR CREATION OF  
VAPOUR CLUSTERS IN A LIQUID

FIG. 2.5

In addition to the activation energy deduced above, it is assured that the energy required for the transition from one phase to other should be considered. Berneath<sup>15</sup> put this additional amount of energy to be equal to the molecular heat of vapourisation of the liquid.

Parkas<sup>24</sup>, Kaishev and Stranski<sup>25</sup> and Becker and Döring<sup>26,27</sup> improved Volmer's theory by combining it with the theory of rate process. The equation for the rate formation of vapour nuclei in superheated liquid becomes:

$$J = Z_1 \sqrt{\frac{6\sigma}{\pi m (3-b)}} \exp \left\{ -\frac{\lambda}{RT} - \frac{16\pi\sigma^3}{3RT(P_S - P_L)^2} \right\} \dots (2.18)$$

where  $Z_1$  = number of molecules of superheated liquid,

$$b = \frac{P_S - P_L}{P_S} = \frac{2\sigma}{P_S R_0}$$

$m$  = molecular mass and  $\lambda$  = latent heat of vapourisation per molecule.

#### Limitations of kinetic theory:

The practical difficulty in calculating the maximum superheat temperature to which a liquid could be raised from eq. 2.18, lies in selecting a suitable value for  $J$ , the rate of formation of nuclei. This is somewhat

arbitrarily settled by defining nucleation to be the process of appearance of a bubble in a reasonable time. The reasonable time usually taken is one second. Since the limiting superheat temperature is mainly determined by the value of surface tension and molecular heat of vapourisation of the liquid, the selection of reasonable time as 1 sec., though not critical, is not considered to be a source of large error. Fisher<sup>28</sup> calculated the fracture pressure of water at 300°K and found that the ratio of the maximum to the minimum fracture pressure (tensile strength) is only 1.58, although the corresponding time ratio is  $10^{33}$ .

The physical meaning of the rate of formation of bubbles in a superheated liquid (or a liquid under tension or stress),  $J$ , is explained according to Volmer as follows: As soon as a single metastable nucleus gains in size, the liquid will explode in a moment, and the state of tension ( $P < 0$ ) or the metastable condition of the superheated liquid will be brought to an end. Therefore, for thermodynamical considerations to apply, such nuclei must be removed from the liquid as soon as they appear. Thus there arises a steady state of current of molecules in the system. This is the flux  $J$  itself.

Limitations of the equation deduced from the kinetic view point lies mainly in the inexactness of the assumptions made in its derivation. These as pointed out by Westwater<sup>19</sup> are; (i) that the change of one phase into another is an equilibrium process, (ii) That a nucleus is bodily removed from the liquid, (iii) that the boundary between a liquid phase and a vapour phase is a plane of zero thickness; (iv) that the value of the various physical constants, such as surface tension determined for the bulk liquids, are the same for microscopic bodies. Despite these limitations of theory, most of the results obtained by Wismer et al,<sup>41</sup> Wakeshima and Takata,<sup>42</sup> Jalaluddin and Sinha,<sup>32</sup> Skripov et al<sup>33</sup> and Apfel,<sup>34</sup> are found to agree generally among themselves and also fairly with those deduced from the Döring's equation.

Wakeshima<sup>23</sup> has criticized the theories of fracture of liquids-those of Temperley, Döring and Fisher- in view of the observations mainly of Briggs. He took into consideration the effect of bubble size on surface tension according to Tolmann<sup>35</sup> theory. As the result was not satisfactory, he proposed a new hypothesis for the curvature



effect. This shows a reduction in the theoretical values and a better agreement of nucleation theory with Briggs data.

### 3. Homogeneous nucleation and heterogeneous nucleation:

Though the kinetic model of Volmer and others for nucleation has proved to be qualitatively correct and extremely useful, doubt still exists as to its quantitative validity. Part of this uncertainty lies in the macroscopic nature of the theoretical formulation, and part lies in a lack of direct experimental measurements of the nucleation rate. Most phase transformations proceed discontinuously through the birth and the subsequent growth of small embryos or nuclei of new phase. In the absence of catalytic agents, these nuclei appear at random throughout the original phase, and the nucleation process is termed homogeneous.

The most important reason for the incongruence between the theoretical<sup>and</sup>/experimental results is the introduction of heating surface. This results in a heterogeneity in the system which is not taken into account in the Volmers theory of nucleation.

When a liquid is heated in contact with a solid, the work required for the formation of a bubble at the solid-liquid interface is given by Fisher<sup>28</sup> to be

$$W = 2\pi R^2(1-m)\sigma + \pi R^2(1-m^2)(\sigma_{SV} - \sigma_{SL}) \\ - \frac{\pi R^3}{3}(2 - 3m - m^3)P_S \quad \dots\dots\dots (2.19)$$

$$\text{where } m = \frac{d}{R} = \frac{(\sigma_{SV} - \sigma_{SL})}{\sigma}$$

and  $2\pi R^2(1-m)$  is the area of the liquid-vapour interface,  $\pi R^2(1-m^2)$  is the area of the solid-liquid interface,  $(\pi R^3/3)(2-3m+m^3)$  is the volume of the bubble. The maximum value of  $W$ , corresponding to a bubble of critical size, is

$$W = \frac{16\pi\sigma^3\phi}{3(P_S - P_L)^2} \quad \dots\dots\dots (2.20)$$

$$\text{where } \phi = (2+m)(1-m^2)/4 \quad \dots\dots\dots (2.21)$$

Excepting the inclusion of the term  $\phi$ , the equation 2.20 is identical with eq.2.15 obtained for a homogeneous system. Thus equation becomes same for  $\phi = 1$ , i.e. the contact angle between the solid and liquid is zero. With

the increase of the contact angle,  $W$  becomes smaller and nucleation becomes easier. If the angle of contact between a liquid and solid is zero, we have the possibility of a wide range of maximum superheat values. However, although most organic liquids and water form zero contact angle with glass, silica and metallic surfaces, when they are scrupulously clean, ordinarily these surfaces behave differently.

#### 4. Factors affecting the phase transition:

Most solid substances have numerous small cracks on their surfaces. If such a crack or cavity has a sharp apex, the trapped gas in it can serve as a nucleation site. The gas can gain vapour easily and can grow to a bubble of critical size. If the surfaces are marked rough, the contact angle observed will not be the true angle representing the work of adhesion of liquid to solid. The effect of roughness is to increase the apparent angle if the true is greater than  $90^\circ$

If the gases are adsorbed on the surface of the solid, the free energy or the surface tension of the solid surface is diminished, sometimes, to a small fraction of its original value. Often, heating or other treatments can not

tear away the adsorbed layer. Langmuir<sup>36</sup> found that if there are layers of grease, even one molecule thick, it can increase the contact angle considerably.

If the contaminations are not uniformly distributed over the whole surface, but are concentrated over certain isolated portions of the surface, the nucleation of the liquid on heating starts from these points. Dust particles or other solid particles are usually contained in the liquid. The surface of these impurities can play the same role as the surface of the vessel. In comparison of other substances, glass seems to be the most suited for the experiments to determine the superheat of liquids. With the experimental methods reported by Wisner et al<sup>41</sup>, Wakeshima and Takata,<sup>42</sup> Skripov et al,<sup>33</sup> Jalaluddin et al<sup>32</sup> and Apfel,<sup>34</sup> it was found possible to produce very high degree of superheat, nearly the theoretical value predicted by the kinetic theory, in the case of organic liquids viz. diethyl ether, methyl alcohol etc in contact with pyrex glass.

##### 5. Effects of ionizing radiation and electric field:

In 1952, Glaser<sup>43</sup> first confirmed the fact that ionizing particles produce nucleation in superheated liquids.

This phenomenon was very ingeniously used for the development of bubble chambers, which are considered to be the most efficient devices presently available for the registration of tracks of elementary particles. Glaser tried to develop the theory of formation of bubbles by ionizing particles on the same lines as done by Wilson<sup>14</sup> in the case of formation of tracks in cloud chamber according to which the coulomb repulsion produced by cluster of similar charges at the surface of embryonic droplets facilitate their spontaneous growth to microscopic size. But Glaser's suggestion was later on discarded by Seitz<sup>15</sup> and others on the grounds that in the case of liquids the recombination time of oppositely charged particles is much smaller than the time required for the growth of nuclei to their critical sizes. The formation of tracks in bubble chambers is now explained to be due to the ultimate conversion of the energy of the ionizing particles into heat energy spread over the microscopic volumes comparable to the size of the nuclei of bubbles. A bubble chamber becomes sensitive to ionizing radiations only when the degree of superheat and the energy contribution of the particle are sufficiently high for

spontaneous growth of bubble nuclei. However, the success of the energy contribution theory in explaining the formation of tracks in bubble chambers should not minimize the importance of the coulomb repulsion theory as a possible factor for phase transition in liquids, including the case of liquid-vapour transition. The effectiveness of the coulombic repulsion of charged particles in producing nucleation in liquids should become evident only when free charges of the same kind are capable of existing in the liquid for sufficient time. The first evidence of induced nucleation in liquids due to external electric fields was reported in 1962 by Jalaluddin and Sinha.<sup>46</sup> As an external electric field always produces space charges at the interface of a conductor and insulator or at the boundary of two different dielectrics, it should be possible to correlate the intensity of electric field at the interface of a liquid with the maximum degree of superheat attainable under its presence.

While studying the electric strength of liquids, many workers<sup>51</sup> have observed that the breakdown in liquid dielectrics is sometimes preceded by the formation of bubbles at the surface of the electrodes. According to them the

bubble can be formed by one, or more, of the following mechanisms:

- (a) gas pockets on the electrode surface,
- (b) electrostatic repulsion between space charges- positive ions in the cathode region and negative in the body of the liquid . This force may be sufficient to overcome the surface tension of the liquid, when bubbles could form,
- (c) gaseous products of ionization of the molecules by energetic electrons,
- (d) vapourisation of liquid by corona-type discharge from points and asperities on the electrodes.

It has been observed in the above experiments that small conduction currents flow between the anode and the cathode even when the liquid used is known to be a good dielectric. This is primarily due to the presence of ionic impurities in the liquid and ionization of liquid by cosmic ray particles. The presence of such conduction current always produces a heating effect in the liquid and disturbs its thermodynamic equilibrium. It is therefore necessary to avoid the conduction current when one attempts to study the effect of electric field on phase transition

in liquid under thermodynamic equilibrium or quasi-equilibrium. This could be done by altogether removing the cathode from the liquid medium itself and considering the anode to be immersed in an infinite liquid dielectric contained by a good insulator like glass, and putting the earthed terminal just out side the glass container.

As has been pointed out earlier, a liquid hardly withstands superheat when it is in contact with metallic surfaces. Hence the application of an electric field to a superheated liquid poses serious problem. In the present work this problem has been solved by depositing a very thin layer of tin oxide on the surface of glass which makes the glass surface highly conducting without actually introducing any irregularity on it. It is thus possible to produce intense electric fields at the edge of this tin oxide layer where it has got sharp boundaries. According to the well known laws of electrostatics,<sup>15</sup> such an intense field produces mechanical pressure in the boundary layer of the liquid. This may also give rise to electrostriction.<sup>18</sup> Due to the finite potential difference between the tin oxide layer and the liquid layer adjacent to it, an electric double layer effect might also be present at the interface.<sup>16</sup>



Several authors<sup>49,50</sup> observed that the stress developed at the solid-liquid interface due to the presence of surface charge generally tend to reduce the surface tension of the liquid at the interface. Apart from effecting the microscopic interfacial tension, an external electric field might also facilitate any fluctuation or gradient of density of the liquid that might be present near the tin oxide boundary. It is not unlikely that an electric field gradient might also produce space charge at the 'boundary' of sub-critical nuclei in a superheated liquid. A critical value of this space charge might thus create a condition for the spontaneous growth of such a nucleus.

#### 6. Aims and scope of present study :

In the present work, we report a new method of inducing nucleation in stable and metastable liquids with the help of external electric field. The external electric field is applied in the liquid in such a way that it does not produce any heating in the liquid. With the help of this device it has been found possible to formulate a relationship between the attainable degree of superheat of the liquid and the field applied. Apart from having

some practical importance, this relationship enables us to determine the limit of stability of liquids on extrapolation.

The first part of the present work (Chapter III) deals with the design of the present experiment. Chapter IV deals with the experimental results and the interpretation of the results and the conclusions are given in Chapter V.

ccccc

# REFERENCES

1. Gibbs J.W., "Scientific Papers," Longman and Green, 1906.
2. Lebowitz J.L., and Penrose O., J. Math. Phys. 2, 1, 98 (1966).
3. (a) Kac M., Phys. Fluid. 2, 8 (1959).  
(b) Kac M., Uhlenback G.E., Hemmer P., J. Math. Phys., 4, 216 (1963).
4. Fisher M.E., Physics, 3, 255 (1967).
5. Langer J., Ann. Phys. N.Y., 41, 108 (1967).
6. Temperley H.N.V., Proc. Phys. Soc. (Lond.), 49, 203 (1947).
7. Fürth R., Proc. Camb. Phil. Soc., 37, 252 (1941).
8. Van der Waals J., thesis (Liden, 1873).
9. Maxwell J.C., "Scientific Papers" (Dover Reprint, N.Y.) p. 425.
10. Penrose O. and Lebowitz J.L., J. Stat. Phys., 3, 2, 211 (1971).
11. Ruelle D., "Statistical Mechanics" (Benjamin, N.Y., 1969).
12. Temperley, H.N.V., Rowlinson J.S. and Rushbrooke G.S., "Physics of Simple Liquids," H.H. Publ. Co., 1968.
13. Volmer M., "Kinetik der Phasebildung," (Stekikopff, Dresden and Leipzig, 1939).
14. Kerneth L., Ind. Engg. Chem., 44, 1310 (1952).
15. Fisher J.C., J. Appl. Phys., 19, 1062 (1948).
16. Frenkel J., "Kinetic theory of liquids", (Dover publications Inc., N.Y., 353, 1946).

17. Döring W., Zeits. f. Physik. Chem. B36, 371 (1937).
18. Apfel R., Acou. Res. Lab. Harvard Univ. Tech. Memo. No. 62 (1970).
19. Westwater J.W., "Advances in Chemical Engg.", Ch. I, (Academic Press, N.Y., 1956).
20. Wakeshima H., J. Phys. Soc. Japan, 16, 6 (1961).
21. Henderson D., Ann. Rev. Phys. Chem., 1964.
22. Neece G.A., and Widom B., Ann. Rev. Phys. Chem., (1969).
23. Smoluchowski M.V., Ann. d. Physik., 25, 205 (1908).
24. Farkas, Ze. f. Phys. Chem., 125, 236 (1927).
25. Kailash and Stronski, Ze.f. Phys. Chem., 1326, 317 (1934).
26. Becker and Döring W., Ann. d. Phys., 24, 719 (1935).
27. Döring W., Zeits. f. Physik. Chem., B38, 292 (1938).
28. Fisher J., J. Appl. Phys., 19, 1062 (1948).
29. Beams J.W., Phys. Rev., 104, 880 (1956).
30. Briggs L.J., J. Appl. Phys., 21, 721 (1950).
31. Chu M.L., Jr., Ph.D. Dissertation, Univ., Houston, Texas (1967).
32. Sinha D.B. and Jalaluddin A.K., Ind. J. Phys., 35, 6, 311 (1961).
33. Skripov V.P. and Ermakov G.V., Zur. Fisi. Khim., 38, (1964) In Russian.
34. Apfel R., J. Acou. Soc. America, 49, 1, Part 2, 145 (1971).

35. Tolman R.C., J. Chem. Phys., 17, 333 (1949).
36. Langmuir I., Tran. Fara. Soc., 15, 69 (1920).
37. Clark F.H., J. Frank. Inst. 216, 429 (1933).
38. Ref. 37, 39 (1933).
39. Ref. 37, p. 430.
40. Ref. 37, p. 434.
41. Wigner K.L., J. Phys. Chem., 26, 301 (1922).
42. Wakechima H. and Tokata K., J. Phys. Soc. Japan, 13, 1398 (1958).
43. (a) Glaser D.A., Phys. Rev., 87, 665 (1952).  
 (b) Glaser D.A., Sci. Amer., 192, 2, 46 (1955).  
 (c) Glaser D.A., Nuovo Cimento; 11, supp. 2, 361 (1954).
44. Wilson J.G., "The principles of cloud chamber Technique", Camb. Univ. Press, London, 1953.
45. Seitz F., Phys. Fluids, 1, 1,2 (1958).
46. Jalaluddin A.K. and Sinha D.B., Nuovo Cimento, Supp. 26, Ser.X, 234 (1962).
47. Stratton J.D., "Electromagnetic theory", McGraw Hill Co. N.Y., 1941.
48. Jeans J.H., "The mathematical theory of electricity and magnetism", Camb. Univ. Press, 1925.
49. Nayyar N.K. and Murty G.S., Proc. Phys. Soc., 75, 369 (1960).
50. Cade R., Proc. Phys. Soc., 82, 216 (1964).

EXPERIMENTAL SETUP AND WORKING PRINCIPLE

The present experimental set-up consists of:

- i) a miniature bubble chamber for subjecting the liquid to superheated (metastable) condition;
- ii) an electrical device for introducing electric field at the liquid-glass interface; and
- iii) set of electronic devices to indicate change in pressure of the liquid, application of the electric field and initiation of boiling at the interface.

The chamber and the electrical and electronic systems have been designed and fabricated in the laboratory.

### 3.1 Principles of bubble chamber technique:

In a bubble chamber, a closed volume of the liquid is thermostated at a temperature much higher than its boiling point, i.e., it remains at pressures much higher than the atmospheric pressure. On sudden expansion of the flexible wall of the chamber, the pressure inside the chamber drops down rapidly and the liquid becomes superheated. Since the compressibility of the liquid is comparatively small, the change of temperature inside the liquid during the expansion is rather very small and its thermodynamic state may be represented by the working temperature  $T$  and the instantaneous pressure  $P_L$ .

The life time of a superheated liquid goes on decreasing with the increase in the degree of the superheat, represented by  $\Delta p = P_G - P_L$ , where  $P_G$  is the saturated vapour pressure of the liquid. The metastable superheated condition is generally destroyed by parasitic bubble formation which, among other factors, may be caused by the incident cosmic ray particles, presence of dust particles, the existence of heterogeneity or cleavages on the internal surface of the chamber or due to application of an electric field at the interface. The waiting time or the time interval,  $\Delta t$ , between the moment at which the pressure falls to a given value below the saturated vapour pressure and the moment at which boiling is initiated under the given thermodynamic state depends mainly on the magnitude of  $\Delta p$  and the construction of the chamber. With the increase of  $\Delta p$ ,  $\Delta t$  decreases exponentially and at a given temperature  $\Delta p$  may reach such a high value  $\Delta P_m$  that spontaneous boiling starts almost simultaneously althroughout the volume of the superheated liquid, the phenomenon being known as homogeneous phase transition of a liquid into vapour. The waiting time,  $\Delta t$ , should be zero when  $\Delta p$  reaches the limiting value  $\Delta P_m$ .



### 3.2 Experimental set-up.

In any experiment with superheated liquids, the main experimental requirement is to make the test liquid and its container free from agents responsible for initiating heterogeneous boiling. This can be accomplished by using as small quantity of liquid as possible as the sample and a scrupulously cleaned homogeneous glass surface to contain it. On the other hand in order to study the effect of any variable external factor, like an external electric field, in inducing nucleation in the superheated liquid one has to introduce foreign bodies, e.g., metallic electrodes into the liquid itself which are most likely to act as sources of heterogeneous nucleation in the liquid under very small degrees of superheat. The present experiment is so designed as to avoid introducing any external source of nucleation while introducing an external electric field.

In the present experimental set-up, a thick walled glass capillary has been chosen as the chamber proper and in order to avoid boiling from the joints sealing the glass capillary with the expansion device, the superheating of the test liquid is confined to the upper

half of the capillary. The liquid in the lower half of the capillary and in the expansion system is always kept at subcooled temperatures. A thin transparent film of tin oxide deposited on the inner wall of the capillary serves as the high voltage electrode. There is no other electrode in the liquid itself. This requirement is considered stringent because the presence of both the electrodes in the same liquid generally gives rise to the flow of small conduction currents through the liquid which results in its consequent heating. It can be theoretically estimated that even in the absence of the second electrode in the test liquid, the intensity of the electric field at the sharp edge of tin oxide layer may be raised to a sufficiently high value in order to induce nucleation at the interface.

The main requirements in the design of a bubble chamber for the present study are:

- (a) The inner wall of the chamber proper should be free from all surface irregularities and joints. In other words it should be an all glass chamber without any sharp bend in order to reduce the probability of bubble formation from permanent sites.

- (b) The mechanism of the expansion of the chamber should be capable of producing a desired  $\Delta p$  for more or less a wide range of temperature.
- (c) There should be an automatic arrangement for the application of the electric field in the chamber liquid at a desired value of  $\Delta p$ . The instant of the application of the electric field should also be indicated somewhere in the measuring arrangement.

The details of the construction of the setup follows:

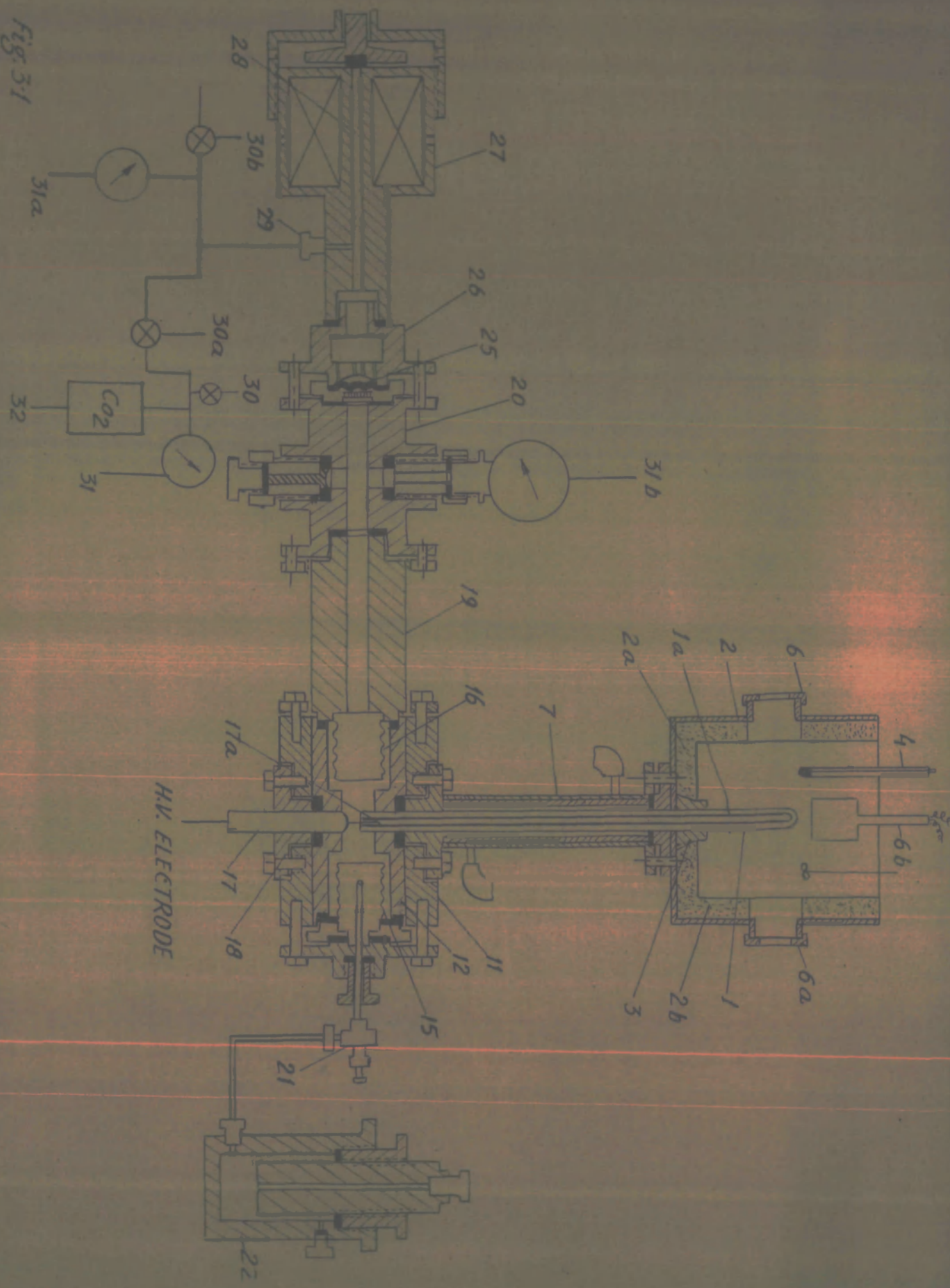
### 3.3. The Chamber:

A schematic diagram of the chamber expansion mechanism and other accessories is given in Fig.3.1. It is a composite system of two chambers and functions on the same principle as that of bubble chambers.

#### (a) The Experimental Liquid Chamber:

A thick walled coming glass tube(1) (i.d. = 2.5 mm, o.d. = 9 mm) constitute the chamber proper. The inner wall of the glass tube is coated with tin oxide (1a) in order to make it conducting. The tin oxide coating is

Fig. 31



thin (thickness  $\approx 10^{-5}$  cm), transparent and highly conducting, and it has a sharp boundary near the upper sealed end of the glass capillary. The lower end of this glass tube is sealed with the steel-ebonite chamber (11) with the help of rubber gaskets and a cylindrical brass flange (7). The ebonite chamber (12) insulates the experimental liquid from all the metallic parts of the chamber. The metallic body (11) is used only to give strength to the chamber. To pressurise and to change the volume of the liquid in the chamber, two metallic bellows (15, 16) are used at either end of the steel - ebonite chamber and are sealed with it with rubber gaskets. A metallic high voltage electrode (17) is inserted at the bottom of the ebonite chamber and sealed with it with the help of an ebonite flange (18). The electrode touches the tin oxide coating (17a) of the glass tube. Cooling of the lower portion of the glass tube and other parts of the chamber is done by circulating cold water through the gap between the glass capillary and the cylindrical brass tubing.

(b) The Buffer Chamber:

The chamber (20) filled with an insulating liquid is meant for damping down the oscillations during the expansion of the chamber. A static pressure gauge (31b) is inserted in this chamber as shown in Fig.3.1. The chamber is made of steel and an ebonite separator (19) separates it from the experimental liquid chamber. The separator is used only to avoid any probable sparking between the experimental liquid chamber and the buffer chamber in case the high voltage electrode or the liquid at high voltage in the experimental liquid chamber accidentally touches the metallic parts of the chamber. A dynamic capacitance pressure gauge (23) is also inserted below the static pressure gauge in order to record the time variation of pressure during the expansion. On the other end of the chamber, there is a rubber diaphragm (25) on which the pressure from outside can be applied from a CO<sub>2</sub> gas cylinder (32). The pressure can be released by operating an electromagnetic valve (28).

(c) The Pressure Generator

In order to control the initial volume of the liquid in the capillary, a pressure generator-piston in a cylinder-is used. It consists of a hollow steel cylinder (22) 10 cm in length, 4 cm outer diameter and closed at one end. A steel solid cylindrical rod (22a) is made to slide into this cylinder by means of screw thread arrangement. The arrangement is made pressure proof by teflon O-ring. The hollow cylinder is filled with a liquid and the pressure is generated in the liquid by moving the cylindrical rod in the forward direction. The pressure thus generated can be transmitted to the experimental liquid chamber through a stainless steel tubing.

(d) The Volume Control System

To keep the liquid in the heated portion of the capillary even after boiling has taken place, it is necessary to fix the initial level of the meniscus of the test liquid in the capillary. This is done by fixing the sylvphon (15) at a suitable position with the help of the pressure generator (22). Once the level of

the meniscus in the capillary is fixed, the pressure generator is disconnected from the main chamber by closing the needle valve (21).

(e) The Temperature Control System:

The upper portion of the vertical glass chamber(1) containing the test liquid is maintained at higher temperature whereas its lower portion and other chambers are maintained at room temperature. This is done by means of two different thermostating systems.

The room temperature thermostating is done by circulating cold water through a brass cylinder (7), containing two opposite slits covered by perspex cylinder. The perspex is transparent and thus the liquid column in the glass tube could be visualised through it. The brass cylinder surrounds the middle and lower portions of the glass capillary.

The upper portion of the vertical glass tube is maintained at higher temperatures (70-185°C). A glass cylinder (2b) 5 cm in diameter and 7 cm in length, open at the upper end, is sealed coaxially with the capillary by a rubber cork (3). This cylinder is protected by a copper box (2). To

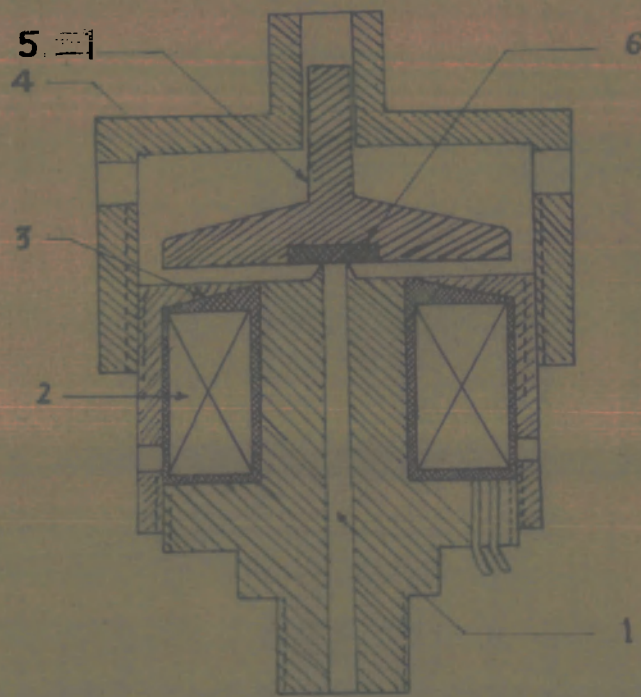


visualise boiling in the capillary, two glass windows (6 & 6a), 2 cm in diameter, are fitted in the centre of the vertical walls of the copper box. Another glass window, fitted at the centre of the third vertical wall of the box, is used for illuminating the capillary. To avoid heat losses to atmosphere from the glass thermostat, the gap between the glass cylinder and the copper box is filled with glass wool leaving the windows free.

Glycerine is used as the thermostating liquid. It is chosen because of its high boiling point ( $300^{\circ}\text{C}$ ) and refractive index. A 100 watt immersion heater (6b), fabricated for the setup is used for heating the thermostating liquid from the top. The current in the heater is controlled by a variac. The thermostating liquid is stirred with the help of a stirrer. A thermometer ( $0-300^{\circ}\text{C}$ ) with  $0.5^{\circ}\text{C}$  accuracy is used to measure the temperature of the thermostat.

(f) The Electromagnetic Valve:

An electromagnetic valve (Fig.3.2) is used for the expansion of the chamber. It consists of two coils surrounding an iron core. One of the coils has no. of



ELECTROMAGNETIC VALVE

FIG. 3.2

turns 3000 and resistance 350 ohms while the other has the no. of turns 1000 and resistance 40 ohms. There is a central hole (1) in the iron core coaxially with the coils which is connected with the gas inlet to the rubber diaphragm. When a current (90-110mA in  $350\Omega$  and 350 - 450 mA in  $40\Omega$ ) is passed through coils, the iron core becomes magnetised and it attracts the iron disc (5) in which a teflon disc (6) is fitted in the center. The outlet for the gas is thus closed by passing current through the coils (2); when the current through the coils is switched off, the iron core becomes demagnetised and the iron disc is pushed back by the gas pressure thus opening the outlet for the gas. The horizontal movement of the iron disc forward and backward is facilitated with the help of the aluminium cover (4). The time required for opening the electromagnetic valve is of the order of milli-seconds.

(g) The Optical Indicator of Boiling:

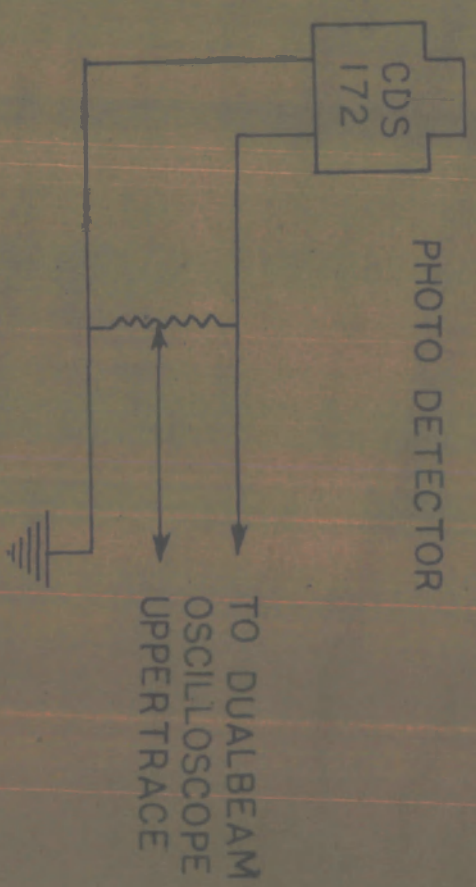
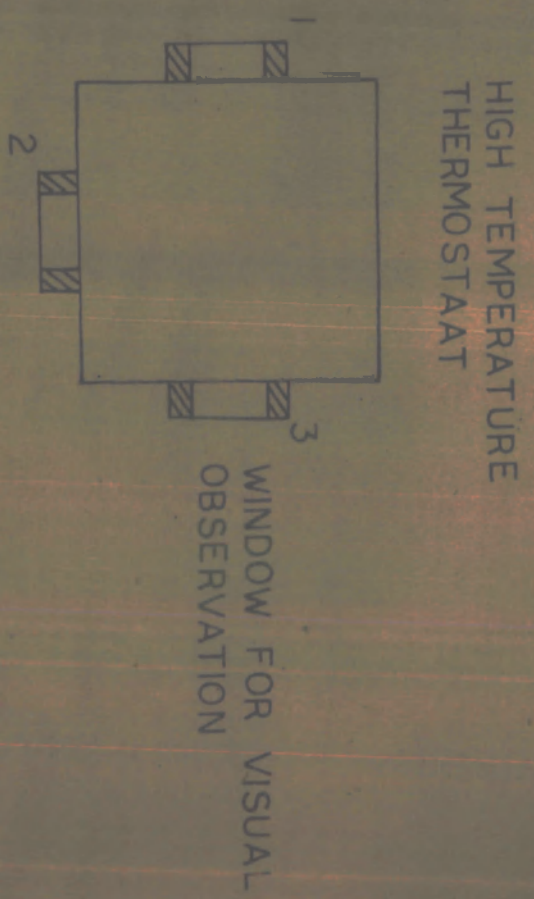
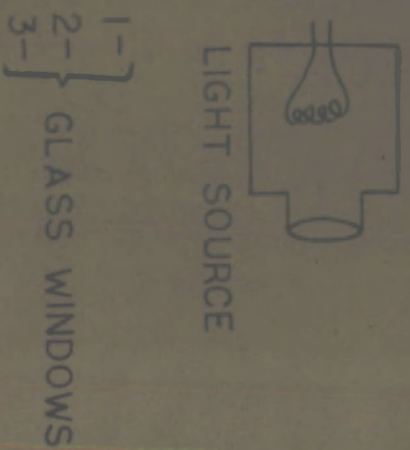
The method of light scattering has been widely applied in the study of the critical opalescence.<sup>3</sup> As formation of minute vapour bubbles in a liquid causes appreciable variation in the intensity of light

scattered from the liquid, the method of scattering has been used as an indicator of the initiation of boiling in the test liquid.

The change in intensity in the scattered light at  $90^\circ$  is detected with the help of a photo diode (Pioneer CDS 712) using an optical scheme shown in Fig.3.3. The electrical signal from the photo detector is fed to an oscilloscope (upper trace) by putting a load in the circuit as shown in Fig.3.3. Thus any change in intensity in the scattered light on boiling could be detected on the oscilloscope screen.

(1) The High Voltage Unit: An 8 KV rectifier unit as shown in Fig. 3.4 has been assembled in the laboratory.

The a.c. voltage is available from a 220-20 KV step-up transformer and it is rectified by a diode valve (1B3GT, Haltron). In designing the rectifier care has been taken to make the direct current (d.c.) output voltage free from ripples by using filters. A two step filter circuit, with 3 capacitors each of  $4\mu\text{f}$ , 4KV working voltage and  $10\text{ M}\Omega$  resistance in each



OPTICAL SCHEME FOR INDICATION OF BOILING IN THE GLASS CAPILLARY

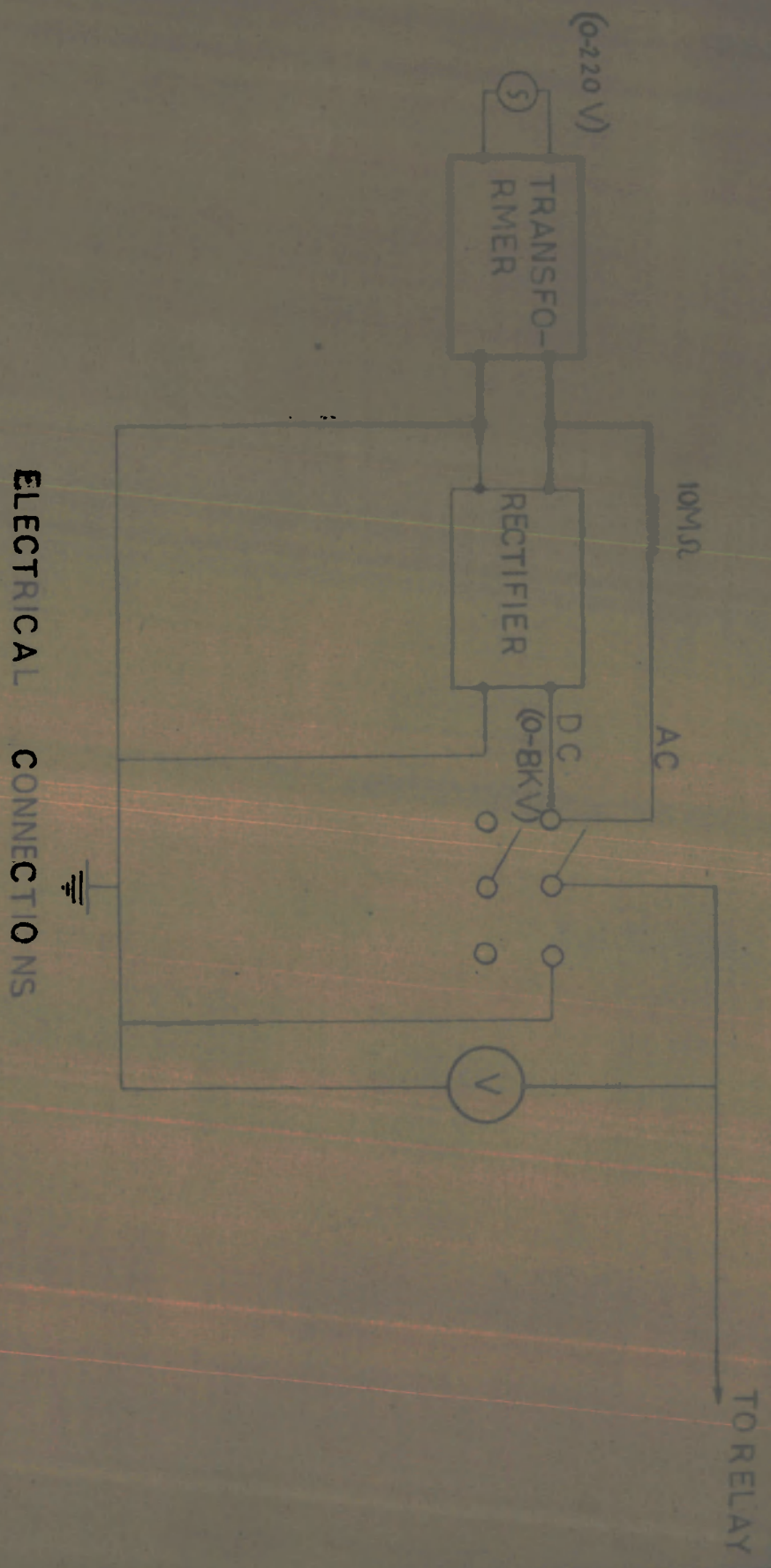
FIG. 3.3



HIGH VOLTAGE  
TERMINAL

step is used. Since the maximum current capacity of the transformer windings is 1 mA, a 100 mA fuse is used with the primary of the transformer to avoid any possible damage of the transformer in the case the high voltage terminal is short circuited to earth due to possible leakage through the body of the chamber.

(11) The Electrical Connections : A schematic representation of the electrical connections used in the experimental setup is given in Fig. 3.5. The high voltage source is switched on and off through a double - pole double - throw switch in such a way that the liquid in the chamber could be earthed immediately after the high voltage electrode is disconnected from the power supply. When an a.c supply is required, the rectifier unit is disconnected from the secondary of the high voltage transformer and a  $10\text{ M}\Omega$  resistance is put in series with the electrode. In order to check the effect of polarity of the high voltage electrode on nucleation, a 0-4 KV variable polarity stabilised power supply (Type 200, manufactured by Dynatron Radio Ltd., Maidenhead) has been used.



ELECTRICAL CONNECTIONS

FIG. 3.5



An auto-transformer is included in the circuit in the input of the voltage supply unit. This is used to change the output voltage, both alternating (50HZ) and unidirectional (+ ve polarity). All the components used in the circuit have high voltage insulation and the electrical connections have been made with cables having 40 KV insulation. Proper precautions have been taken to prevent any possible leakage.

The high voltage terminal of the double-pole double-throw switch is connected to the high voltage electrode of the experimental liquid chamber through an electromagnetic relay, which could introduce a desired delay in the application of the electric field. The relay is operated by a regulating switch which also operates the electromagnetic valve simultaneously as shown in Fig. 3.6. The voltage is measured with 0-5KV and 0-30KV (electrostatic) voltmeters.

#### 3.4 Cleaning and Filling of the High Pressure Chamber :

The superheating of liquids is very much affected by impurities, particularly suspended dust particles, oily deposits on the surface or air or gas bubbles

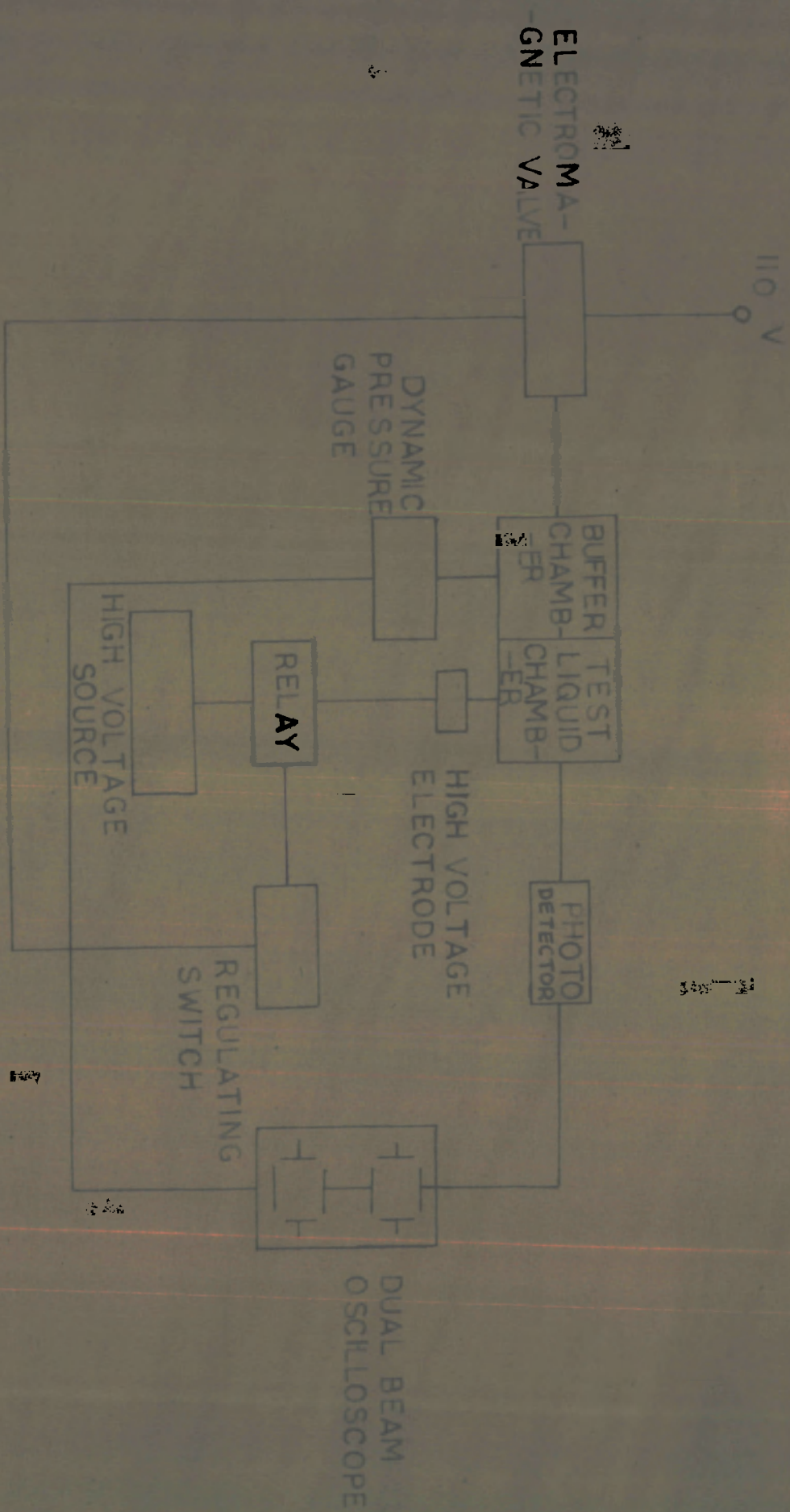


FIG. 3.6  
BLOCK DIAGRAM OF THE CONTROL MECHANISM.

dissolved in the liquid used. Therefore the glass capillary is cleaned with chromic acid and then dried in an oven. The ebonite chamber is also first washed with distilled water and then dried by blowing hot air through it. It is then rinsed with the experimental liquid. The experimental liquids used for the present study are of high purity and have been supplied by E. Merck, W. Germany (n-Hexane 99%, n-Pentane 95% , iso-pentane 95%).

In order to ensure that no air bubble is entrapped in the experimental liquid chamber, it is evacuated before filling it with the test liquid. The evacuation is done by means of a rotary oil vacuum pump connected with a three way stop cock. The chamber is mounted on a table with the capillary downwards. The vacuum system is sealed with it through the flange for the high voltage electrode and sealed with the chamber with the help of rubber O-rings. The test liquid contained in a bottle is sucked into the chamber when the stop cock is rotated to disconnect the pump and connect the chamber with the container of the test liquid. To remove any air bubble that might have been entrapped

in the chamber inspite of following the above procedure and also to free the test liquid from dissolved air, the chamber thus filled is again connected to the vacuum pump through a vapour and liquid trap. Under the reduced pressure the liquid is allowed to boil and the chamber is refilled. This procedure is repeated until the spurious boiling of the chamber liquid stopped and occasional bumping of the liquid is observed. This ensures the fact that the test liquid has been properly degassed. The vacuum system is then disconnected from the chamber and an electrode, a copper rod, is inserted into the chamber in such a way that a thin tungsten wire soldered to it always touches the tin oxide film coated on the inner surface of the glass capillary. The length of the thin wire is so adjusted that it is always confined to that volume of the liquid which is kept at room temperature. The electrode is then sealed with the chamber by a flange and O-ring arrangement. The buffer chamber is also filled with an insulating liquid (n-Hexane) in the same manner and a dummy metallic piece in place of capacitance monometer

is used for this purpose. When the buffer chamber is filled with the liquid, the dummy arrangement is replaced by the capacitance manometer. The chamber is then removed from the table and supported on wooden and metallic stands in such a way that the pressure gauge in the buffer chamber and the glass capillary are kept vertically upwards and the rest of the body of the chamber is horizontal. The pressure generator system for volume control is then incorporated into the chamber.

The electromagnetic valve is then sealed at the other end of the buffer chamber. The copper tubing circuit with the high pressure valves and pressure gauges are sealed with the gas inlet of the electromagnetic valve. The coils of the electromagnet are then energised by a 110V d.c. supply through a set of resistances which were used to control the currents in the coils.

On completing all the connections, the high voltage terminal of the power supply is connected to the <sup>-age</sup> high voltage electrode through the double-pole double-throw switch and the electromagnetic relay as shown in Fig. 3.6.

The general lay out of the experimental arrangement is thus shown in Fig. 3.7.

### 3.5. Mechanism of the expansion of the chamber :

Internal pressure of the experimental liquid chamber is counteracted by subjecting the buffer chamber to a pressure from outside through the rubber diaphragm.  $\text{CO}_2$  from the cylinder is used for this purpose. When the external pressure slightly exceeds the internal pressure, saturated vapour of the working liquid at the given temperature begins to condense and the level of the liquid in the glass tube rises till the last trace of the vapour phase disappears. While <sup>is</sup> pressurizing the chamber, the outlet for the  $\text{CO}_2$  gas is closed by the electromagnetic valve.

On switching off the current through the coils of the electromagnet, pressure in the chamber suddenly drops down. The rate of fall of pressure is mainly determined by the inertia of the rubber diaphragm and the bellows.

### 3.6. Dynamic measurement of pressure :

Since the present experiment is designed for studying the thermodynamic properties of liquids, an accurate knowledge of the instantaneous pressure is

considered to be very important here. In the present experiment, a capacitance pressure gauge is used to record the change of pressure in the chamber during its expansion. A schematic diagram of the pressure gauge is given in Fig. 3.8. In fact, it is a parallel plate condenser, one of the plates (a membrane 5) of which happens to be a part of the wall of the chamber. The other plate (6) is kept rigidly fixed. The capacitance of the condenser is given by the formula

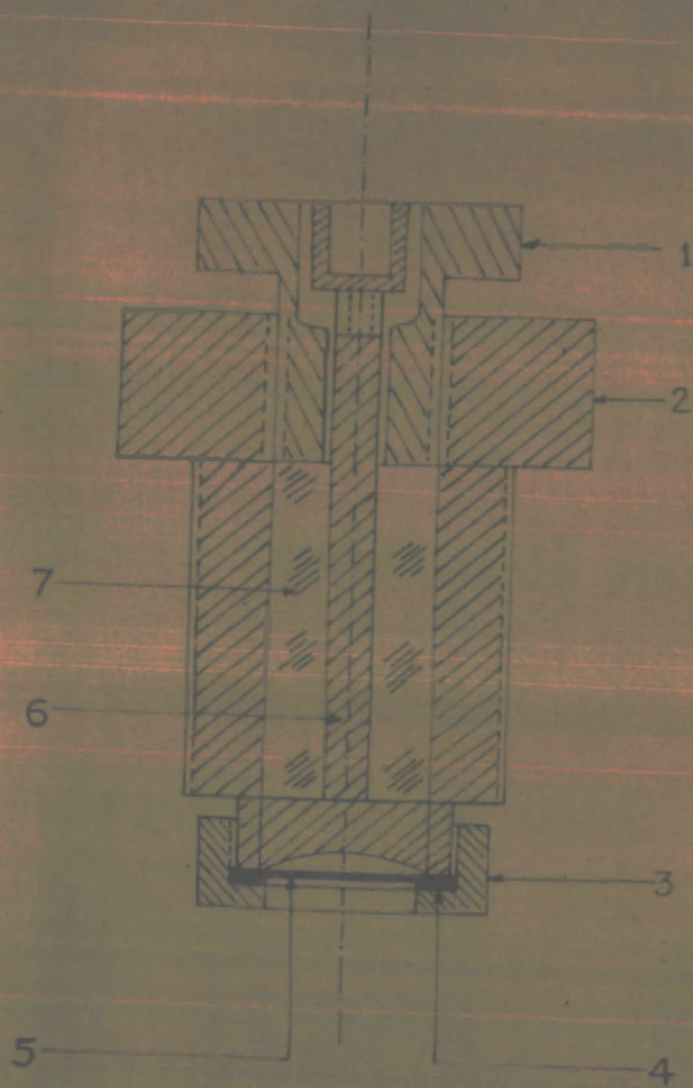
$$C = \frac{S \varepsilon}{3.6 \pi d} \mu\mu_f \dots\dots\dots (3.1)$$

where  $S$  is the area of the membrane in  $\text{cm}^2$ ,  $d$  is the gap between the two plates in  $\text{cm}$ ,  $\varepsilon$  - the relative dielectric constant of the medium between the plates.

The surface of the inner plate (5) is made curved inside, the depth being 0.1 mm. With the change of pressure the gap  $d$  changes correspondingly, and this in turn alters the capacitance. For small displacement of the membrane the sensitivity of the membrane is given by

$$\eta = \frac{S \varepsilon}{3.6 \pi (d - \Delta d)^2} \mu\mu_f / \text{cm.}, \dots\dots (3.2)$$





CAPACITANCE MANOMETER

FIG. 3.8



where  $\Delta d$  is the displacement of the membrane for a change of pressure  $\Delta p$  atms. This relation is reliable only when  $\Delta d/d \ll 1$ . The capacitance of the manometer and consequently its sensitivity is increased by placing condenser paper of 0.05 mm thickness between the plates. In the working range of pressure the change in the capacity of the condenser is about 1  $\mu\text{mf/at.}$ , and the maximum deviation from linearity is about 3%. The capacitance gauge is calibrated by comparing it with standard manometers (tested by Lucas Pressure Gauge Co., Ltd., Birmingham, England.) under both static and dynamic variation of pressure.

Kuznetsov's<sup>4</sup> circuit has been used to record change of capacitance of the gauge (Fig. 3.9). With the help of this circuit a change in the capacitance is converted into a change in the voltage by producing an amplitude modulation of the frequency of the circuit. A detector separates out the modulating voltage.

The circuit consists of an oscillator with inductive coupling and a measuring circuit  $L_5C$ . The resonance frequency of the measuring circuit is close to that of the oscillator (1 MHz). The coupling coils

$L_3L_4$  help in maintaining the forced oscillations in the measuring circuit at the frequency of the oscillator. The capacitance gauge is directly connected to the measuring circuit. A change in the capacitance of the gauge disturbs the setting of  $L_5C$  which was previously set for producing resonance with the generating frequency. This in turn brings about a change in the current through  $L_3L_4$ . This current is rectified by the detector having  $R_H$  as load. Potential across  $R_H$ , which is proportional to the change of the capacitance of the gauge, is fed into an oscilloscope.

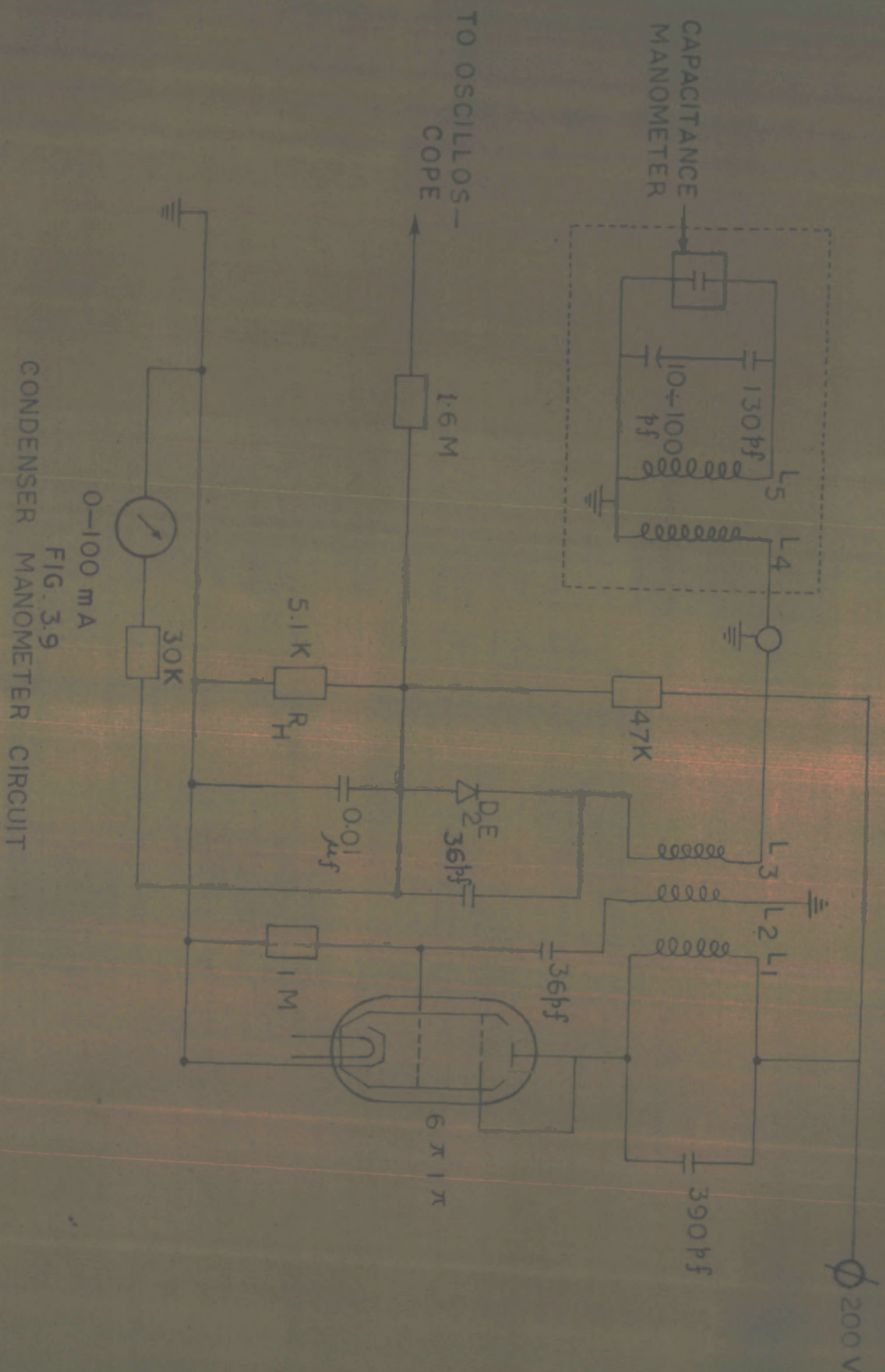
High fidelity of the measuring circuit is ensured by the following factors:

(a) The measurement of the capacitance is made inertialess by selecting the frequency of the circuit (1 MHz) much above the natural frequency of vibration of the membrane of the gauge which is of the order of 30 KHZ as calculated from the following formula

$$f = 1.2 \times 10^6 \times \frac{h'}{g} \text{ Hz , } \dots\dots\dots (3.3)$$

where  $h'$  is the thickness of the membrane in cm.

(b) The difficulty with connecting cables have been avoided by fixing the measuring circuit with the gauge in sit.



(c) The stability of the circuit is achieved by using highly stabilised supply voltages.

The output of the oscillator circuit is fed into the lower trace of the dual beam oscilloscope. Thus any change in the pressure is converted into an electrical signal which could be detected on the oscilloscope screen and the instantaneous pressure could be determined by photographing the oscilloscope beam with the help of a reflex camera.

### 3.7. Procedure :

Since the experimental chamber is completely filled with the degassed liquid before the temperature of the liquid occupying the upper portion of the glass capillary is raised it is necessary to ensure that the siphons separating the auxiliary chamber from the experimental chamber are flexible enough to accommodate the increase in the volume of the liquid caused due to the thermal expansion of the hot liquid. This is done by raising the temperature of the hot liquid in the upper half of the capillary and simultaneously observing the pressure indicated by the pressure gauge sealed with

the auxillary chamber. Usually no rise in the pressure is observed when the temperature of the liquid is raised to a value much above its boiling point. Under this condition the hot liquid was superheated. After prolonged waiting, vapour bubbles are found to be formed at the top of the capillary and the meniscus of the liquid is found to move downwards under the vapour pressure of the liquid. The level of the meniscus in the capillary is then adjusted by readjusting the position of the sylvan by generating pressure in the pressure generator till the vapour phase remained confined to about 2 cm of the height of the capillary at the top. While thus controlling the volume of the vapour phase in the capillary, care is taken to see that the pressure indicated by the pressure gauge corresponds to the actual vapour pressure of the liquid when the level of the meniscus of the liquid in the capillary occupies the final position. Temperature of the high temperature thermostat is raised to a desired value and simultaneously cold water from a reservoir is circulated at a constant pressure through the brass cylinder to keep the lower portion of the vertical glass capillary and

other parts of the chamber at room temperature. The temperature of the thermostat can be controlled by controlling the current through the immersion heater with the help of a variac. With the rise of the temperature of the test liquid, the pressure inside the chamber also rises. The readings of the pressure gauge always correspond to the saturated vapour pressure of the test liquid at given temperatures. In order to bring the test liquid to the superheated state once again it is necessary to completely remove the vapour phase in the capillary by applying  $\text{CO}_2$  pressure from outside and wait till the temperature of the liquid attains the thermostat value.

### 3.8. Control mechanism :

Block diagram of the control mechanism for the simultaneous measurement of pressure, light intensity at  $90^\circ$ , and the instant of the application of the electric field is shown in Fig. 3.6. A complete cycle of the expansion, recompression, and electric field application is realized in the following stages:

The current is passed through the electromagnet and thus the outlet for the gas is closed. The chamber is pressurised by  $\text{CO}_2$  by opening the control valve to

a pressure slightly higher than the saturated vapour pressure of the liquid at the temperature of the thermostat. Thus the saturated vapour of the working liquid begins to condense and the level of the liquid rises till the last trace of the vapour disappears. Disappearance of the vapour is observed through the window for the immergent light. The chamber is left in this position for two-three minutes in order to facilitate temperature equalisation in the liquid. During this interval the electron beams of the double trace oscilloscope are adjusted in their reference positions. The shutter of the reflex camera in front of the screen of the oscilloscope is opened and after a second or two of this, the regulating switch of the overall system is pressed down, thus switching off the current in the electromagnet and operating the electromagnetic relay. The process of switching off of the current in the electromagnet produces a spark in the regulating switch which is sufficient for the triggering of the electron beams of the oscilloscope. After 15-20 msec of the switching off process the electromagnetic valve opens and the pressure begins

to fall. Within 50 msec it attains the atmospheric value. Signal from the capacitance gauge (lower trace) and that from the photo-cell (upper trace) are simultaneously registered on the film of the camera. The time delay between the instances of the release of the electron beams and the application of the electric field is already fixed by adjusting the separation between the contact points of the relay. By altering the separation between the contact points, the electric field can be applied at the given pressure  $P_L$  of the chamber below the saturated vapour pressure  $P_g$  of the liquid at temperature  $T$ . The minimum critical voltage required (0-5KV) at the high voltage electrode for inducing nucleation in liquid at a given degree of superheat expressed either as  $(\Delta p)_T$  (= saturated vapour pressure  $P_g$  minus the external pressure  $P_L$ ) or as  $(\Delta T)_p$  (= temperature of the liquid,  $T$  minus the boiling point at the given pressure) is determined by gradually raising the potential at the electrode in steps of 20 volts only.

The above procedure is repeated at different pressures (1-15 atms.) by altering the separation between

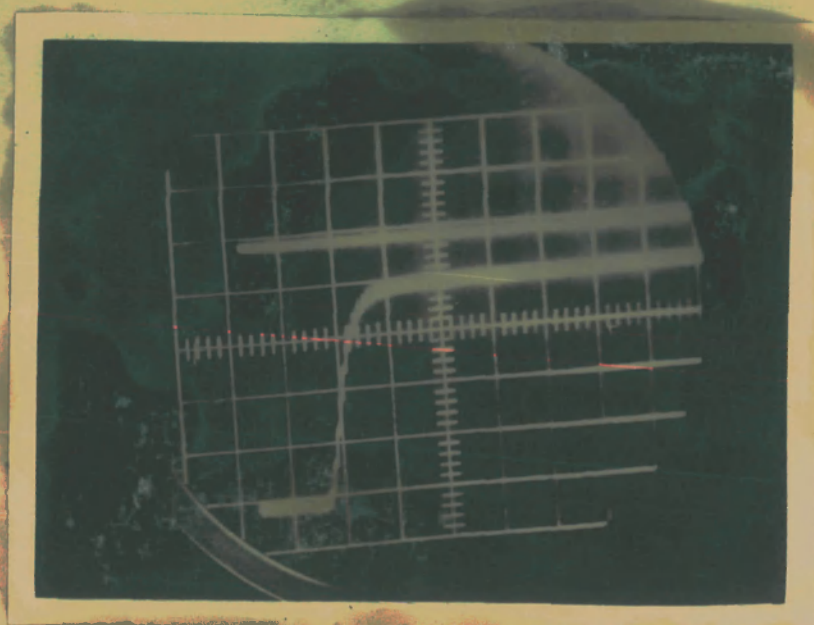


the two contact points of the electromagnetic relay and at different temperatures of the liquid (90-185°C) until the life-time of the superheated state becomes as high as few seconds.

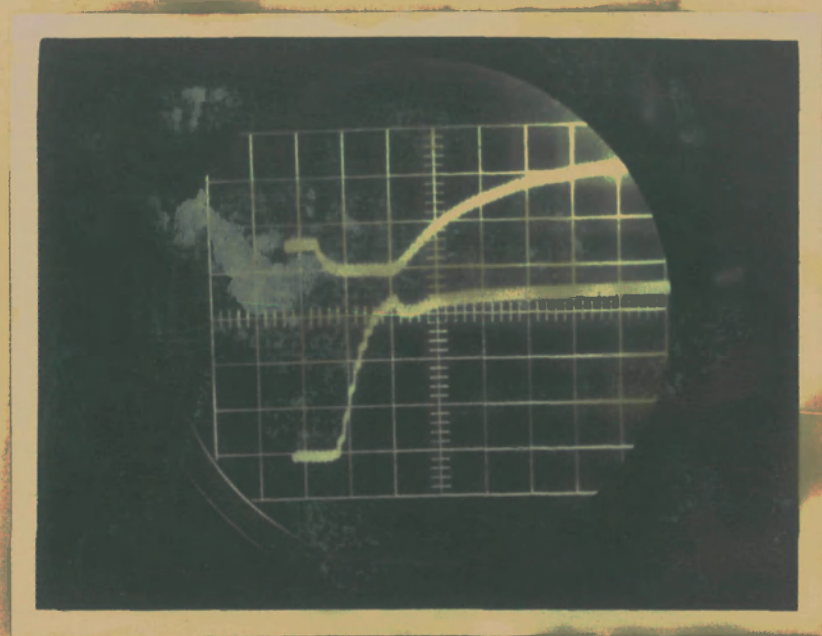
Four typical double-trace oscillograms, characterising the process of application of the external electric field, growth of intensity of scattered light at an angle  $90^\circ$  to the incident light on the initiation of boiling, and the development of pressure on boiling of the liquid are shown in Fig.3.10

In (a) the lower trace represents the drop of pressure from 20 to 1 atms. in the chamber during its expansion in the absence of external electric field while the upper one characterises the intensity scattered at  $90^\circ$ . As there was no boiling in this case, the intensity of the scattered light remain unaltered.

Oscillogram (b) shows change in the intensity of the scattered light at the point of application of the electric field during the expansion of the chamber. The initial small fall of intensity of the scattered beam seems to be due to the application of the field but the actual correlation between the two is not obvious.



(a)

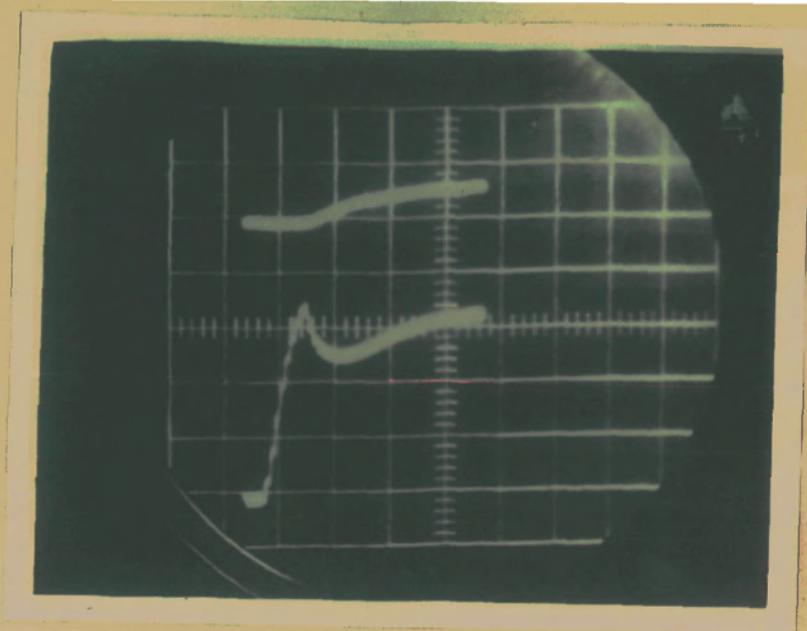


(b)

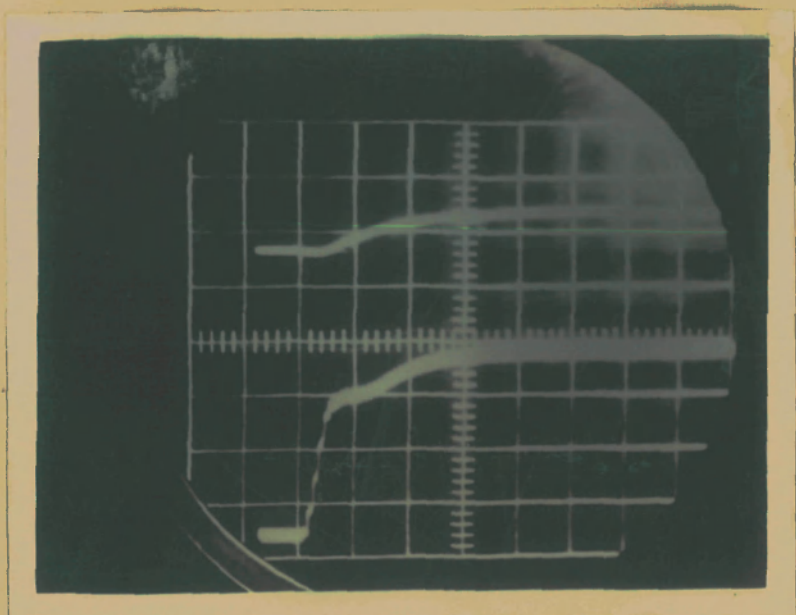
FIG.3.10

However, the sharp rise in the intensity in the later phase, which almost coincides with the minimum in the pressure curve, has been visually ascertained to be due to the initiation of boiling. Soon after the boiling of the liquid, there is a rapid increase of pressure in the chamber, which is indicated by a rise in the pressure. The pressure again falls down due to the depression of the liquid column into cooler region of the thermostat.

The phenomenon of instantaneous nucleation due to critical voltage  $V_c$  is shown in oscillogram(c). In this case the pressure falls from the initial value of 20 atm. and as soon it reaches the value of 3 atm., the electric field corresponding to the critical voltage  $V_c$  ( $= 600$  volts for *n*-pentane at  $T = 120.0^\circ\text{C}$ ) is automatically applied. The instantaneous nucleation due to the field is indicated by a sudden rise of the upper beam. The rise is instantaneous and thus the mark of the application of the electric field does not appear. The pressure attains the saturated vapour pressure value ( $= 9.0$  atm.). After boiling has taken place, the liquid column in the glass capillary falls down to the cold liquid region resulting a pressure drop again, as indicated in the oscillogram.



(c)



(d)

FIG.3.10

The instantaneous nucleation in the stable region i.e. at a pressure (10.0 ats) above the saturated vapour pressure, (9.0 ats. at  $T = 120^{\circ}\text{C}$ ) is shown in oscillogram (d). It should be noted that in this case pressure rise in the chamber due to boiling of the liquid is not perceptible because of the fact that the pressure is already higher than the saturated vapour pressure.

The  $V_c(T, \Delta p)$  values obtained from these type of oscillograms are given in Tables 1-34 for the three liquids used in the present study. These results are plotted in Figs. 4.1 (a,b,c). The  $V_c(P, \Delta T)$  values determined from the above tables are given in Tables 35-37 and the  $V_c$  versus  $\Delta T$  are plotted in Figs. 4.2 (a,b,c).

REFERENCES

1. Delone N.B., "Puzirkovskiy Kameri", Moscow (1963).
2. Kratochvil J.P., "Light scattering", Rev. Ann. Chem., 36, 458R (1964).
3. Conf. on Crit. Phen., Natl. Bur. Stan., Washington (1965) Science, 150, 229 (1965).
4. Kuznetsov E., Tekhnika Eksperimentov No.1, 58(1956)
5. Kratochvil J.P., "Light scattering" Rev. Ann. Chem., 38, 517R (1966).

\*\*\*\*\*

### EXPERIMENTAL RESULTS

TABLE -1- Minimum voltage ( $V_c$ ) of the applied field giving rise to instantaneous nucleation at different degrees of superheat  $\Delta P = (P_S - P_L)$ .

n = Hexane

Boiling point =  $68.7^\circ\text{C}$        $T = 100^\circ\text{C}$   
 $T_c = 234.7^\circ\text{C}$        $P_S = 2.4 \text{ ats.}$   
 $P_c = 30.4 \text{ ats.}$

Pressure in the Chamber ats.		$\Delta P = P_S - P_L$	$V_c$ Volts.
Initial higher P	Final lower P <sub>L</sub>	ats.	D.C.
20	1.0	1.4	1300
20	1.5	0.9	1350
20	2.0	0.4	1350
20	2.5	-0.1	1500
20	3.0	-0.6	2750
20	3.5	-1.1	Not upto maximum measurable



TABLE 2 - Minimum voltage  $V_c$  of the applied field giving rise to instantaneous nucleation at different degrees of superheat ( $P_S - P_L$ ).

n-Hexane

Boiling point =  $68.7^\circ\text{C}$

$T = 105^\circ\text{C}$

$T_c = 234.7^\circ\text{C}$

$P_S = 2.6$  ats.

$P_c = 30.4$  ats.

Pressure in the Chamber $\Delta p = P_S - P_L$ ats.			$V_c$ Volts	
Initial higher P	Final lower $P_L$	ats.	D.C. + ve	D.C. -ve
20	1.0	1.6	1200	1200
20	1.5	1.1	1250	1240
20	2.0	0.6	1300	1300
20	2.5	0.1	1400	1400
20	3.0	-0.4	1550	1575
20	3.5	-0.9	2750	2700
20	4.0		Not upto Max. measurable	Not upto Max. measurable

TABLE 3 - Minimum voltage  $V_c$  of the applied field giving rise to instantaneous nucleation at different degrees of superheat  $\Delta p = (P_S - P_L)$ .

n - Hexane

Boiling point =  $68.7^\circ\text{C}$   
 $T_c = 234.7^\circ\text{C}$   
 $P_c = 30.4 \text{ ats.}$

$T = 110^\circ\text{C}$   
 $P_S = 3.10 \text{ ats.}$

Pressure in the Chamber ats.		$\Delta p = P_S - P_L$ ats	$V_c$ Volts.	
Initial higher $P$	Final lower $P_L$		D.C. + ve	D.C. - ve
20	1.0	2.0	1100	1100
20	1.5	1.5	1100	1100
20	2.0	1.0	1150	1150
20	2.5	0.5	1250	1250
20	3.0	0.0	1350	1350
20	3.5	-0.5	1500	1550
20	4.0	-1.0	2100	2150
20	4.5	-1.5	Not upto maximum measurable	Not upto maximum measur- able

TABLE 4 - Minimum voltage  $V_c$  of the applied field giving rise to instantaneous nucleation at different degrees of superheat  $\Delta p = P_S - P_L$ .

n - Hexane

Boiling point =  $68.7^\circ\text{C}$

$T = 115^\circ\text{C}$

$T_c = 234.7^\circ\text{C}$

$P_S = 3.5$  ats.

$P_c = 30.4$  ats

Pressure in the Chamber ats.		$\Delta p = P_S - P_L$ ats.	$V_c$ Volts.	
Initial higher P	Final lower P <sub>L</sub>		D.C.	A.C. (50 HZ)
20	1.0	2.5	1000	1150
20	1.5	2.0	1000	1250
20	2.0	1.5	1100	1350
20	2.5	1.0	1150	1500
20	3.0	0.5	1200	2500
20	3.5	0.0	1300	Not upto Max. measurable.
20	4.0	-0.5	1500	
20	4.5	-1.0	1900	
20	5.0	-1.5	3000	Not upto max. measurable.
20	5.5	-2.0		

TABLE 5 - Minimum voltage  $V_0$  of the applied field giving rise to instantaneous nucleation at different degrees of superheat  $\Delta p = P_S - P_L$

n - Hexane

Boiling point =  $68.7^\circ\text{C}$

$T = 120^\circ\text{C}$

$T_c = 234.7^\circ\text{C}$

$P_S = 4.0 \text{ ats.}$

$P_c = 30.4 \text{ ats.}$

Pressure in the Chamber ats.		$\Delta p = P_S - P_L$ ats.	$V_0$ Volts.	
Initial higher P	Final lower P <sub>L</sub>		D.C.	A.C. (50 Hz)
20	1.0	3.0	900	1000
20	1.5	2.5	920	1050
20	2.0	2.0	950	1150
20	2.5	1.5	980	1250
20	3.0	1.0	1050	1350
20	3.5	0.5	1100	1600
20	4.0	0.00	1150	2100
20	4.5	-0.5	1350	3200
20	5.0	-1.0	1600	Not upto Max. measurable.
20	5.5	-1.5	Not upto max. measurable	

TABLE 6 - Minimum voltage  $V_c$  of the applied field giving rise to instantaneous nucleation at different degrees of superheat  $\Delta p = P_g - P_L$ .

n - Hexane

Boiling point =  $68.7^\circ\text{C}$   
 $T_c = 234.7^\circ\text{C}$   
 $P_c = 30.4 \text{ ats.}$

$T = 125^\circ\text{C}$   
 $P_g = 4.5 \text{ ats.}$

Pressure in the Chamber ats.		$\Delta p = P_g - P_L$ ats.	$V_c$ Volts.	
Initial higher P	Final lower $P_L$		D.C. +ve	D.C. -ve
20	1.0	3.5	800	800
20	1.5	3.0	800	800
20	2.0	2.5	850	850
20	2.5	2.0	900	850
20	3.0	1.5	950	950
20	3.5	1.0	1000	1000
20	4.0	0.5	1050	1000
20	4.5	0.0	1150	1100
20	5.0	-0.5	1350	1300
20	5.5	-1.0	1600	1600
20	6.0	-1.5	1950	1950
20	6.5	-2.0	2750	2800
20	7.0	-2.5	Not upto max. measurable.	Not upto max. measurable.

TABLE 7 - Minimum voltage  $V_c$  of the applied field giving rise to instantaneous nucleation at different degrees of superheat  $\Delta p = P_g - P_L$ .

n - Hexane

Boiling point =  $68.7^\circ\text{C}$   
 $T_c$  =  $234.7^\circ\text{C}$   
 $P_g$  = 30.4 ats.

$T$  =  $130^\circ\text{C}$   
 $P_g$  = 5.0 ats.

Pressure in the Chamber ats.		$\Delta p = P_g - P_L$ ats.	$V_c$ Volts.	
Initial higher P	Final lower $P_L$		D.C. +ve	D.C. -ve
20	1.0	4.0	750	700
20	1.5	3.5	750	750
20	2.0	3.0	775	750
20	2.5	2.5	780	800
20	3.0	2.0	800	800
20	3.5	1.5	850	850
20	4.0	1.0	900	900
20	4.5	0.5	950	950
20	5.0	0.0	1050	1050
20	5.5	-0.5	1150	1150
20	6.0	-1.0	1300	1300
20	6.5	-1.5	1500	1500
20	7.0	-2.0	2100	2100
20	7.5	-2.5	Not upto max. measurable	Not upto max. measurable.

TABLE 8 - Minimum voltage  $V_c$  of the applied field giving rise to instantaneous nucleation at different degrees of superheat  $\Delta p = P_g - P_L$

n - Hexane

Boiling point =  $68.7^\circ$                        $T = 135^\circ\text{C}$   
 $T_c = 234.7^\circ\text{C}$                        $P_g = 5.4 \text{ ats.}$   
 $P_c = 30.4 \text{ ats.}$

Pressure in the Chamber ats.		$\Delta p = P_g - P_L$ ats.	$V_c$ Volts.	
Initial higher P	Final lower P <sub>L</sub>		D.C. +ve	D.C. -ve
20	1.0	4.4	650	650
20	1.5	3.9	650	650
20	2.0	3.4	680	690
20	2.5	2.9	700	700
20	3.0	2.4	750	725
20	3.5	1.9	775	775
20	4.0	1.4	825	825
20	4.5	0.9	850	825
20	5.0	0.4	900	900
20	5.5	-0.1	1000	1000
20	6.0	-0.6	1100	1100
20	6.5	-1.1	1250	1250
20	7.0	-1.6	1450	1400
20	7.5	-2.1	1750	1800
20	8.0	-2.6	2250	2300
20	8.5	-3.1	Not upto max. Not upto max. measurable. measurable.	

TABLE 9 - Minimum voltage  $V_c$  of the applied field giving rise to instantaneous nucleation at different degrees of superheat  $\Delta p = P_g - P_L$ .

n - Hexane

Boiling point =  $68.7^\circ\text{C}$   
 $T_c = 234.7^\circ\text{C}$   
 $P_c = 30.4 \text{ ats.}$

$T = 150^\circ\text{C}$   
 $P_g = 7.4 \text{ ats.}$

Pressure in the Chamber ats.		$\Delta p = P_g - P_L$ ats.	$V_c$ Volts.	
Initial higher P	Final lower $P_L$		D.C.	A.C. (50 Hz)
20	1.0	6.4	500	575
20	1.5	5.9	500	575
20	2.0	5.4	525	625
20	2.5	4.9	525	650
20	3.0	4.4	550	725
20	3.5	3.9	575	750
20	4.0	3.4	625	800
20	4.5	2.9	675	850
20	5.0	2.4	700	925
20	5.5	1.9	750	1000
20	6.0	1.4	800	1125
20	6.5	0.9	850	1250
20	7.0	0.4	950	1350
20	7.5	-0.1	1050	1600
20	8.0	-0.6	1150	1850
20	8.5	-1.1	1250	2250
20	9.0	-1.6	1450	3000
20	9.5	-2.1	1950	Not upto max. measurable.
20	10.0	-2.6	Not upto maximum measurable.	



TABLE 10 - Minimum voltage  $V_c$  of the applied field giving rise to instantaneous nucleation at different degrees of superheat  $\Delta p = P_S - P_L$ .

n - Hexane

Boiling point =  $68.7^\circ\text{C}$        $T = 155^\circ\text{C}$   
 $T_c = 234.7^\circ\text{C}$        $P_S = 8.7 \text{ ats.}$   
 $P_c = 30.4 \text{ ats.}$

Pressure in the Chamber ats.		$\Delta p = P_S - P_L$ ats.	$V_c$ volts	
Initial higher P	Final lower P <sub>L</sub>		D.C.	A.C. (50 HZ)
20	1.0	7.7	425	500
20	1.5	7.2	450	500
20	2.0	6.7	450	525
20	2.5	6.2	475	525
20	3.0	5.7	500	550
20	3.5	5.2	500	575
20	4.0	4.7	550	625
20	4.5	4.2	550	675
20	5.0	3.7	600	700
20	5.5	3.2	625	750
20	6.0	2.7	650	800
20	6.5	2.2	700	850
20	7.0	1.7	750	950
20	7.5	1.2	800	1050
20	8.0	0.7	900	1150
20	8.5	0.2	1000	1250
20	9.0	-0.3	1125	1450
20	9.5	-0.8	1250	1950
20	10.0	-1.3	1550	3000
20	10.5	-1.8	1900	Not upto max. measurable.
20	11.0	-2.3	2500	
20	11.5	-2.8	Not upto maximum measurable.	

TABLE 11 = Minimum voltage  $V_c$  of the applied field giving rise to instantaneous nucleation at different degrees of superheat  $\Delta p = P_S - P_L$ .

n - Hexane

Boiling point =  $68.7^\circ\text{C}$

$T = 160^\circ\text{C}$

$T_c = 234.7^\circ\text{C}$

$P_S = 9.0 \text{ ats.}$

$P_c = 30.4 \text{ ats.}$

Pressure in the Chamber ats.		$\Delta p = P_S - P_L$ ats.	$V_c$ Volts.	
Initial higher P	Final lower P <sub>L</sub>		D.C. (+ve)	D.C. (-ve)
20	1.0	8.0	375	375
20	1.5	7.5	375	375
20	2.0	7.0	400	400
20	2.5	6.5	420	450
20	3.0	6.0	450	450
20	3.5	5.5	450	475
20	4.0	5.0	450	450
20	4.5	4.5	480	480
20	5.0	4.0	500	500
20	5.5	3.5	525	525
20	6.0	3.0	550	550
20	6.5	2.5	570	575
20	7.0	2.0	600	625
20	7.5	1.5	650	650
20	8.0	1.0	700	700
20	8.5	0.5	750	750
20	9.0	0.0	850	825
20	9.5	-0.5	900	900
20	10.0	-1.0	1050	1100
20	10.5	-1.5	1250	1250
20	11.0	-2.0	1500	1500
20	11.5	-2.5	2250	2250
20	12.0	-3.0	Not upto max. measurable	Not upto max. measurable.

TABLE 12 - Minimum voltage  $V_c$  of the applied field giving rise to instantaneous nucleation at different degrees of superheat  $\Delta p = P_S - P_L$ .

n - Hexane

Boiling point =  $68.7^\circ\text{C}$ .       $T = 165^\circ\text{C}$   
 $T_c = 234.7^\circ\text{C}$        $P_S = 9.6 \text{ ats.}$   
 $P_c = 30.4 \text{ ats.}$

Pressure in the Chamber ats.		$\Delta p = P_S - P_L$ ats.	$V_c$ Volts	
Initial higher P	Final lower $P_L$		D.C. (+ve)	A.C. (50 HZ)
20	1.0	8.6	300	500
20	1.5	8.1	300	500
20	2.0	7.6	320	520
20	2.5	7.1	325	520
20	3.0	6.6	350	550
20	3.5	6.1	375	600
20	4.0	5.6	400	620
20	4.5	5.1	400	680
20	5.0	4.6	450	700
20	5.5	4.1	450	750
20	6.0	3.6	500	820
20	6.5	3.1	520	870
20	7.0	2.6	520	950
20	7.5	2.1	550	1050
20	8.0	1.6	600	1150
20	8.5	1.1	675	1250
20	9.0	0.6	725	1450
20	9.5	0.1	775	1950
20	10.0	-0.4	850	3100
20	10.5	-0.9	950	Not upto max. measurable.
20	11.0	-1.4	1000	
20	11.5	-1.9	1200	
20	12.0	-2.4	1500	
20	12.5	-2.9	2000	
20	13.0	-3.4	3300	
20	13.5	-3.9	Not upto max. measurable.	

TABLE 13 - Minimum voltage  $V_c$  of the applied field giving rise to instantaneous nucleation at different degrees of superheat  $\Delta p = P_g - P_L$ .

n - Hexane

Boiling point = 68.7°C

T = 170°C

$T_c = 234.7^\circ\text{C}$

$P_g = 10.7$  ats.

$P_c = 30.4$  ats.

Pressure in the Chamber ats.		$\Delta p = P_g - P_L$ ats.	$V_c$ Volts	
Initial higher P	Final lower $P_L$		D.C. +ve	D.C. -ve
20	1.0	9.7	300	300
20	1.5	9.2	300	300
20	2.0	8.7	320	300
20	2.5	8.2	320	320
20	3.0	7.7	350	340
20	3.5	7.2	350	340
20	4.0	6.7	375	370
20	4.5	6.2	375	370
20	5.0	5.7	400	400
20	5.5	5.2	400	400
20	6.0	4.7	425	425
20	6.5	4.2	425	425
20	7.0	3.7	425	425
20	7.5	3.2	450	450
20	8.0	2.7	470	470
20	8.5	2.2	470	470
20	9.0	1.7	500	500
20	9.5	1.2	550	550
20	10.0	0.7	600	620
20	10.5	0.2	650	650
20	11.0	-0.3	750	720
20	11.5	-0.8	850	850
20	12.0	-1.3	950	950
20	12.5	-1.8	1100	1150
20	13.0	-2.3	1400	1420
20	13.5	-2.8	2300	2350
20	14.0	-3.3	Not upto max. measurable	Not upto max. measurable.

TABLE 14 - Minimum voltage  $V_c$  of the applied field giving rise to instantaneous nucleation at different degrees of superheat  $\Delta p = P_g - P_L$ .

n - Hexane

Boiling point =  $68.7^\circ\text{C}$        $T = 180^\circ\text{C}$   
 $T_c = 234.7^\circ\text{C}$        $P_g = 12.7^\circ\text{C}$  at.  
 $P_c = 30.4$  at.

Pressure in the Chamber at. Initial higher    Final lower P                      P <sub>L</sub>		$\Delta p = P_g - P_L$ at.	$V_c$ Volts. D.C.	-
20	1.0	11.7	250	-
20	1.5	11.2	250	-
20	2.0	10.7	250	-
20	2.5	10.2	250	-
20	3.0	9.7	250	-
20	3.5	9.2	250	-
20	4.0	8.7	250	-
20	4.5	8.2	250	-
20	5.0	7.7	250	-
20	5.5	7.2	250	-
20	6.0	6.7	250	-
20	6.5	6.2	250	-
20	7.0	5.7	250	-
20	7.5	5.2	250	-
20	8.0	4.7	250	-
20	8.5	4.2	270	-
20	9.0	3.7	300	-
20	9.5	3.2	320	-
20	10.0	2.7	350	-
20	10.5	2.2	380	-
20	11.0	1.7	400	-
20	11.5	1.2	420	-
20	12.0	0.7	450	-
20	12.5	0.2	500	-
20	13.0	-0.3	600	-
20	13.5	-0.8	650	-
20	14.0	-1.3	750	-
20	14.5	-1.8	850	-
20	15.0	-2.3	1000	-
20	15.5	-2.8	1400	-
20	16.0	-3.3	1700	-
20	16.5	-3.8	Not upto max. measurable.	

TABLE 15 - Minimum voltage  $V_c$  of the applied field giving rise to instantaneous nucleation at different degrees of superheat  $\Delta p = P_S - P_L$ .

n - Pentane

Boiling point =  $36.1^\circ\text{C}$

$T = 90^\circ\text{C}$

$T_c = 196.6^\circ\text{C}$

$P_S = 4.6 \text{ ats.}$

$P_c = 33.8 \text{ ats.}$

Pressure in the Chamber ats.		$\Delta p = P_S - P_L$ ats.	$V_c$ volts.	
Initial P	higher Final lower P <sub>L</sub>		D.C. +ve	D.C. -ve
20	1.0	3.6	800	800
20	1.5	3.1	850	850
20	2.0	2.6	900	900
20	2.5	2.1	1025	1000
20	3.0	1.6	1100	1100
20	3.5	1.1	1250	1250
20	4.0	0.6	1500	1500
20	4.5	0.1	2400	2350
20	5.0	-0.4	Not upto max. measurable.	Not upto max. measurable.

TABLE 16 - Minimum voltage  $V_c$  of the applied field giving rise to instantaneous nucleation at different degrees of superheat  $\Delta p = P_S - P_L$ .

n - Pentane

Boiling point =  $36.1^\circ\text{C}$        $T = 95^\circ\text{C}$   
 $T_c = 196.6^\circ\text{C}$        $P_S = 5.2 \text{ ats.}$   
 $P_c = 33.8 \text{ ats.}$

Pressure in the Chamber ats.		$\Delta p = P_S - P_L$ ats.	$V_c$ Volts.	
Initial P	Final P <sub>L</sub>		D.C.	-
20	1.0	4.2	700	-
20	1.5	3.7	750	-
20	2.0	3.2	800	-
20	2.5	2.7	870	-
20	3.0	2.2	1000	-
20	3.5	1.7	1100	-
20	4.0	1.2	1250	-
20	4.5	0.7	1450	-
20	5.0	0.2	1800	-
20	5.5	-0.3	2780	-
20	6.0	-0.8	Not upto max. measurable.	

TABLE 17 - Minimum voltage  $V_c$  of the applied field giving rise to instantaneous nucleation at different degrees of superheat  $\Delta p = P_S - P_L$ .

n - Pentane

Boiling point =  $36.1^\circ\text{C}$        $T = 100^\circ\text{C}$   
 $T_c = 196.6^\circ\text{C}$        $P_S = 5.8 \text{ ats.}$   
 $P_c = 33.8 \text{ ats.}$

Pressure in the Chamber ats.		$\Delta P = P_S - P_L$ ats.	$V_c$ Volts	
Initial higher P	Final lower P <sub>L</sub>		D.C.	A.C. (50 HZ)
20	1.0	4.8	600	800
20	1.5	4.3	650	850
20	2.0	3.8	700	900
20	2.5	3.3	750	1025
20	3.0	2.8	800	1125
20	3.5	2.3	850	1250
20	4.0	1.8	1000	1500
20	4.5	1.3	1100	2400
20	5.0	0.8	1250	3300
20	5.5	0.3	1750	Not upto max. measurable.
20	6.0	-0.2	2500	
20	6.5	-0.7	Not upto max. measurable.	



TABLE 18 - Minimum voltage  $V_c$  of the applied field giving rise to instantaneous nucleation at different degrees of superheat  $\Delta p = P_S - P_L$ .

n - Pentane

Boiling point = 36.1°C

$T = 105^\circ\text{C}$

$T_c = 196.6^\circ\text{C}$

$P_S = 6.4 \text{ ats.}$

$P_c = 33.8 \text{ ats.}$

Pressure in the Chamber ats.		$\Delta p = P_S - P_L$ ats.	$V_c$ Volts	
Initial higher P	Final lower P <sub>L</sub>		D.C. +ve	D.C.* +ve
20	1.0	5.4	500	500
20	1.5	4.9	550	550
20	2.0	4.4	600	600
20	2.5	3.9	650	650
20	3.0	3.4	700	700
20	3.5	2.9	750	750
20	4.0	2.4	850	850
20	4.5	1.9	950	950
20	5.0	1.4	1050	1100
20	5.5	0.9	1200	1250
20	6.0	0.4	1400	1400
20	6.5	-0.1	1750	1700
20	7.0	-0.6	2600	2700
20	7.5	-1.1	Not upto max. measurable.	

\* A  $20M\Omega$  resistance was connected in series with the high voltage electrode.

TABLE -19 - Minimum voltage  $V_c$  of the applied field giving rise to instantaneous nucleation at different degrees of superheat  
 $\Delta p = P_S - P_L$

n - Pontane

Boiling point = 36.1°      T = 110°C  
 $T_c$  = 196.6°C       $P_S$  = 7.2 ats.  
 $P_c$  = 33.8 ats.

Pressure in the Chamber ats.		$\Delta p = P_S - P_L$	$V_c$ Volts	
Initial higher P	Final lower $P_L$	ats.	D.C.	-
20	1.0	6.2	450	-
20	1.5	5.7	500	-
20	2.0	5.2	500	-
20	2.5	4.7	550	-
20	3.0	4.2	600	-
20	3.5	3.7	650	-
20	4.0	3.2	700	-
20	4.5	2.7	750	-
20	5.0	2.2	800	-
20	5.5	1.7	900	-
20	6.0	1.2	1000	-
20	6.5	0.7	1200	-
20	7.0	0.2	1450	-
20	7.5	-0.3	2250	-
20	8.0	-0.8	Not upto max. measurable.	
20	8.5	-1.3		

TABLE -20-Minimum voltage  $V_c$  of the applied field giving rise to instantaneous nucleation at different degrees of superheat  $\Delta p = P_S - P_L$ .

n - Pentene

Boiling point =  $36.1^\circ\text{C}$   
 $T_c = 196.6^\circ\text{C}$   
 $P_c = 33.8 \text{ ats.}$

$T = 115^\circ\text{C}$   
 $P_S = 8.0 \text{ ats.}$

Pressure in the Chamber ats.			$\Delta p = P_S - P_L$ ats.	$V_c$ Volts
Initial P	higher P <sub>L</sub>	Final lower P <sub>L</sub>		D.C.
20	1.0		7.0	400
20	1.5		6.5	420
20	2.0		6.0	450
20	2.5		5.5	450
20	3.0		5.0	500
20	3.5		4.5	525
20	4.0		4.0	600
20	4.5		3.5	620
20	5.0		3.0	700
20	5.5		2.5	750
20	6.0		2.0	800
20	6.5		1.5	900
20	7.0		1.0	1100
20	7.5		0.5	1300
20	8.0		0.0	1600
20	8.5		- 0.5	2100
20	9.0		- 1.0	Not upto max. measurable.

TABLE -21 - Minimum voltage  $V_0$  of the applied field giving rise to instantaneous nucleation at different degrees of superheat  $\Delta p = P_S - P_L$ .

n - Pontane

Boiling point =  $36.1^\circ\text{C}$

$T = 120^\circ\text{C}$

$T_c = 196.6^\circ\text{C}$

$P_S = 8.9 \text{ ats.}$

$P_c = 33.8 \text{ ats.}$

Pressure in the Chamber ats.			$\Delta p = P_S - P_L$	$V_0$ Volts
Initial P	higher P <sub>L</sub>	Final lower P <sub>L</sub>	ats.	D.C.
22	1.0		7.9	350
22	1.5		7.4	350
22	2.0		6.9	370
22	2.5		6.4	370
22	3.0		5.9	400
22	3.5		5.4	425
22	4.0		4.9	450
22	4.5		4.4	500
22	5.0		3.9	550
22	5.5		3.4	600
22	6.0		2.9	650
22	6.5		2.4	700
22	7.0		1.9	800
22	7.5		1.4	900
22	8.0		0.9	1000
22	8.5		0.4	1250
22	9.0		-0.1	1550
22	9.5		-0.6	2200
22	10.0		-1.1	3900
22	10.5		-1.6	Not upto maximum measurable.

TABLE -22 - Minimum voltage  $V_c$  of the applied field giving rise to instantaneous nucleation at different degrees of superheat  $\Delta p = P_S - P_L$ .

n = Pentane

Boiling point =  $36.1^\circ\text{C}$        $T = 125^\circ\text{C}$   
 $T_c = 196.6^\circ\text{C}$        $P_S = 9.8 \text{ ats.}$   
 $P_c = 33.8 \text{ ats.}$

Pressure in the Chamber ats.			$\Delta p = P_S - P_L$	$V_c$ Volts
Initial higher P	Final lower P <sub>L</sub>		ats.	D.C.
20	1.0		8.8	300
20	1.5		8.3	300
20	2.0		7.8	320
20	2.5		7.3	320
20	3.0		6.8	350
20	3.5		6.3	370
20	4.0		5.8	400
20	4.5		5.3	420
20	5.0		4.8	450
20	5.5		4.3	470
20	6.0		3.8	500
20	6.5		3.3	580
20	7.0		2.8	630
20	7.5		2.3	700
20	8.0		1.8	800
20	8.5		1.3	900
20	9.0		0.8	1025
20	9.5		0.3	1200
20	10.0		-0.2	1500
20	10.5		-0.7	2100
20	11.0		-1.2	3000
20	11.5		-1.7	Not upto maximum measurable.

TABLE -23- Minimum voltage  $V_c$  of the applied field giving rise to instantaneous nucleation at different degrees of superheat  $\Delta p = P_g - P_L$ .

n - Pentane

Boiling point = 36.1°C

T = 130°C

$T_c = 196.6^\circ\text{C}$

$P_g = 10.9$  ats.

$P_c = 33.8$  ats.

Pressure in the Chamber ats.		$\Delta p = P_g - P_L$	$V_c$ Volts
Initial higher P	Final lower P <sub>L</sub>	ats.	D.C.
20	1.0	9.9	250
20	1.5	9.4	250
20	2.0	8.9	250
20	2.5	8.4	250
20	3.0	7.9	275
20	3.5	7.4	275
20	4.0	6.9	300
20	4.5	6.4	300
20	5.0	5.9	350
20	5.5	5.4	350
20	6.0	4.9	400
20	6.5	4.4	450
20	7.0	3.9	500
20	7.5	3.4	550
20	8.0	2.9	600
20	8.5	2.4	650
20	9.0	1.9	700
20	9.5	1.4	800
20	10.0	0.9	900
20	10.5	0.4	1050
20	11.0	-0.1	1250
20	11.5	-0.6	1900
20	12.0	-1.1	2900
20	12.5	-1.6	Not upto maximum measurable.

TABLE-24- Minimum voltage  $V_0$  of the applied field giving rise to instantaneous nucleation at different degrees of superheat  $\Delta p = P_S - P_L$ .

n - Pentane

Boiling point = 36.1°C

T = 135°C

$T_c$  = 196.6°C

$P_S$  = 12.0 ats.

$P_c$  = 33.8 ats.

Pressure in the Chamber ats.		$\Delta p = P_S - P_L$ ats.	$V_0$ Volts. D.C.
Initial higher P	Final lower $P_L$		
20	1.0	11.0	200
20	1.5	10.5	200
20	2.0	10.0	200
20	2.5	9.5	200
20	3.0	9.0	200
20	3.5	8.5	220
20	4.0	8.0	250
20	4.5	7.5	250
20	5.0	7.0	280
20	5.5	6.5	300
20	6.0	6.0	330
20	6.5	5.5	350
20	7.0	5.0	350
20	7.5	4.5	400
20	8.0	4.0	450
20	8.5	3.5	500
20	9.0	3.0	550
20	9.5	2.5	600
20	10.0	2.0	700
20	10.5	1.5	800
20	11.0	1.0	900
20	11.5	0.5	1100
20	12.0	0.0	1300
20	12.5	-0.5	1750
20	13.0	-1.0	2500
20	13.5	-1.5	Not upto maximum measurable.

TABLE - 25- Minimum voltage  $V_c$  of the applied field giving rise to instantaneous nucleation at different degrees of superheat ( $P_S - P_L$ ).

iso-Pentane

Boiling point =  $27.8^\circ\text{C}$   
 $T_c = 187.8^\circ\text{C}$   
 $P_c = 30.3 \text{ ats.}$

$T = 70^\circ\text{C}$   
 $P_S = 3.5 \text{ ats.}$

Pressure in the Chamber ats.		$\Delta P = P_S - P_L$ ats.	$V_c$ Volts	
Initial higher P	Final lower $P_L$		D.C. +ve	D.C. -ve
20	1.0	2.5	900	900
20	1.5	2.0	950	950
20	2.0	1.5	1000	1050
20	2.5	1.0	1125	1150
20	3.0	0.5	1200	1200
20	3.5	0.0	1350	1300
20	4.0	-0.5	1600	1650
20	4.5	-1.0	2500	2400
20	5.0	-1.5	Not upto max. measurable.	Not upto max. measurable.



TABLE-26-Minimum voltage  $V_c$  of the applied field giving rise to instantaneous nucleation at different degrees of superheat ( $P_S - P_L$ ).

iso-Pentane

Boiling point = 27.8°C                       $T = 75^\circ\text{C}$   
 $T_c = 187.8^\circ\text{C}$                        $P_S = 4.0 \text{ ats.}$   
 $P_c = 30.3 \text{ ats.}$

Pressure in the Chamber ats.			$\Delta p = P_S - P_L$		$V_c$ Volts.	
Initial P	higher Final	lower $P_L$	ats.		D.C. +ve	D.C. -ve
20		1.0	3.0		800	800
20		1.5	2.5		850	850
20		2.0	2.0		900	880
20		2.5	1.5		970	950
20		3.0	1.0		1070	1075
20		3.5	0.5		1200	1200
20		4.0	0.0		1350	1350
20		4.5	- 0.5		1550	1600
20		5.0	- 1.0		1900	1950
20		5.5	- 1.5	Not upto max. measurable	Not upto max. measurable.	Not upto max. measurable.

TABLE-27 - Minimum voltage  $V_c$  of the applied field giving rise to instantaneous nucleation at different degrees of superheat ( $P_g - P_L$ ).

iso-Pentane

Boiling point =  $27.8^\circ\text{C}$        $T = 80^\circ\text{C}$   
 $T_c = 187.8^\circ\text{C}$        $P_g = 4.5 \text{ ats.}$   
 $P_c = 30.3 \text{ ats.}$

Pressure in the Chamber ats.		$\Delta p = P_g - P_L$ ats.	$V_c$ Volts.	
Initial higher $P$	Final lower $P_L$		D.C.	A.C. (50 HZ)
20	1.0	3.5	700	800
20	1.5	3.0	750	900
20	2.0	2.5	800	1000
20	2.5	2.0	850	1125
20	3.0	1.5	900	1200
20	3.5	1.0	950	1350
20	4.0	0.5	1100	1600
20	4.5	0.0	1200	2500
20	5.0	-0.5	1350	Not upto max. measurable.
20	5.5	-1.0	1850	
20	6.0	-1.5	2600	
20	6.5	-2.0	Not upto max. measurable.	

TABLE-28 - Minimum voltage  $V_c$  of the applied field giving rise to instantaneous nucleation at different degrees of superheat ( $P_S - P_L$ ).

iso-Pentane

Boiling point =  $27.8^\circ\text{C}$   
 $T_c = 187.8^\circ\text{C}$   
 $P_c = 30.3 \text{ ats.}$

$T = 85^\circ\text{C}$   
 $P_S = 5.0 \text{ ats.}$

Pressure in the Chamber ats.		$\Delta p = P_S - P_L$	$V_c$
Initial higher P	Final lower P <sub>L</sub>	ats.	D.C. ats.
20	1.0	4.0	600
20	1.5	3.5	625
20	2.0	3.0	700
20	2.5	2.5	750
20	3.0	2.0	800
20	3.5	1.5	875
20	4.0	1.0	950
20	4.5	0.5	1050
20	5.0	0.0	1150
20	5.5	- 0.5	1300
20	6.0	- 1.0	1500
20	6.5	- 1.5	1800
20	7.0	- 2.0	2750
20	7.5	- 2.5	Not upto max. measurable.

TABLE -29- Minimum voltage  $V_c$  of the applied field giving rise to instantaneous nucleation at different degrees of superheat ( $P_g - P_L$ ).

iso-Pentane

Boiling point =  $27.8^\circ\text{C}$        $T = 90^\circ\text{C}$   
 $T_g = 187.8^\circ\text{C}$        $P_g = 5.6 \text{ ats.}$   
 $P_e = 30.3 \text{ ats.}$

Pressure in the Chamber ats.		$\Delta p = P_g - P_L$	$V_c$ Volts.
Initial higher P	Final lower P <sub>L</sub>	ats.	D.C.
20	1.0	4.6	550
20	1.5	4.1	600
20	2.0	3.6	620
20	2.5	3.1	650
20	3.0	2.6	700
20	3.5	2.1	750
20	4.0	1.6	800
20	4.5	1.1	850
20	5.0	0.6	900
20	5.5	0.1	1000
20	6.0	- 0.4	1100
20	6.5	- 0.9	1300
20	7.0	- 1.4	1500
20	7.5	- 1.9	2300
20	8.0	- 2.4	Not upto max. measurable.

TABLE-30- Minimum voltage  $V_c$  of the applied field giving rise to instantaneous nucleation at different degrees of superheat ( $P_S - P_L$ ).

iso-Pentane

Boiling point =  $27.8^\circ\text{C}$

$T = 95^\circ\text{C}$

$T_c = 187.8^\circ\text{C}$

$P_S = 6.2 \text{ ats.}$

$P_c = 30.3 \text{ ats.}$

Pressure in the Chamber ats.		$\Delta p = P_S - P_L$	$V_c$ Volts
Initial higher $P$	Final lower $P_L$	ats.	D.C.
20	1.0	5.2	500
20	1.5	4.7	500
20	2.0	4.2	550
20	2.5	3.7	570
20	3.0	3.2	600
20	3.5	2.7	650
20	4.0	2.2	650
20	4.5	1.7	750
20	5.0	1.2	800
20	5.5	0.7	850
20	6.0	0.2	920
20	6.5	0.3	1025
20	7.0	0.8	1200
20	7.5	1.3	1350
20	8.0	1.8	1500
20	8.5	2.3	2050
20	9.0	2.8	Not upto max. measurable.

TABLE-31- Minimum voltage  $V_c$  of the applied field giving rise to instantaneous nucleation at different degrees of superheat ( $P_S - P_L$ ).

1a0-Pentane

Boiling point =  $27.8^\circ\text{C}$   
 $T_c = 187.8^\circ\text{C}$   
 $P_c = 30.3$  ats.

$T = 100^\circ\text{C}$   
 $P_S = 7.0$  ats.

Pressure in the Chamber ats.		$\Delta p = P_S - P_L$	$V_c$ Volts.
Initial P	Final P <sub>L</sub>	ats.	D.C.
20	1.0	6.0	450
20	1.5	5.5	470
20	2.0	5.0	470
20	2.5	4.5	490
20	3.0	4.0	510
20	3.5	3.5	530
20	4.0	3.0	550
20	4.5	2.5	600
20	5.0	2.0	650
20	5.5	1.5	700
20	6.0	1.0	750
20	6.5	0.5	800
20	7.0	0.0	900
20	7.5	-0.5	1000
20	8.0	-1.0	1100
20	8.5	-1.5	1350
20	9.0	-2.0	1650
20	9.5	-2.5	2300
20	10.0	-3.0	4000
20	10.5	-3.5	Not upto max. measurable.

TABLE-32- Minimum voltage  $V_c$  of the applied field giving rise to instantaneous nucleation at different degrees of superheat ( $P_g - P_L$ ).

iso-Pentane

Boiling point =  $27.8^\circ\text{C}$

$T = 105^\circ\text{C}$

$T_c = 187.8^\circ\text{C}$

$P_g = 7.8 \text{ ats.}$

$P_c = 30.3 \text{ ats.}$

Pressure in the Chamber ats.		$\Delta p = P_g - P_L$	$V_c$ Volts
Initial higher P	Final lower P <sub>L</sub>	ats.	D.C.
20	1.0	6.8	350
20	1.5	6.3	370
20	2.0	5.8	400
20	2.5	5.3	420
20	3.0	4.8	450
20	3.5	4.3	470
20	4.0	3.8	500
20	4.5	3.3	550
20	5.0	2.8	550
20	5.5	2.3	600
20	6.0	1.8	650
20	6.5	1.3	700
20	7.0	0.8	750
20	7.5	0.3	820
20	8.0	-0.2	900
20	8.5	-0.7	1050
20	9.0	-1.2	1250
20	9.5	-1.7	1400
20	10.0	-2.2	1700
20	10.5	-2.7	2500
20	11.0	-3.2	Not upto max. measurable.

TABLE -33- Minimum voltage  $V_c$  of the applied field giving rise to instantaneous nucleation at different degrees of superheat ( $P_S - P_L$ ).

iso-Pentane

Boiling point = 27.8°C      T = 110°C  
 $T_e$  = 187.8°C       $P_S$  = 8.6 ats.  
 $P_c$  = 30.3 ats.

Pressure in the Chamber ats.			$\Delta p = P_S - P_L$		$V_c$ Volts.	
Initial P	higher Final $P_L$	lower $P_L$	ats.		D.C.	D.C.*
20	1.0		7.6		320	300
20	1.5		7.1		320	320
20	2.0		6.6		340	340
20	2.5		6.1		340	340
20	3.0		5.6		370	360
20	3.5		5.1		370	360
20	4.0		4.6		400	400
20	4.5		4.1		420	400
20	5.0		3.6		450	450
20	5.5		3.1		500	500
20	6.0		2.6		550	550
20	6.5		2.1		600	600
20	7.0		1.6		650	650
20	7.5		1.1		700	700
20	8.0		0.6		750	750
20	8.5		0.1		800	800
20	9.0		- 0.4		900	900
20	9.5		- 0.9		1000	1000
20	10.0		- 1.4		1150	1150
20	10.5		- 1.9		1350	1300
20	11.0		- 2.4		2000	2000
20	11.5		- 2.9		3000	3000
20	12.0		- 3.4		Not upto max. Not upto max. measurable. measurable.	

\* A 20 M $\Omega$  resistance was connected in series with the high voltage electrode.



TABLE -34- Minimum voltage  $V_c$  of the applied field giving rise to instantaneous nucleation at different degrees of superheat ( $P_S - P_L$ ).

iso-Pentane

Boiling point =  $27.8^\circ\text{C}$   
 $T_c = 187.8^\circ\text{C}$   
 $P_c = 30.3 \text{ ats.}$

$T = 115^\circ\text{C}$   
 $P_S = 9.6 \text{ ats.}$

Pressure in the Chamber ats.		$\Delta p = P_S - P_L$	$V_c$ Volts.
Initial higher P	Final lower P <sub>L</sub>	ats.	D.C.
20	1.0	8.6	250
20	1.5	8.1	270
20	2.0	7.6	270
20	2.5	7.1	300
20	3.0	6.6	300
20	3.5	6.1	300
20	4.0	5.6	320
20	4.5	5.1	350
20	5.0	4.6	400
20	5.5	4.1	400
20	6.0	3.6	450
20	6.5	3.1	470
20	7.0	2.6	520
20	7.5	2.1	550
20	8.0	1.6	620
20	8.5	1.1	680
20	9.0	0.6	800
20	9.5	0.1	900
20	10.0	- 0.4	1000
20	10.5	- 0.9	1100
20	11.0	- 1.4	1350
20	11.5	- 1.9	2000
20	12.0	- 2.4	2600
20	12.5	- 2.9	Not upto max. measurable.

TABLE 35 - Minimum voltage ( $V_c$ ) of the applied field giving rise to instantaneous nucleation at different degrees of superheat of liquid (T-B.P.) and atmospheric pressure.

n - Hexane

Boiling point =  $68.7^{\circ}\text{C}$       Nature of applied electric field- D.C.  
 $T_c = 234.7^{\circ}\text{C}$   
 $P_c = 30.4 \text{ ats.}$

Temperature $T$ $^{\circ}\text{C}$	Saturated vapour pressure $P_s$ ats.	Degree of superheat $\Delta T (= T - \text{B.P.})$ $^{\circ}\text{C}$	$V_c$ Volts.
100	2.4	31.3	1300
105	2.6	36.3	1200
110	3.0	41.3	1100
115	3.5	46.3	1000
120	4.0	51.3	900
125	4.5	56.3	800
130	5.0	61.3	750
135	5.4	66.3	650
150	7.4	81.3	500
155	8.7	86.3	425
160	9.0	91.3	375
165	9.6	96.3	300
170	10.7	101.3	300
180	12.7	111.3	250

TABLE 36 - Minimum voltage  $V_c$  of the applied field giving rise to instantaneous nucleation at different degrees of superheat of the liquid (T-B.P.) and atmospheric pressure.

n - Pentane

Boiling point =  $36.1^\circ$  Nature of applied electric field = D.C.

$T_o = 196.6^\circ\text{C}$

$P_o = 33.8$  ats.

Temperature $T$ $^\circ\text{C}$	Saturated Vapour pressure $P_s$ ats.	Degree of superheat $\Delta T = (T - T_o)$ $^\circ\text{C}$	$V_c$ Volts.
90	4.6	53.9	800
95	5.2	58.9	700
100	5.8	63.9	600
105	6.4	68.9	500
110	7.2	73.9	450
115	8.0	78.9	400
120	8.9	83.9	350
125	9.8	88.9	300
130	10.9	93.9	250
135	12.0	98.9	200

TABLE 37- Minimum voltage  $V_c$  of the applied field giving rise to instantaneous nucleation at different degrees of superheat of liquid (T- B.P.) and atmospheric pressure.

Iso-Pentane

Boiling point =  $27.8^{\circ}\text{C}$       Nature of the applied electric  
 $T_c = 187.8^{\circ}\text{C}$                       field = D.C.  
 $P_c = 30.3$  atms.

Temperature T $^{\circ}\text{C}$	Saturated vapour pressure P <sub>s</sub> atms.	Degree of superheat $\Delta T = (T - \text{B.P.})$ $^{\circ}\text{C}$	$V_c$ Volts
70	3.5	42.2	900
75	4.0	47.2	800
80	4.5	52.2	700
85	5.0	57.2	600
90	5.6	62.2	550
95	6.2	67.2	500
100	7.0	72.2	450
105	7.8	77.2	350
110	8.6	82.2	320
115	9.6	87.2	250

DISCUSSIONS AND CONCLUSIONS

The results of the present experiment, as given in tables 1-37, may be summarised as follows :-

- (1) In the test liquid, nucleation is initiated at the glass-liquid interface near the tin oxide boundary when the system is subjected to an external electric field of sufficient strength.
- (2) The effect is observed with both alternating (50HZ) and unidirectional (+ve and -ve) fields.
- (3) It is evident from the graphs (Figs. 4.1 and 4.2) that the slope of the  $V_c$ -T and  $V_c$ - $\Delta p$  curves, in almost all the cases decrease with the increase in the superheat of liquids. This indicates an appreciable change in the rate of fall of the critical value of the applied voltage,  $V_c$ , with the rise of the degree of superheat.
- (4) The general pattern for the  $V_c$  -  $\Delta T$  and  $V_c$  -  $\Delta p$  curves is similar.
- (5) The general pattern of the critical voltage versus the degree of superheat curves is similar for both alternating and unidirectional fields as shown in Fig : 4.3.

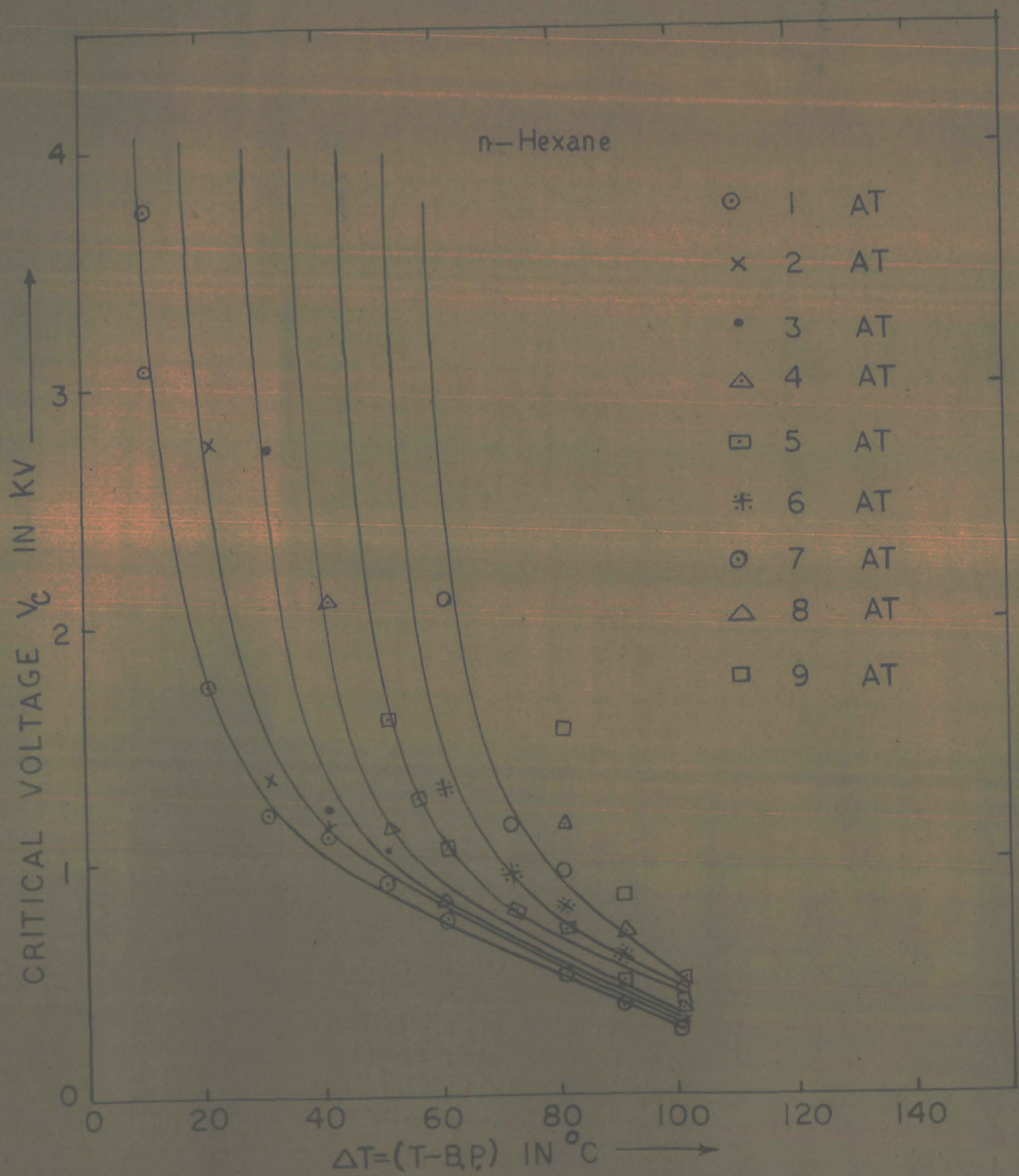


FIG. 4.1(a)

VARIATION OF THE CRITICAL VOLTAGE WITH THE DEGREE OF SUPERHEAT  $\Delta T$  AT DIFFERENT PRESSURES.

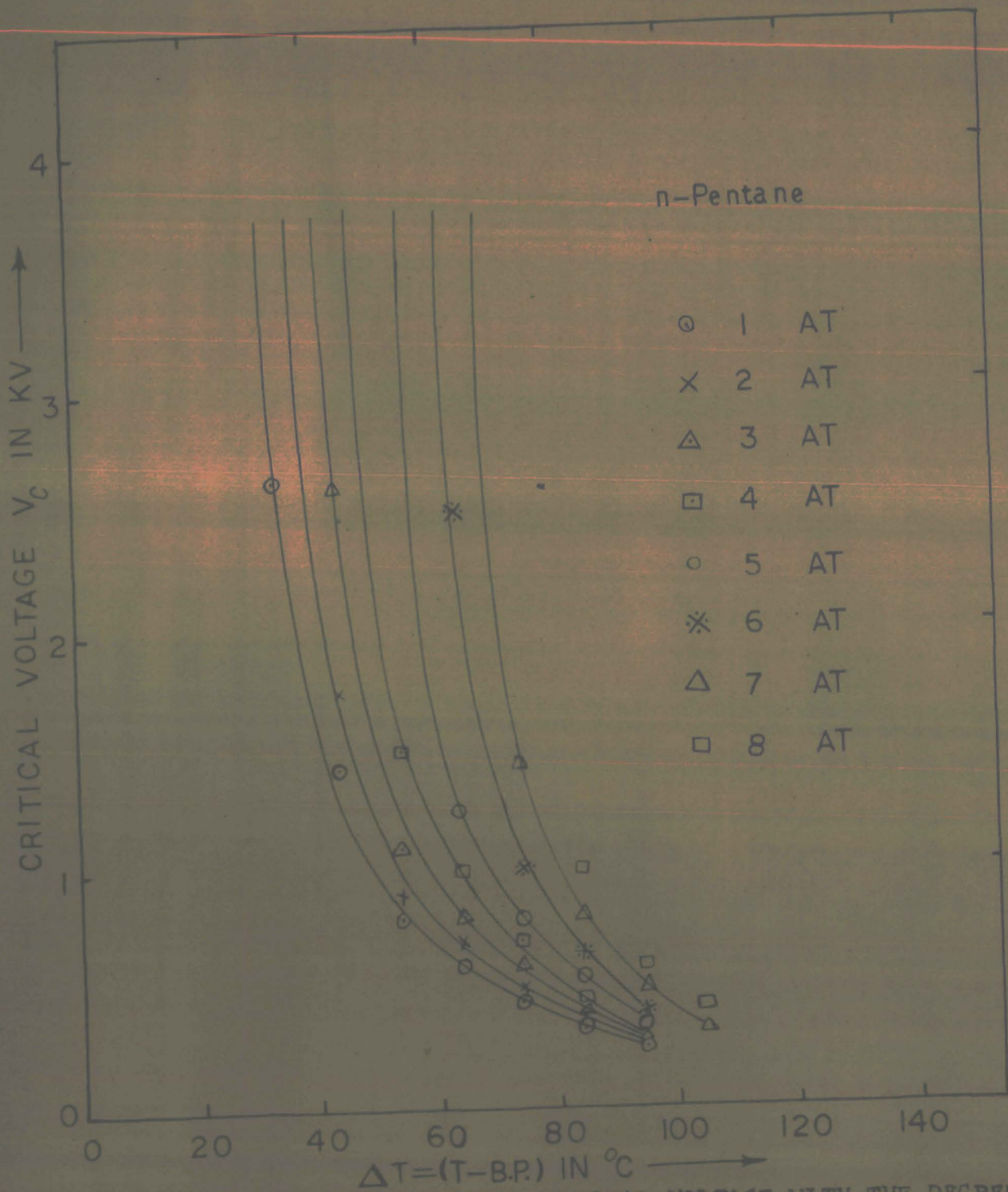


FIG. 4.1(b) VARIATION OF THE CRITICAL VOLTAGE WITH THE DEGREE OF SUPERHEAT  $\Delta T$  AT DIFFERENT PRESSURES.



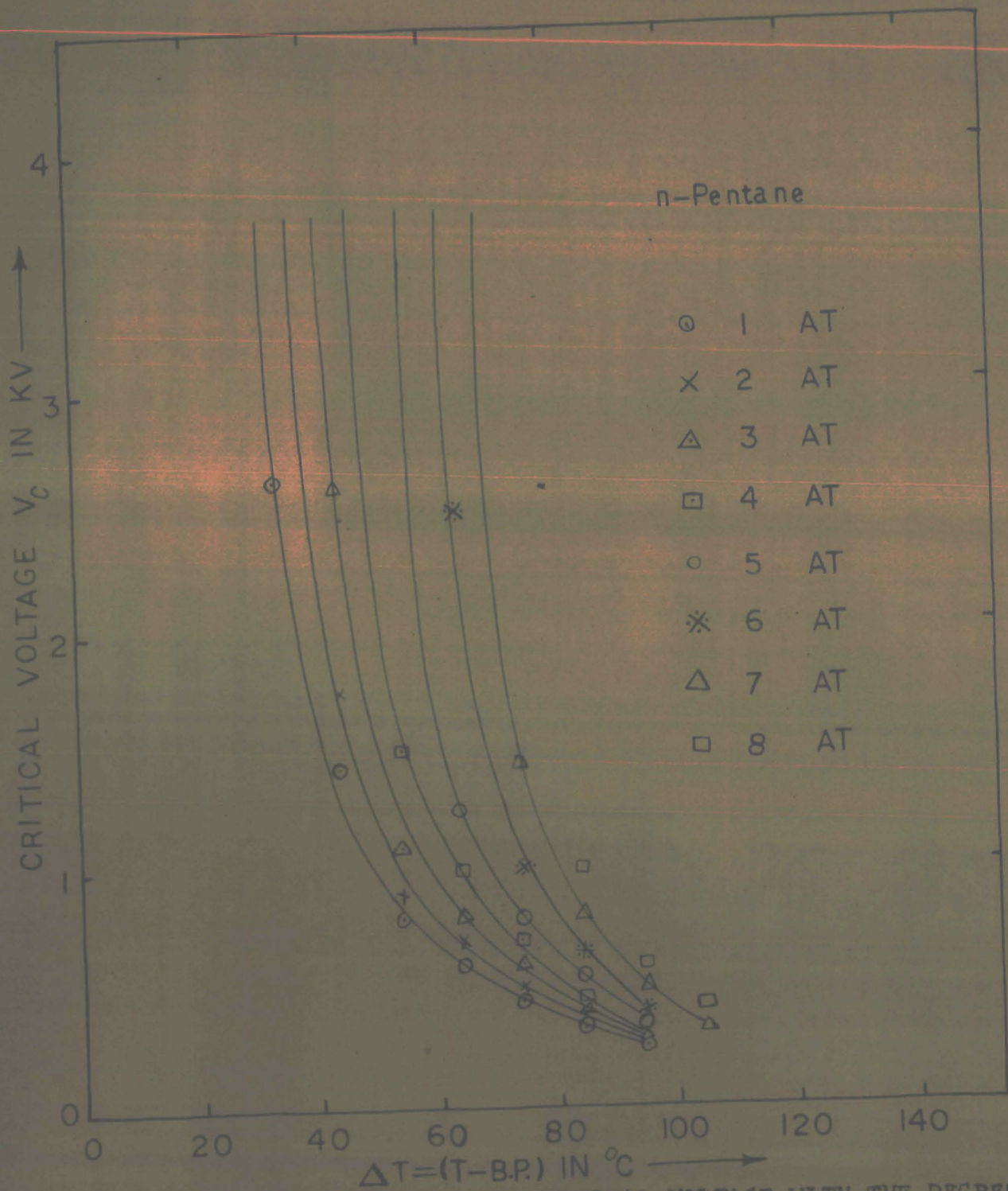


FIG. 4.1(b) VARIATION OF THE CRITICAL VOLTAGE WITH THE DEGREE OF SUPERHEAT  $\Delta T$  AT DIFFERENT PRESSURES.

VARIATION OF THE CRITICAL VOLTAGE WITH THE DEGREE OF SUPERHEAT  $\Delta P$  AT DIFFERENT TEMPERATURES.

$\circ$  — 100°C  
 $\times$  — 110°C  
 $\Delta$  — 120°C  
 $\square$  — 130°C  
 $\times$  — 150°C  
 $\circ$  — 160°C  
 $\Delta$  — 170°C  
 $\square$  — 180°C

n—Hexane

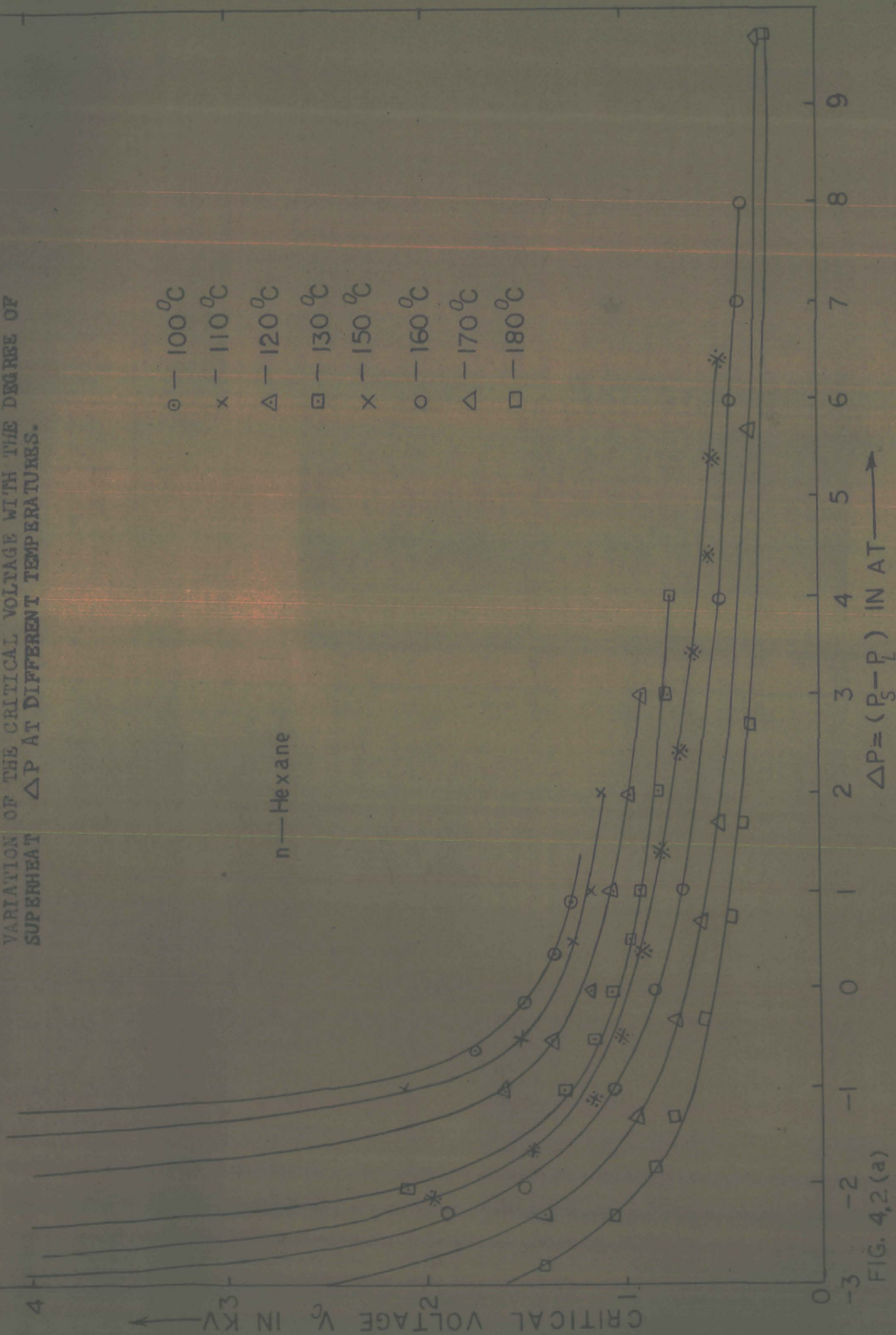


FIG. 4.2 (a)



VARIATION OF THE CRITICAL VOLTAGE WITH THE DEGREE OF  
 SUPERHEAT  $\Delta P$  AT DIFFERENT TEMPERATURES.

○ 90 °C  
 × 100 °C  
 ● 110 °C  
 △ 120 °C  
 □ 130 °C

n-Pentane

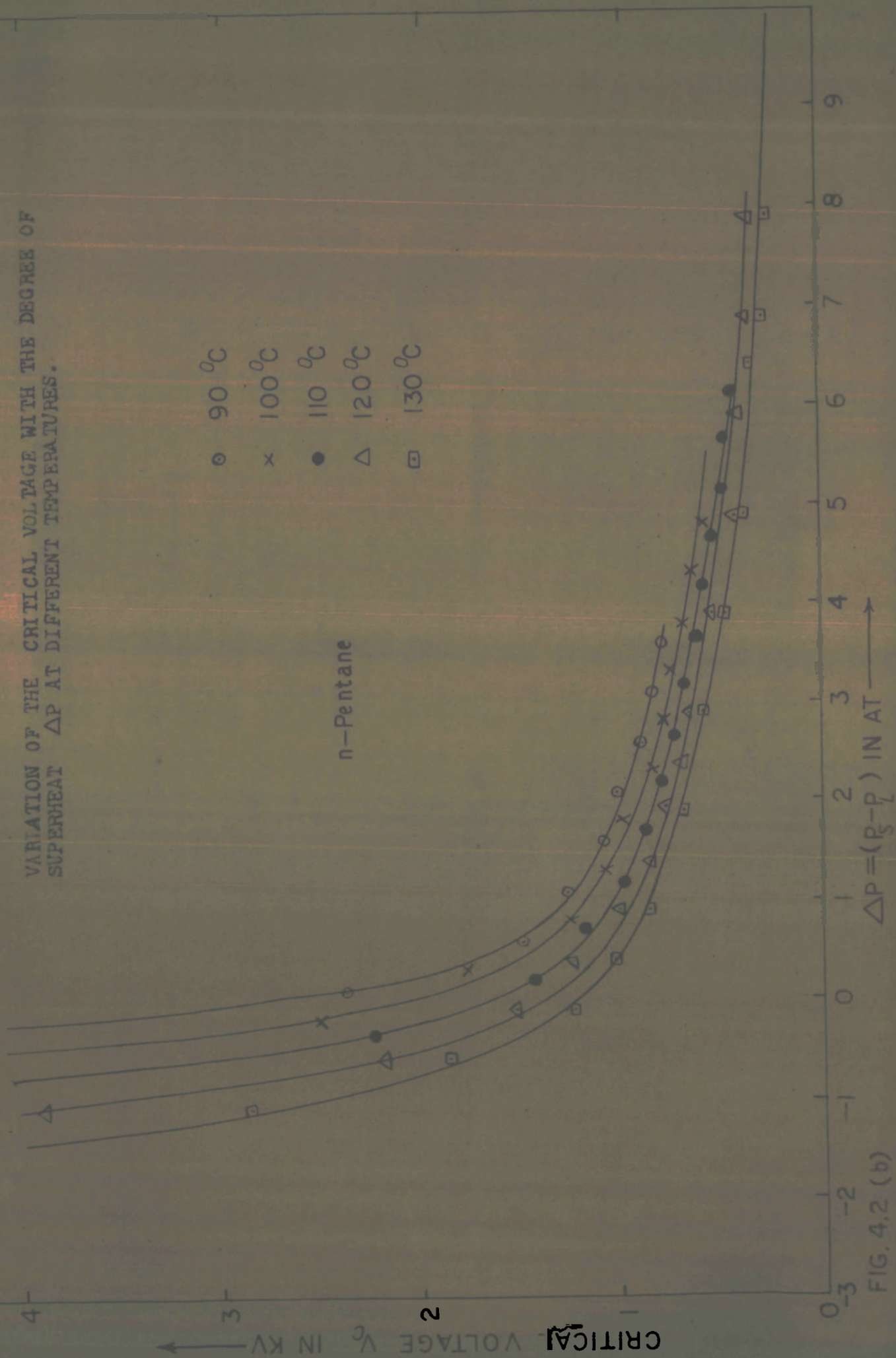


FIG. 4.2 (b)

VARIAION OF THE CRITICAL VOLTAGE WITH THE DEGREE OF  
SUPERHEAT  $\Delta P$  AT DIFFERENT TEMPERATURES.

ISO-PENTANE

○ - 70 °C  
x - 80 °C  
△ - 90 °C  
□ - 100 °C  
● - 200 °C

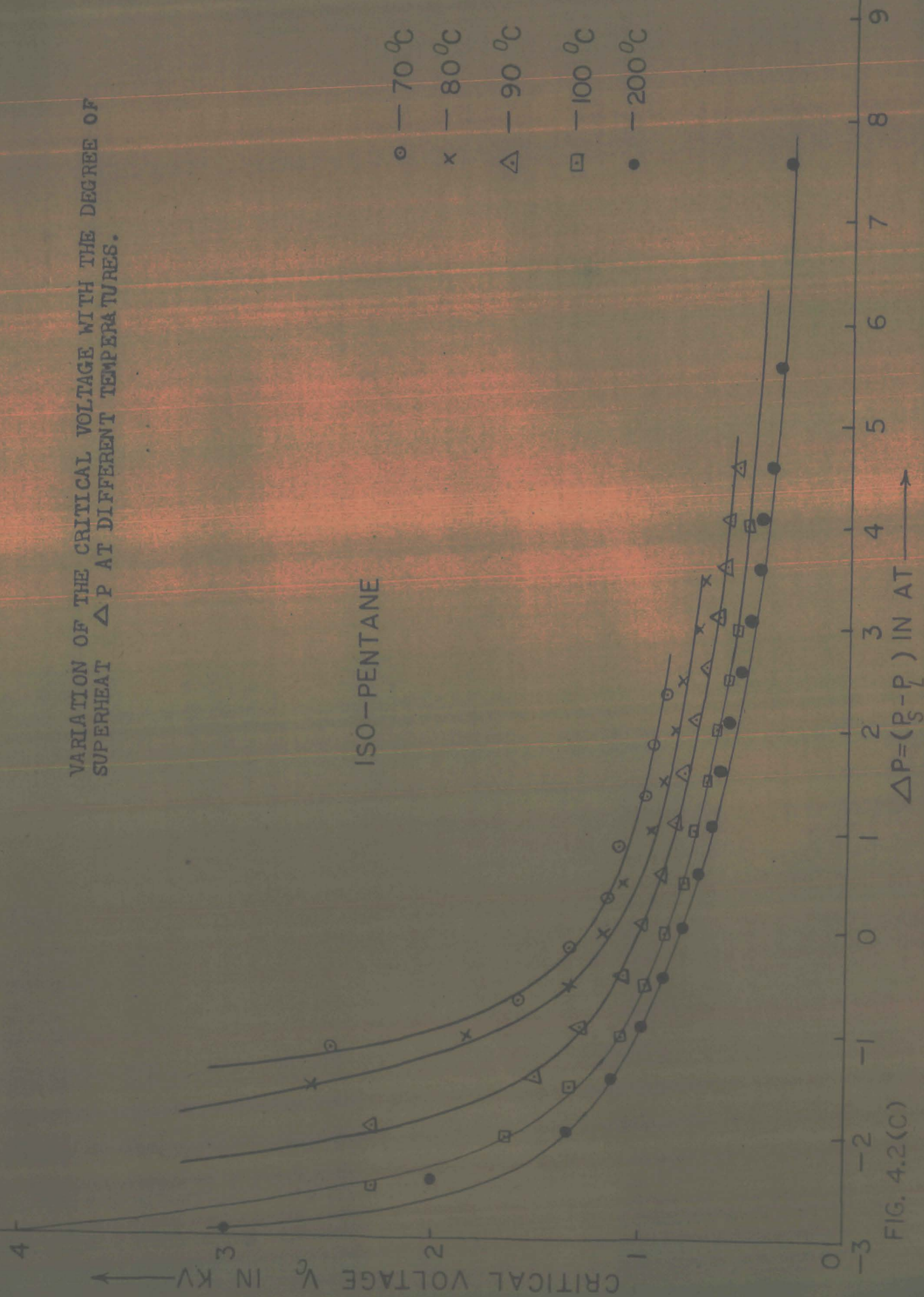


FIG. 4.2(C)



FIG. 4.3

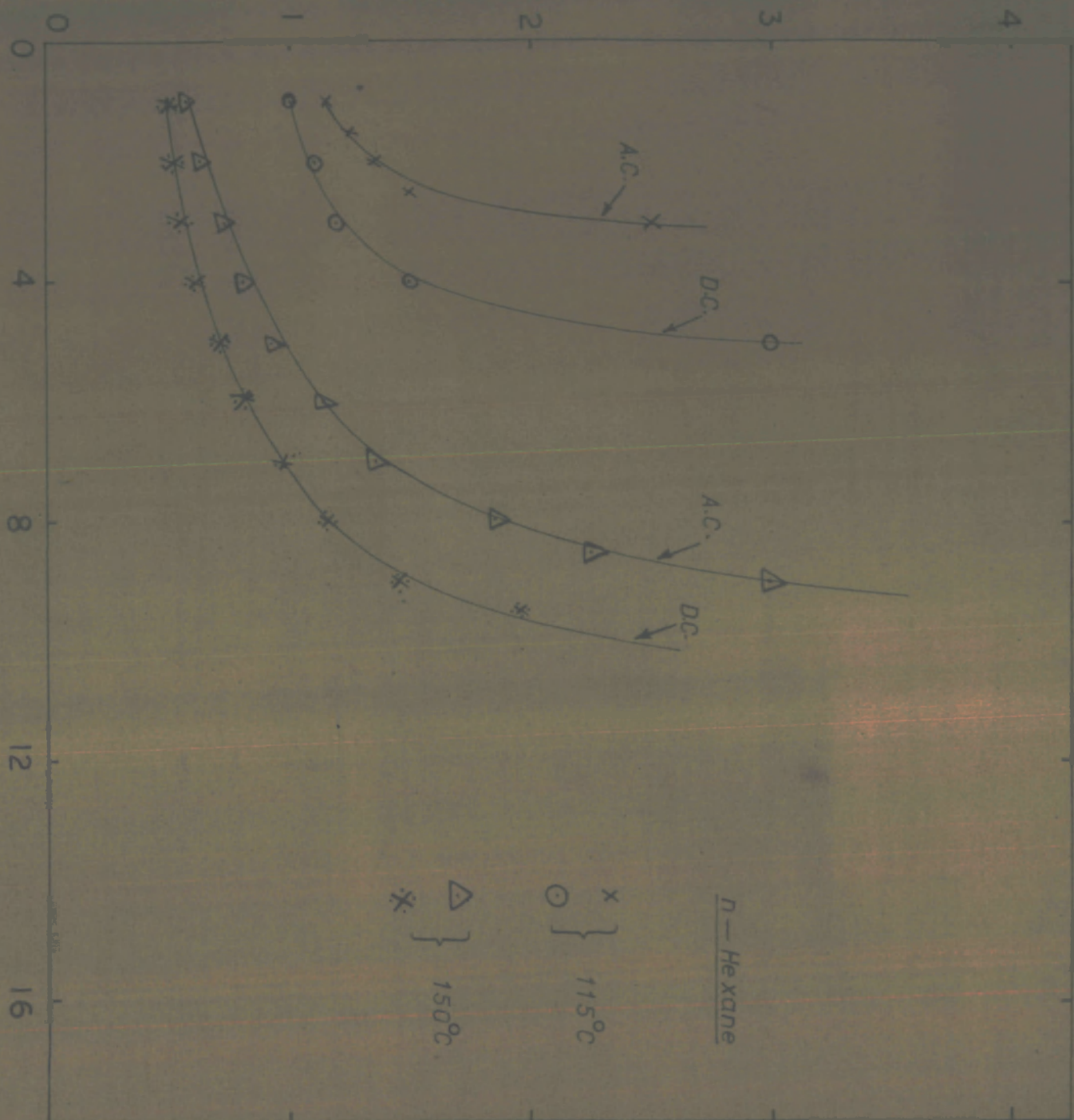
PRESSURE  $P_c$  IN ATS

IN ATS

→

CRITICAL VOLTAGE  $V_c$  IN KV

→



n-He xane

$\times$  } 115°C

$\circ$  }

$\Delta$  } 150°C

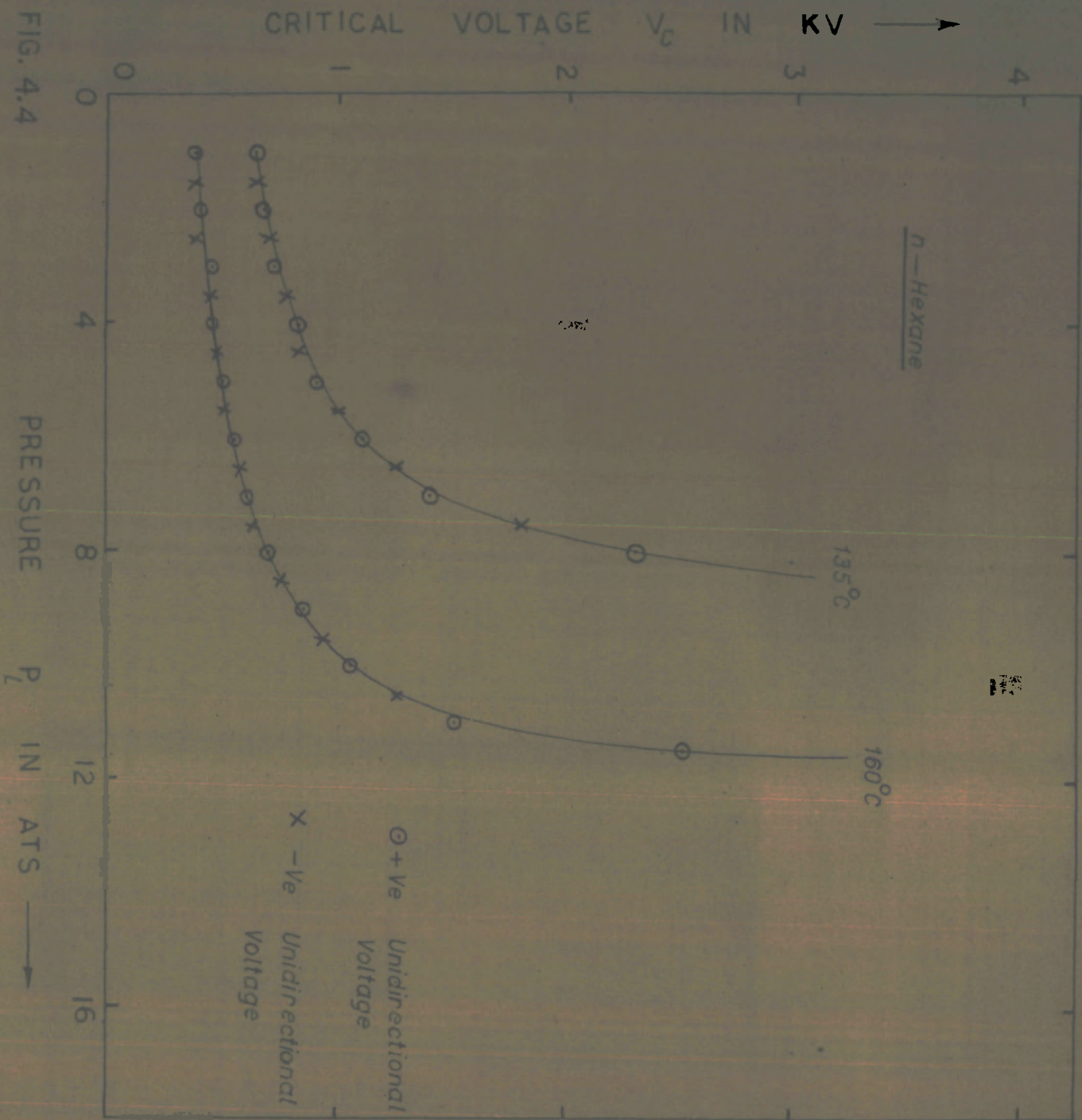
$*$  }

- (6) The change of polarity of the high voltage electrode in the case of the applied unidirectional field does not quantitatively change the results (Fig.4.4).
- (7) The critical voltage requirement for inducing nucleation in a superheated liquid at a given temperature and pressure is higher in case of the alternating as compared to the unidirectional fields.
- (8) In order to change the time constant of the application of the electric field, high resistances of the order of few megohms were connected in series with the high voltage terminal of the power supply and the high voltage electrode. This does not alter the results as shown in Fig. 4.5 for n-Hexane.

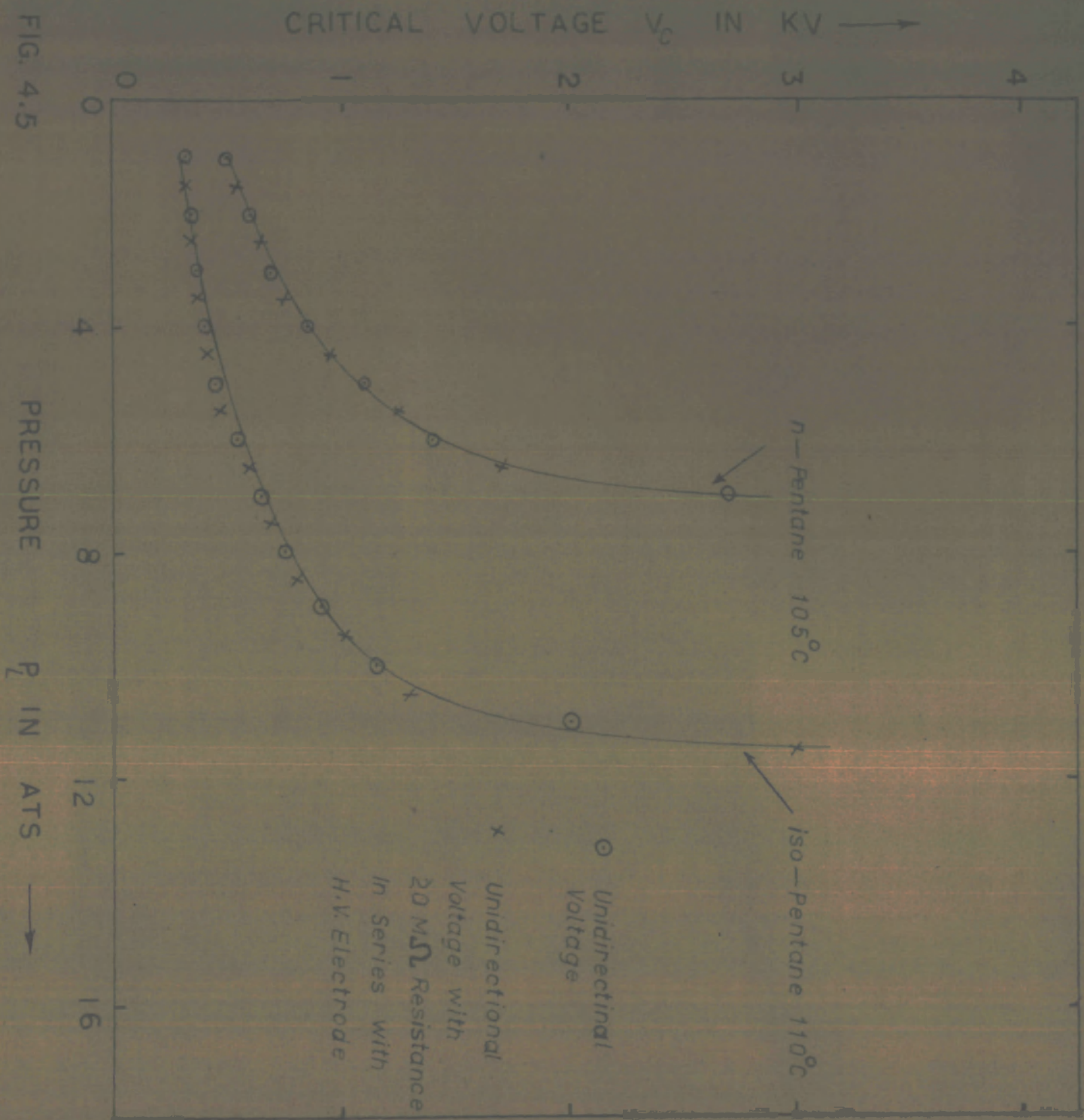
All the sets of observations taken are consistent among themselves and are reproducible. The change in the slope of  $V_c$  versus  $\Delta P$ (or $\Delta T$ ) curves qualitatively agree with the theory proposed by Glaser<sup>(1)</sup> for charge induced nucleation. With the rise in the degree of superheat, the critical voltage required for nucleation decreases in a way predicted by Glaser's equation,<sup>(1)</sup>

$$P_g - P_L = \frac{2\sigma(T)}{\gamma} - \frac{(n_g)^2}{8\pi\epsilon(T)\gamma^4} \quad \dots\dots\dots (5.1)$$

FIG. 4.4









where  $n$  = no. of charges on the bubble of radius  $r$ ,  $e$  = the charge on each ion,  $\sigma(T)$  = the surface tension of the liquid at temperature  $T$ ,  $\epsilon(T)$  = the dielectric constant of the liquid as a function of temperature.

This equation correlates the maximum degree of superheat attainable with the concentration of charges at the interface of a nuclear bubble. The above equation may be interpreted to mean that a subcritical bubble, subjected to an electric field, may grow spontaneously either due to change in surface tension or by fulfilling the condition of criticality of size under the applied field.

### 5.1. The Nature of Interface.

In the present experimental setup, the external electric field is applied through the conducting tin oxide layer coated on the glass wall in contact with the experimental liquid. The tin oxide layer is very thin and has got a sharp boundary in the superheated region of the liquid. In spite of this the thin tin oxide layer is unlikely to produce any inhomogeneity on the surface of the glass which may act as nucleation center. The main reason for the formation of bubbles at the tin oxide boundary seems to be due to the direct effect of the field. In the present experimental setup, the tin oxide coated



therefore plays the dominant role in inducing nucleation. The calculation of this field near the tin oxide boundary is a difficult task because of the geometry. The non-uniformity of the field near the boundary also adds to this difficulty.

However, an attempt can be made to determine the electric field intensity near the tin oxide boundary, to a good approximation, if one considers the boundary as a curved surface, as shown in Fig. 5.1b. The curved surface forms the inner plate of a semicylindrical capacitor surrounded by a composite system of liquid and glass dielectrics. The outer earthed surface of the glass tube forms the other plate.

At point P in the liquid (Fig. 5.1b) situated at a distance  $r$  from the center of curvature of the boundary, the electric field  $E$  has the known value,

$$E = \frac{\rho a}{\epsilon_1 r} \quad \dots\dots\dots (5.1)$$

where  $\rho$  is the surface charge density at the tin oxide boundary,  $a$ , its radius of curvature and  $\epsilon_1$ , the dielectric constant of the liquid. The field thus varies hyperbolically in the space above the tin oxide edge from a maximum value

at points on the surface of the tin oxide boundary to a minimum at points on the outer surface of the glass tube.

The lines of force originating from the points at the boundary have to pass through the liquid and glass media before reaching the outer surface of the glass tube where they terminate. Thus we have to deal in this case with composite dielectrics in series as shown in Fig. 5.1c.

If we assume that the normal component of displacement  $D$  in the two materials is continuous, that is,

$$D_1 = D_2 \quad \dots\dots\dots (5.2)$$

$$\epsilon_1 E_1 = \epsilon_2 E_2, \quad \dots\dots\dots (5.3)$$

where  $E_1$  and  $E_2$  are the field intensities in the liquid and glass dielectrics respectively and  $\epsilon_2$ , the dielectric constant of the glass. If  $V$  is the potential applied to the tin oxide film with reference to the earth, the potentials in the two materials shall be<sup>(2)</sup>

$$V = \int E ds = E_1 S_1 + E_2 S_2 \quad \dots\dots\dots (5.4)$$

where  $S_1$  and  $S_2$  are the thicknesses of the two materials.

Denoting the parts of the total potential difference  $V$  in each material as  $V_1$  and  $V_2$ , and solving eqs. 5.3 and 5.4,

$$V_1 = \frac{V}{1 + (\epsilon_2/\epsilon_1) (s_1/s_2)} = E_1 s_1 \quad \dots (5.5)$$

$$V_2 = \frac{V}{1 + (\epsilon_1/\epsilon_2) (s_2/s_1)} = E_2 s_2 \quad \dots (5.6)$$

It should be noted from eq. 5.5 that the second term in the denominator is negligibly small in comparison with 1 because  $s_1 \ll s_2$  ( $s_1 \simeq r_1$ , the thickness of the tin oxide film for maximum field corresponding to a given voltage,  $V$ ). Thus one can approximate that most of the applied voltage drops across the liquid near the tin oxide boundary and thus the field intensity is greater in the liquid. We can neglect here the accumulation of charge at the glass-liquid interface due to polarisation effects and the difference in conductivities (if any, keeping in view the purity of the liquids given in Table 5.1) of the two materials in comparison with the charge density at the tin oxide layer due to applied voltage.

In consideration of the above conditions the capacitance of the unit length of the cylindrical capacitor

TABLE -5.1.

Some Physical constants for n-Hexane, n-Pentane  
and iso-Pentane.

Constant	n-Hexane	n-Pentane	iso-Pentane
Purity %	99	95	95
Boiling Point (B.P.)°C	68.7	36.1	27.8
Critical Temperature $T_c$ °C	234.7	196.6	187.8
Critical Pressure $P_c$ ats.	30.4	33.8	30.3
Critical density $P_c$ gms/cc.	0.2343	0.2323	0.2343
Katsyama Constant	2.18	2.15	2.13

can be written as,

$$C = \frac{2\pi \epsilon_1}{\log_e(r_2/r_1)} = \frac{2\pi a\sigma}{V} \dots (5.7)$$

or,

$$\sigma = \frac{\epsilon_1 V}{a \log_e (r_2 / r_1)}$$

where  $r_2$  is the thickness of the glass ( = 0.2 cm ).

Therefore, from eq. 5.1, E takes the form,

$$E = \frac{V}{r_1 \log_e (r_2 / r_1)}$$

As on the surface of the  $\text{SnO}_2$  boundary  $r = a \approx r_1$ , we may write

$$E = \frac{V}{r_1 \log_e (r_2 / r_1)} \dots\dots (5.8)$$

The quantity  $r_2$ , the distance of the earthed surface from the  $\text{SnO}_2$  layer appears in this equation in logarithmic term and hence it does not very much affect the value of E.

In the present experiment, the thickness of the tin oxide layer  $r_1$ , was measured by the fringe shift method in

Michelson interferometer. A  $\text{SnO}_2$  film was deposited on a flat glass plate under the same condition as it was done inside the glass tube. The shift is measured in Michelson Interferometer by replacing the simple glass plate by the <sup>one</sup> on which the tin oxide was already deposited. The thickness of the  $\text{SnO}_2$  layer thus measured was found to <sup>be</sup>  $1.41 \times 10^{-5}$  cm. Substituting this value of  $r_1$  in eq. 5.8,  $E$  comes out to be  $\approx 10^6$  volts/cm for the applied voltage  $\approx 1$  KV.

The presence of such a strong field at the glass-liquid interface may produce a number of effects (visible and non-visible). One of the most striking effects would be the increase in the internal energy of a thin layer of liquid in contact with the tin oxide surface above B. This effect might also be interpreted as an induced tension at an interface (and this is more so when the temperature of the system is much higher than the room temperature and it is heated from out side). Any gradient or non-uniformity in the density of a liquid usually gives rise to hydrodynamic flow when the system is subjected to an external electric field.<sup>(3)</sup> Thus the presence of an external electric field may alter the resultant tension at a solid-liquid interface.



In order to verify the above propositions several control experiments were performed.

### 5.3. Experiments :

Dielectric liquids have been previously found to exhibit a number of interesting phenomena under the influence of intense electric forces. The phenomena of electric field induced convection in dielectric liquids<sup>1</sup>, rise of a dielectric liquid along the surface of an electrode due to electric field (the Sumoto effect)<sup>5</sup>, the pumping action of the divergent field<sup>6</sup>, and the electrical breakdown of insulating liquids<sup>7</sup> have been studied by a number of workers<sup>8,9,10</sup>. These effects are considered to be due to strong electric stresses on the liquid in a non-uniform field. As the test liquid in the present experiment happens to be dielectric in nature and the nature of the electric field under which they are subjected fulfils some of the above conditions, a set of control experiments were performed to demonstrate some of the electrohydrodynamic effects.

The effect of dielectrophoretic forces is to move the matter of lower dielectric constant into the regions

of lower field strength. Thus if air or vapour bubbles are mixed in the liquid, the behaviour of the liquid and that of the bubbles under intense electric stress will depend on the nature and direction of the field gradient and the magnitude of the applied field. The three experiments described below include the effect of all the three parameters simultaneously.

(a) Dielectrophoretic creeping of the liquids:

In this experiment, a glass tube (i.d. = 1.2 cm, o.d. = 1.5 cm) open at both the ends was held vertically. The lower portion of the tube was coated with a thin, transparent, and highly conducting film of tin oxide (thickness  $\approx 10^{-5}$  cm) which terminated with a sharp boundary near the middle of the tube as shown in Fig. 5.2a. The lower end of the glass tube is closed with a cork and a high voltage electrode is inserted in the tube through the cork and connected to the tin oxide film. The tube is filled with a liquid upto a height of about 2 mm above the boundary as shown in Fig. 5.2(a). The outer surface of the glass tube is earthed. In the case of insulating liquids, e.g., n-Hexane, Benzene, transformer oil, etc., when

THE LIQUID STARTS CREEPING ALONG THE WALLS OF THE TUBE ON THE APPLICATION OF THE ELECTRIC FIELD.

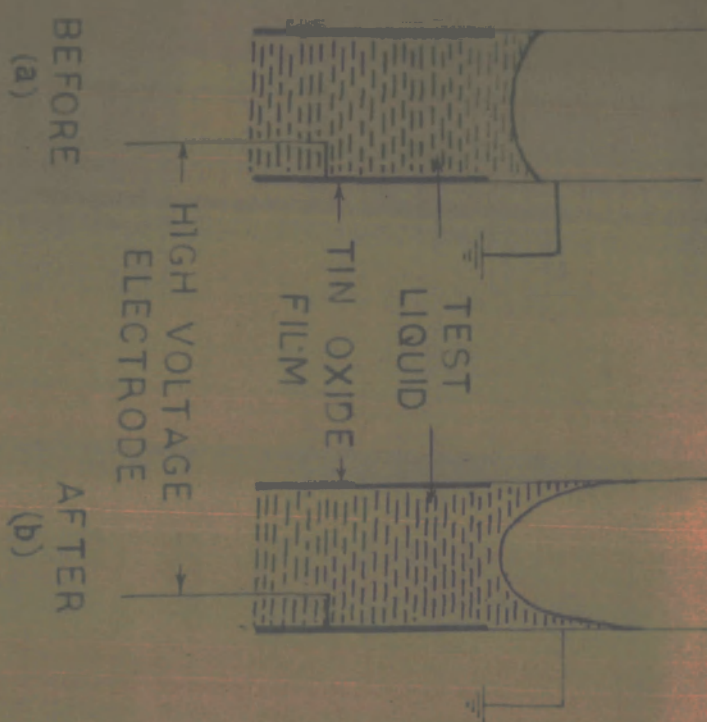


FIG. 5.2

the electrode is connected to a high voltage terminal of a high voltage supply (0-5KV, alternating or unidirectional) the following phenomena are observed: The liquid starts creeping along the walls of the glass tube as shown in Fig.5.2b, (and photographically in Fig.5.2c) both in the case of alternating and unidirectional fields (+ve and -ve polarity). The creeping height increases with increasing applied voltage.

(2) The creeping ceases by removal of the field but in case of the unidirectional field, a momentary creeping is observed when the electrode is earthed just after it is disconnected from the high voltage supply.

(3) The creeping is more vigorous in the case of the alternating fields.

(4) No creeping is observed in case the liquid column lies below the tin oxide layer boundary, i.e., well within the boundaries of the tin oxide cylinder.

(5) The phenomenon is not observed when the liquid used is more or less conducting, i.e., water, alcohol, acetone, etc.

In the light of the above observation some qualitative explanation may be put forward regarding the nature of the

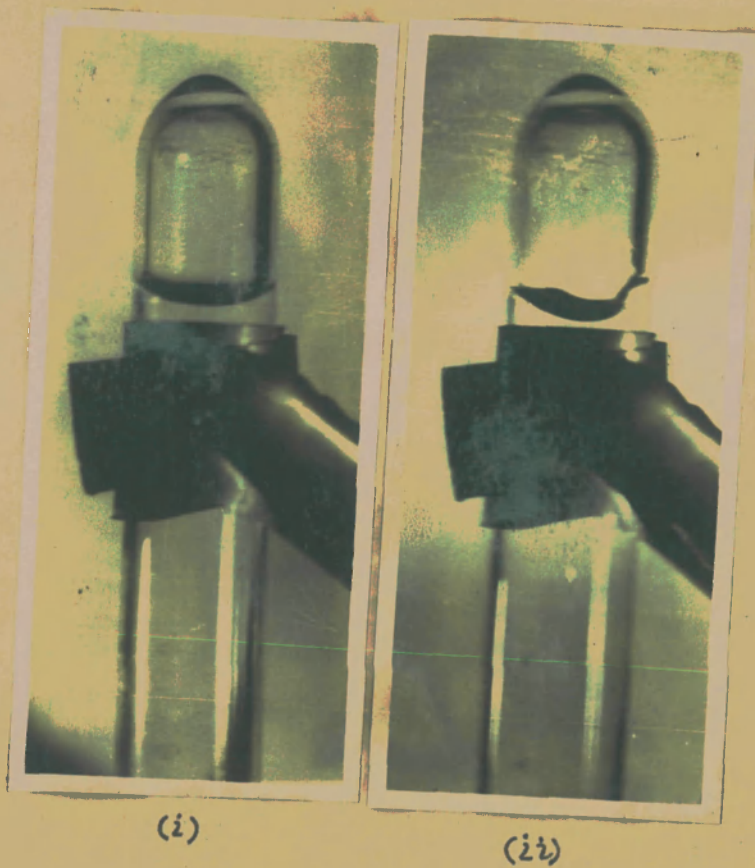


**FIG. 5.2 (c) (i) Level of liquid in the tin oxide coated glass tube in the absence of electric field, (ii) Creeping of the liquid along the walls of the tube on the application of electric field.**

phenomena. The geometry of the apparatus is similar to a cylindrical capacitor as described in section 5.2. The electrostatic field is zero inside the region enclosed by the cylindrical tin oxide layer and highly intense only near the boundaries of the tin oxide layer. Since the liquid remains non-conducting for the applied voltages, the dielectrophoretic forces exerted by the electric field are due exclusively to the local non-uniformity of the field. Thus if  $E$  is the local value of the electric field at the boundary of the tin oxide film,  $\rho$  the density of the liquid at the working temperature, and  $\epsilon$  its dielectric constant, the expression for the dielectrophoretic force is given by<sup>11</sup> the equation

$$F = \rho \text{grad} \left( \frac{\partial \epsilon}{\partial \rho} E^2 \right) \quad \dots\dots (5.9)$$

in which all the quantities are defined in a reference system which is at rest with respect to the liquid (medium) under consideration. The forces given by eq. 5.9 are localised at the free surface of the liquid in contact with air. The specific surface force is given by<sup>12</sup>

$$f_s = \frac{\epsilon - 1}{2} - \frac{(\epsilon - 1)(\epsilon + 2)}{24 \pi} E_{n12}^2 \quad \dots\dots (5.10)$$

where  $n_{12}$  is the unit vector directed towards the second medium, i.e., air. These surface forces, localised in the regions of non-uniform field very near the tin oxide boundary ( $\approx 10^{-5}$  cm) and directed towards the more intense regions of the field, are supposed mainly responsible for the electrohydrodynamic effect reported in this experiment. They exert an "electrical excess pressure" on the liquid which can be calculated at a certain point in the field by integrating the effect of these forces from a point within the liquid but above the tin oxide boundary. This pressure, given by<sup>13</sup>

$$p_e = \frac{(\epsilon-1)(\epsilon+2)}{24\pi} E_{n12}^2, \quad \dots\dots\dots (5.11)$$

depends solely on the dielectric constant of the liquid and the local value of the electric field. The electric intensity at a distance  $r$  from the tin oxide layer is given by the formula (from eq. 5.8)

$$E = \frac{V}{r \log_e (b/a)} \quad \dots\dots\dots (5.12)$$

where  $V$  is the applied voltage,  $a$  and  $b$  are respectively the thickness of the tin oxide layer and the distance of the earthed electrode from the axis of the cylinder.



The surface force (eq. 5.10) and the force due to electrical pressure (eq. 5.11) produce creeping of the liquid while force due to surface tension opposes it. If  $h$  is the height to which the liquid creeps, the equilibrium condition is represented by the equation

$$P_e + f_g - \sigma = \rho gh \quad \text{..... (5.13)}$$

where  $\sigma$  is the value of the surface tension of the liquid and  $g$ , the acceleration due to gravity.

One can estimate the terms appearing in eq. 5.13 and thus compare the calculated and the observed heights (observed  $h = 0.884$  cm for  $V = 3$  KV) for n-Hexane for which  $\sigma = 18.5$  dynes/cm,  $\epsilon = 1.92$  and  $\rho = 0.6543$  gms/cc at  $T = 293^\circ\text{K}$  (the room temperature). The electric field intensity from eq. 5.12 at a distance of  $10^{-2}$  cm (the distance of the liquid layer above the tin oxide boundary) from the tin oxide boundary comes out to be 160 e.s.u./cm and from eq. 5.13,  $h = 1.095$  cm, which is in a fair agreement with the observed height considering the large number of inaccuracies in the calculations.

The observed effects might also be due to the influence of the electric field on surface tension of the



liquid through the displacement of the double layer which exists at the liquid- tin oxide interface even in absence of external electric field.

(b) Control experiment on the effect of dielectrophoretic forces on air bubbles in the liquid :

In this experiment a glass tube partially coated with tin oxide as described above was held vertically with its lower end sealed with a cork. It was almost completely filled with the test liquid (n-Hexane). Small air bubbles were formed at the tip of a nozzle fitted to the cork. The tin oxide coating was connected to a high voltage supply through a connecting electrode. In the absence of any voltage on the tin oxide layer the air bubbles ascend straight to the top of the tube due to buoyancy forces. But if a voltage is applied exceeding a certain value (critical), the following phenomenon is observed:

In case the voltage is applied to the tin oxide layer when the ascending bubble is far below the tin oxide boundary, it is stopped slightly below the (1-2 mm) tin oxide boundary as shown in Fig.5.3 a (photographically in Fig. 5.3 c). If the voltage is applied at an instant when

THE BUBBLE STOPS IN THE  
MIDDLE OF THE TUBE ON THE  
APPLICATION OF THE ELECTRIC  
FIELD.

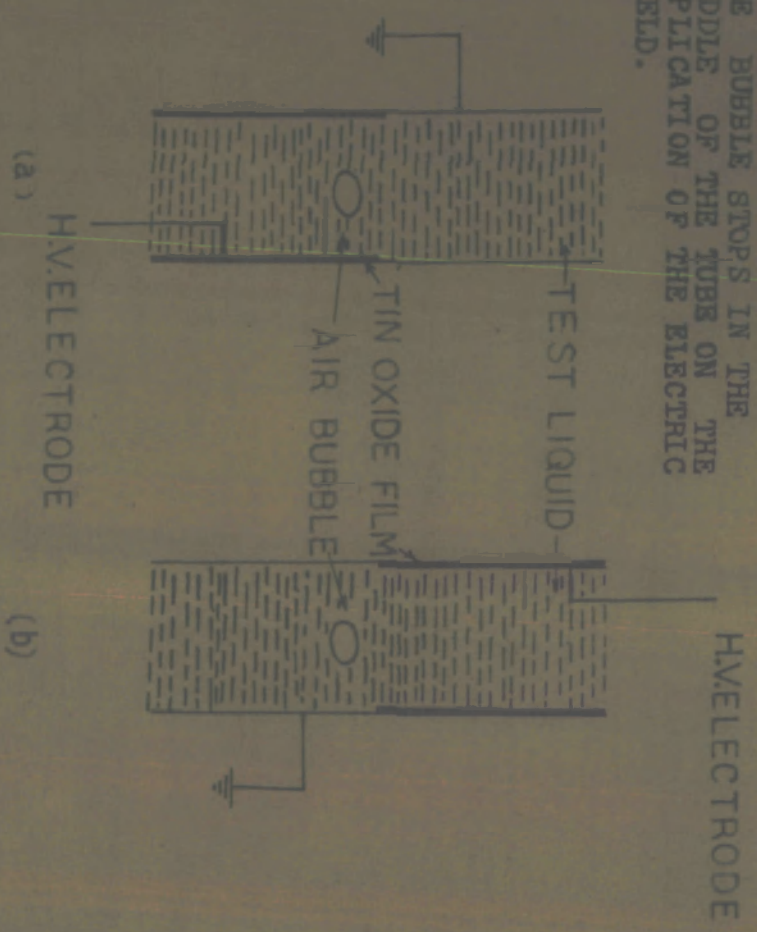


FIG. 5.3



**FIG. 5.3(c) The air bubble ascending in the liquid inside the vertically held glass tube is stopped near the tin oxide boundary on the application of the electric field.**

the ascending bubble is just approaching the boundary, it is pushed downwards while its upward velocity is enhanced if the voltage is applied when it has just crossed the boundary.

The same observations are obtained when the upper portion of the tube is tin oxide coated as shown in Fig. 5.3b.

The behaviour of the bubble described above can be interpreted in terms of the force on the bubble due to viscosity, back diffusion, and the non-uniformity of the electric field. In order to stop the air bubble in the middle, the force,  $F_d$ , on the macroscopic bubble dragging it upwards should be balanced by the electrophoretic forces,  $F_e$ , due to field. The dragging force is given by,

$$\begin{aligned} F_d &= \text{Viscous force} - (\text{mass of the bubble}) \times g \\ &= 6\pi\eta av - \frac{4\pi}{3} a^3 (\rho' - \rho) g \end{aligned}$$

where  $\eta$  and  $\rho$  are respectively the viscosity and density of the liquid while  $a$ ,  $v$  and  $\rho'$  are the radius of the air bubble, its ascending velocity, and density of air respectively. Since  $\rho' \ll \rho$ ,

$$F_d = 6\pi\eta av + \frac{4\pi}{3} a^3 \rho g \quad \dots\dots\dots (5.14)$$

The dielectrophoretic force over the bubble of same size,

$$F_e = \frac{\epsilon E^2}{8\pi} \times 4\pi a^2 = \frac{\epsilon E^2 a^2}{2} \dots\dots (5.15)$$

In an experiment with n-Hexane as the test liquid in a tube (i.d. = 2.5 mm, o.d. = 8.5 mm), the critical voltage at tin oxide layer was  $V_c = 1200$  volts for an air bubble of radius  $a = 1$  mm and its ascending  $v = 1$  cm/sec.

For n-Hexane at  $T = 293^\circ\text{K}$  (the room temperature)  $\epsilon = 1.92$ ,  $\eta = 3.0 \times 10^{-3}$  Poise and  $\rho = 0.6548$  gms/cc. The force  $F_d$  when calculated from eq. 5.14 from these data comes out to be 2.7 dynes while the experimental value of dielectrophoretic force calculated through eqns. 5.12 and 5.15 is found to be 2.1 dynes. The two values are in fair agreement.

(c) Control experiment on dielectrophoretic change in surface tension :

A glass tube (i.d. = 1.2 cm, o.d. = 1.6 cm) with a narrow nozzle was coated inside with a thin, transparent film of tin oxide as shown in Fig. 5.4a. When a liquid is poured into the tube, it first runs out in a smooth jet. When the depth of the liquid is decreased i.e. when the pressure of the depth of the liquid is diminished, the formation of the jet is prevented by surface tension



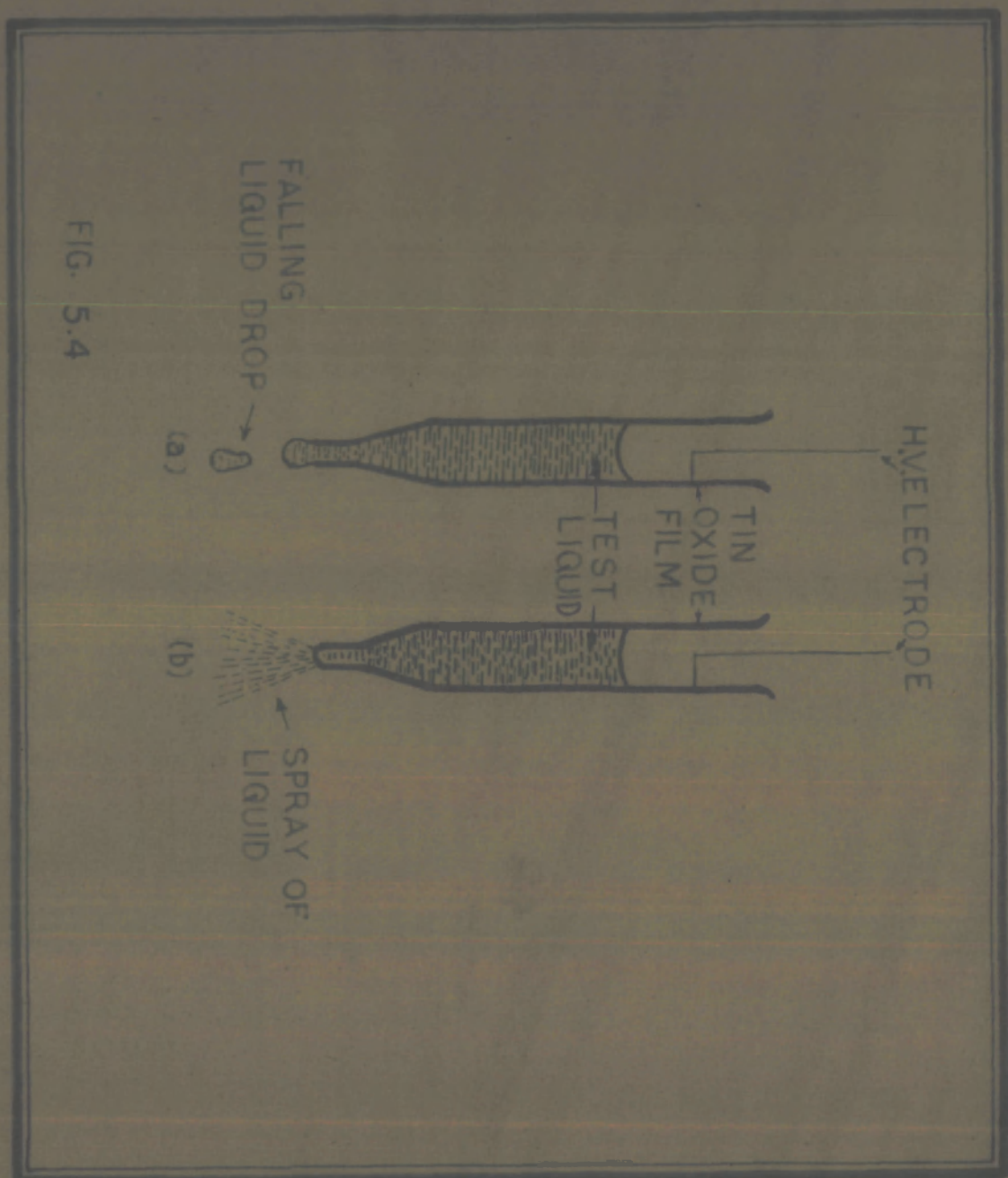


FIG. 5.4

and the liquid merely trickles out slowly in drops. If at this stage the tin oxide layer is connected with the high voltage terminal of a high voltage power supply (0-5KV d.c.) by means of connecting cable, the frequency of the fall of liquid drops increases but their size is reduced. By further increasing the applied voltage, the drop size decreases considerably and at a critical voltage the drops are converted into a spray of liquid from the nozzle as shown in Fig.5.4b.

Since the surface tension causes the liquid to fall in single drops, the size of the falling drops determine the surface tension of the liquid and a decrease in their size demonstrate the decrease in the value of the surface tension. It may be ascribed to the dielectrophoretic forces at the tip of the nozzle where the tin oxide layer has a sharp edge. The sizes of the falling drops for a given fall in the height of liquid in the glass tube were determined by counting the number of falling drops. The radii of the falling drops are plotted against the applied voltages at the tin oxide layer in Fig. 5.4c, for n-Hexane. Similar results are obtained for liquid n-Pentane, Iso-Pentane and polar liquids like water, and alcohol.

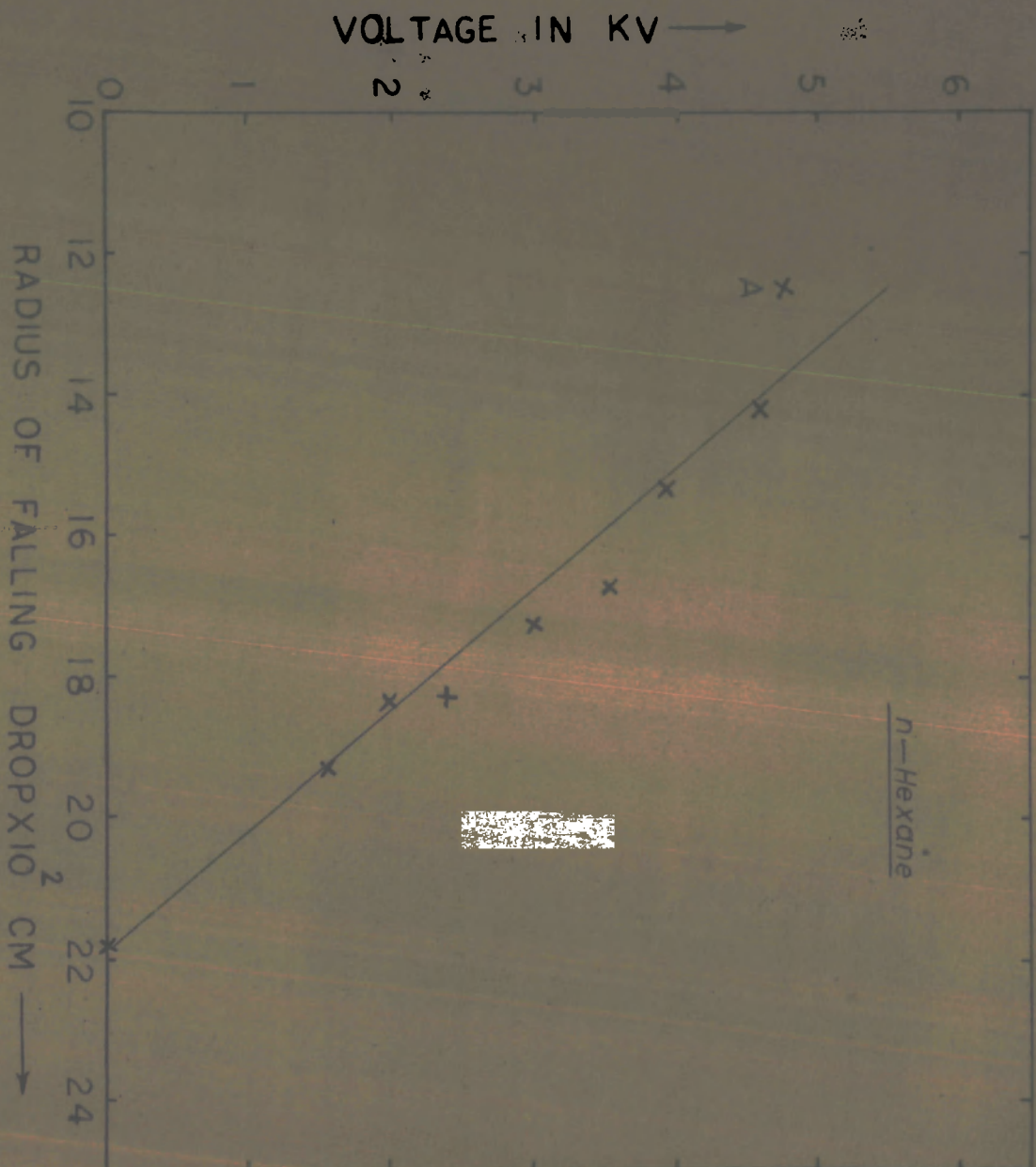


FIG. 5.4 (C)

Radius of the falling drop as a function of the applied voltage at the tin oxide layer. Spray of the liquid starts at point A.



The creeping of the dielectric liquids under strong dielectrophoretic forces, described in the first experiment is quite different from that observed by Sumoto.<sup>14</sup> In Sumoto's experiment the electric field distribution was normal to the electrode surface while the climbing of the liquid took place along the electrode surface. It might be ascribed due to the tendency of the medium of lower dielectric constant to move towards the regions of lower field strength. The air at the region adjoining the tin oxide boundary above the liquid surface (Fig. 5.2a) is displaced due to the electrophoretic forces and a vacuum is created at the region as a result of which the liquid rushes to fill up the space. Krasucki<sup>15</sup> while explaining the phenomenon of electrical breakdown of liquids has suggested the formation of points of zero pressure in these regions. But one can consider the development of regions of negative pressures as well keeping in view the phenomenon of induced nucleation in superheated liquids due to electric fields as reported in this work. This will be dealt with in detail.

All the above control experiments confirm the presence of an intense field at the edge of the tin oxide coating.

The possible reasons for the initiation of nucleation due to electric field in the present experimental set-up may be analysed in the following manner:

#### 5.4 The forces on a conductor :

In an electric field certain forces act on the surface of a conductor. If the conductor is surrounded by a dielectric it should be possible on the pure field theory, to calculate the net force on a given volume of a dielectric in terms of the field condition on the surface element of the volume element. The force on the element of the surface of the body is expressed through a well known stress tensor. Since at the surface of the conductor the field has no tangential component, the force per unit area of the surface (or the pressure) as calculated through the stress tensor becomes,<sup>16</sup>

$$P = \frac{\epsilon E^2}{8\pi}$$

where  $\epsilon$  is the dielectric constant of the liquid in contact with the conductor. In terms of the surface charge density  $\sigma$ , the pressure is given by

$$P = 2\pi\epsilon\sigma^2$$

This pressure acts along the outward normal to the interface. Therefore we can conclude that a "negative pressure" acts on the surface of a conductor, its magnitude is equal to the energy density in the field.

### 5.5 Consequences of the forces at the interface :

The above term for pressure also defines the energy per unit volume of the dielectric due to an external electric field of intensity  $E$  with proper representation of units. Thus while discussing the role of an external electric field on bubble formation in a liquid one may analyse it either as due to the energy contribution by the electric field or due to the mechanical effects. The mechanical effects as obtained through a stress tensor<sup>17</sup> are considered to have different manifestations. As for example, it can be correlated with the general question of the hydrostatics of the body of the liquid which is influenced by an electric field, or as a surface tension effect at the interface.<sup>18</sup> According to Cade,<sup>16</sup> part of the electrostatic stress tensor is the basis of a theory of surface tension and the remainder, representing the effect of applied field, gives a theory of electrocapillarity. Indeed one might go further and introduce the action of applied field

on the electric double layer which might exist<sup>19</sup> at the liquid-tin oxide interface even if there is no externally applied electric field.

It is evident that the problem of calculating the forces (ponderomotive forces) which act on a dielectric in an electric field is fairly complicated and some of the above effects are mutually inclusive. We have therefore made some qualitative estimation of the effect of the field in two ways: (a) Control experiments were set for the estimation of the intensity of the electric field at the sharp tin oxide edge as has been described earlier, (b) the energy contributed by the external electric field to the liquid dielectric (n-Hexane, n-Pentane, Iso-Pentane) was calculated by using estimated values of electric field intensity at the sharp tin oxide edge from eq. 5.8; (c) force due to external electric field when calculated per unit area from eq. 5.14 was compared with the negative pressure required for the formation of a critical bubble from kinetic theory of nucleation at a given temperature.

#### 5.6 Change in surface tension due to external electric field:

The change in surface tension of n-Hexane due to external electric field was determined at room temperature by the liquid drop weight method, as has been described in

sec. 5.3., for the verification of the presence of intense electric stresses at the tin oxide boundary.

It is well known from the equation for the rate of bubble formation<sup>20</sup> as explained in chapter II,

$$J = Z \log \sqrt{\frac{6\sigma}{\pi m(3-b)}} \exp\left(-\frac{\lambda}{RT}\right) \exp\left(-\frac{16\pi\sigma(T)^3}{3RT(P_S - P_L)^2}\right) \dots\dots\dots (5.16)$$

$$\text{where } W = \frac{16\pi\sigma(T)^3}{3(P_S - P_L)^2}$$

that the rate of bubble formation may be increased by decreasing the value of  $W$  in eq. 5.16. The work function for the formation of a critical bubble,  $W$ , can be decreased either by decreasing the value of  $\sigma(T)$  at a given temperature and pressure or by decreasing the external pressure  $P_L$ .

The values of  $J$  from eq. 5.16 were determined at different temperatures and at atmospheric pressure by putting different values for  $\sigma(T)$  in eq. 5.16 and thus the values of  $\sigma(T)$  corresponding to  $J = 1$  were determined by plotting  $J$  versus  $T$  in Fig. 5.5. The values for n-Hexane

Calculation of temperature corresponding to  $J=1$  ( $\log J=0$ )  
at different values of surface tension according to  
Kinetic Theory.

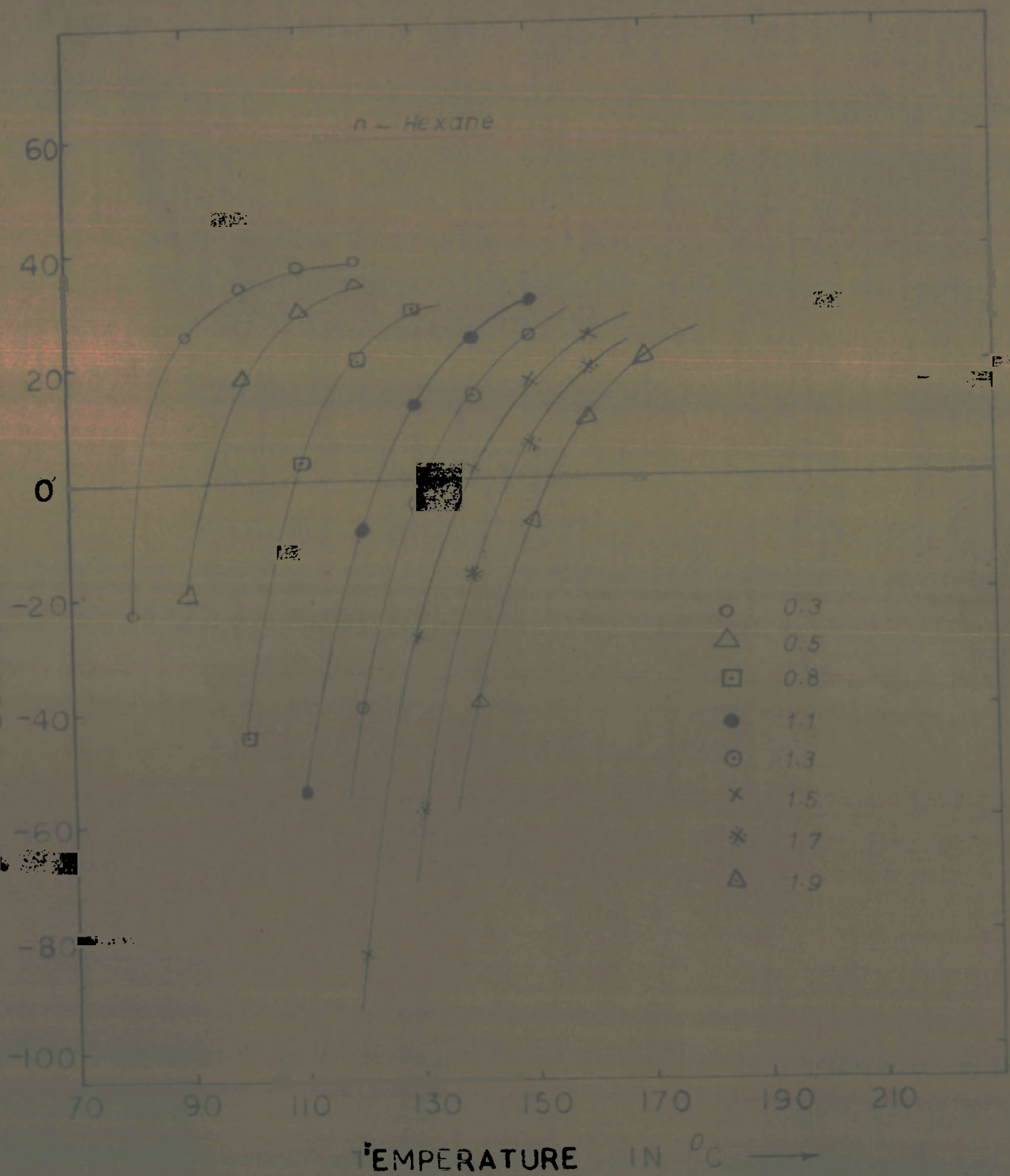


FIG. 55

are given in Table 5.2 and their graphical representation is shown in Fig.5.6. The required change in surface tension  $\Delta\sigma$  is plotted in Fig.5.7. It should be clear that the required change in surface tension corresponding to a given temperature is a linear function of temperature.  $\Delta\sigma = 0$  at  $T = T_m$  according to kinetic theory.

It should be noted from Fig.5.4c that the change in surface tension produced due to external electric field as determined by the liquid drop weight method is also an almost linear function of  $V_c$ , the applied voltage. Thus it seems that the external electric field produces a change in surface tension of the liquid. As we have not taken into account the variation of  $V_c$  with  $T$  for a given change in surface tension, we should not draw any exact quantitative conclusion from this experiment.

### 5.7 Force due to external electric field:

The force per unit area on the surface of a conductor in an electric field  $E$ , as already stated earlier, is given by

$$P = \frac{\epsilon E^2}{8\pi}$$

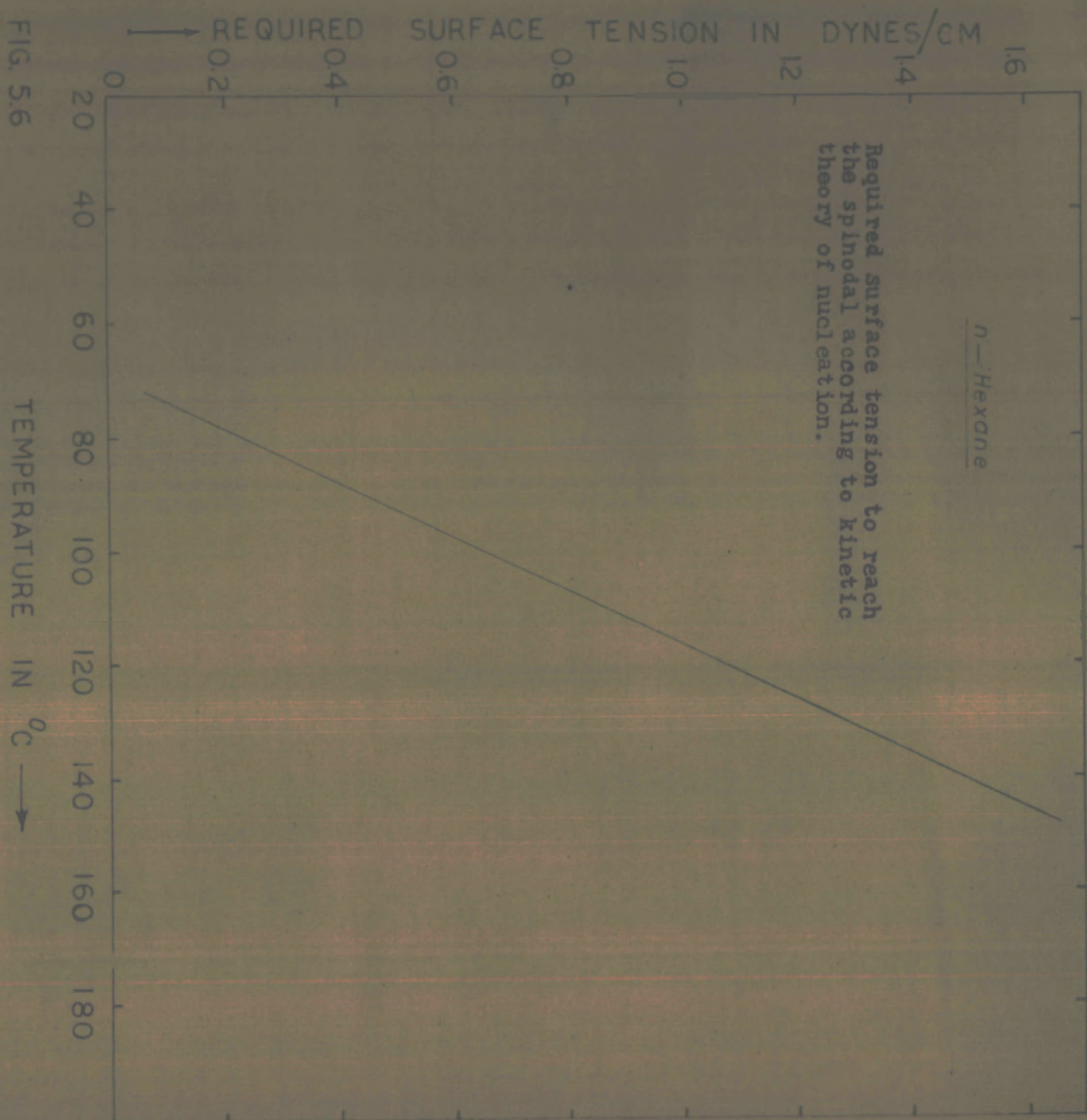
TABLE 5.2.

Required change in surface tension  $\Delta\sigma$  calculated from kinetic equation (eq.5.16) at different temperatures of n-Hexane for  $J = 1 \text{ bubble cm}^{-3}\text{Sec}^{-1}$

Temperature $^{\circ}\text{C}$	Surface Tension dynes/cm	Required surface Tension, dynes/cm	Required change in surface Tension dynes/cm
70	13.4	0.1	13.3
80	12.4	0.3	12.1
90	11.4	0.5	10.9
100	10.5	0.7	9.8
110	9.6	0.9	8.7
120	8.7	1.1	7.6
130	7.8	1.3	6.5
140	6.9	1.5	5.4
150	6.0	1.8	4.2
160	5.1	2.0	3.1
170	4.3	2.5	1.8



FIG. 5.6



The change in surface tension  $\Delta\sigma$  required according to kinetic theory to reach the spinodal.

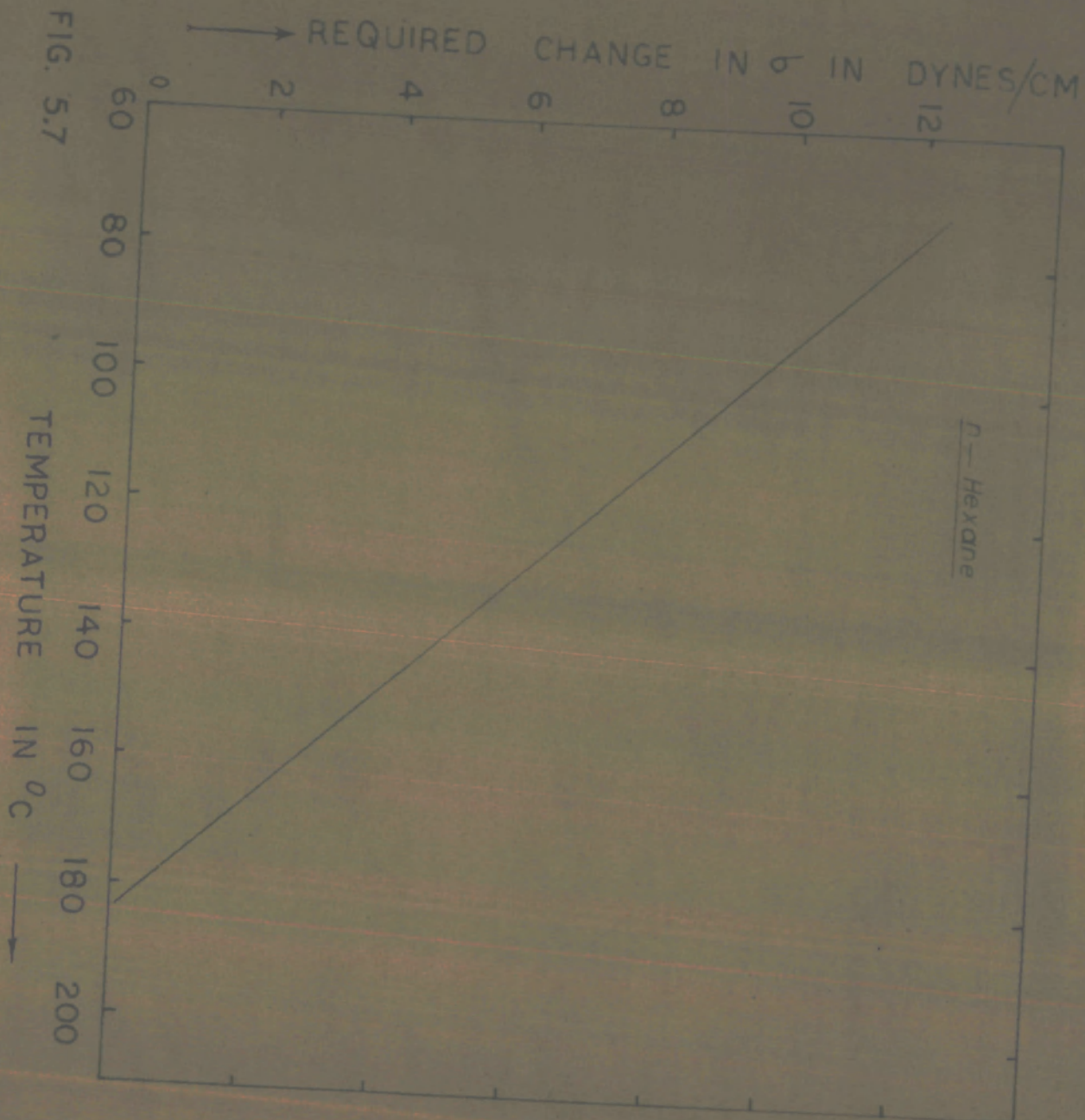


FIG. 5.7

This pressure acts along the outward normal to the interface; i.e., a pressure acts normal to the inner glass wall of the tin oxide coated glass tube towards the liquid side. This pressure is maximum near the tin oxide boundary where  $E$  is maximum. We can thus conclude that something similar to the phenomenon of "negative pressure" acts in the liquid at the surface its magnitude being equal to the energy density in the field.

In case the nucleation is induced due to electric field  $E_c$  corresponding to a critical voltage  $V_c$  at specified temperature and pressure, the negative pressure is,

$$P = \frac{\mathcal{E}(T) E_c^2}{8\pi},$$

where  $\mathcal{E}(T)$  has been taken as a function of temperature. This pressure may be called the tensile strength of the liquid at the given temperature.

A comparison between the values of the limiting negative pressure calculated from the above equation from the given values of the electric field intensities corresponding to various critical voltages and temperatures

with those calculated theoretically from the kinetic<sup>20</sup> and Fürth's equations<sup>21</sup> is given in tables 5.3 (a,b,c) and graphically represented in Fig. 5.8 (a,b,c) for the three liquids.

It should be noted that the tensile strength of the liquids determined from the present experiment are higher than those obtained from the kinetic theory. However, the tensile strength calculated from Fürth's equation happens to be higher than both the above values.

#### 5.8 Energy contributed by the electric field :

It should be noted that the term  $\frac{\mathcal{E}(T) E^2}{8\pi}$  is also defined as the energy per unit volume of the medium.

According to kinetic theory,<sup>20</sup> it is assumed that the density fluctuations in a liquid cause the rapid formation and destruction of subnuclear vapour bubbles; the probability that one of these fluctuations develops into an observable vapour cavity in a reasonable period of time is then calculated. The work function  $W_m^*$  for the formation of a cavity of critical size  $r_c$  is given by the equation,

$$W_m^* = \frac{16 \pi \sigma^3(T)}{3(P_g - P_L)^2} \dots\dots\dots (5.18)$$

TABLE - 5.3(a)

$P_m$  values obtained from Kinetic equation, Fürth's equation, and as an electrical pressure from the present experiment for n-Hexane ( $P_m$  is a negative pressure).

Temperature °C	Critical Voltage $V_c$ Volts.	$\times 10^{-6}$ Volts/Cm	$\frac{\epsilon(T) E^2}{8\pi}$ ats.	$P_m$ (Kinetic equation) ats.	$P_m$ (Fürth's equation) ats.
90	1600	12.3	205.7	114.0	300.0
100	1300	10.1	150.0	97.0	220.0
110	1100	8.48	118.7	82.0	177.0
120	900	5.65	85.0	68.0	145.0
130	750	4.71	75.6	55.0	118.0
140	600	3.86	58.5	42.0	92.0
150	500	3.41	45.4	32.0	70.0
160	375	2.35	38.0	22.0	53.0
170	300	1.88	23.0	13.0	36.0
180	250	1.34	10.5	4.0	20.0

TABLE - 5.3(d)

$P_m$  values obtained from Kinetic equation, Fürth's equation, and as an electrical pressure from the present experiment for n-Pentane ( $P_m$  is a negative pressure).

Temperature °C	Critical Voltage $V_c$ Volts.	$E \times 10^{-6}$ Volts/Cm.	$\frac{E(T) E^2}{8\pi}$ ats.	$P_m$ (Kinetic equation) ats.	$P_m$ (Fürth's equation) ats.
70	1300	10.57	145	79	150
80	900	6.06	97	60	118
90	750	4.81	72	45	94
100	600	3.77	47	34	75
110	450	2.83	37	25	57
120	350	2.20	24	17	42
130	250	1.57	15	10	30

TABLE - 5.3(c)

$P_m$  values obtained from Kinetic equation, Fürth's equation, and as an electrical pressure from the present experiment for iso-Pentane ( $P_m$  is a negative pressure).

Temperature °C	Critical Voltage $V_c$ Volts	$E \times 10^{-6}$ Volts/cm.	$\frac{\mathcal{E}(T) E^2}{8\pi}$ ats.	$P_m$ (Kinetic equation) ats.	$P_m$ (Fürth's equation) ats.
70	900	5.02	99	66	128
80	650	4.08	84	55	101
90	500	3.14	65	44	80
100	400	2.51	50	34	65
110	300	1.76	33	25	52
120	250	1.29	20	16	40
130	220	1.20	10	7	28



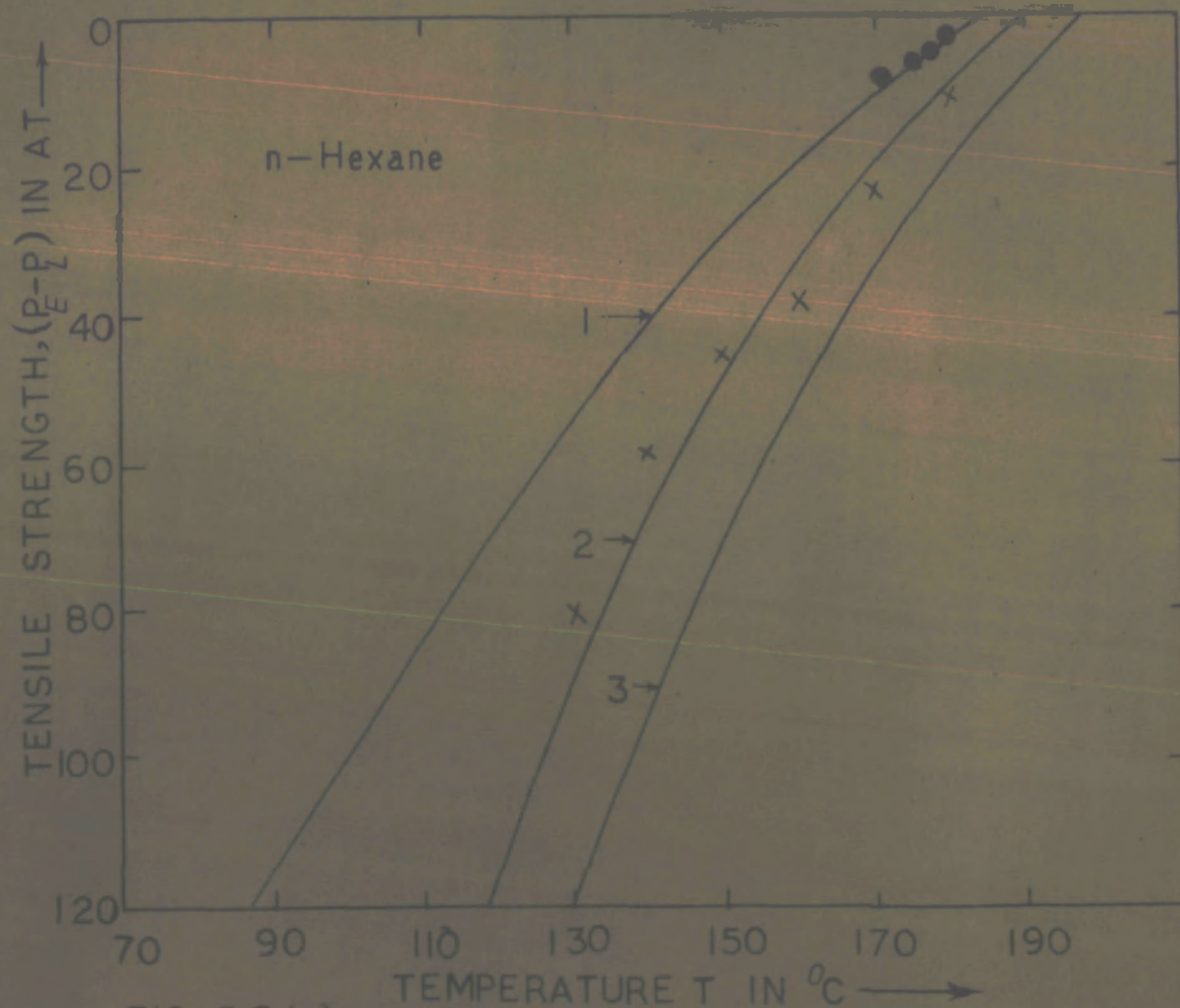


FIG. 5.8 (a)

TENSILE STRENGTH OF n-HEXANE AT DIFFERENT TEMPERATURES. 1 - CALCULATED FROM KINETIC THEORY OF NUCLEATION, ● - EXPERIMENTAL POINTS OBTAINED BY APPEL. 2 - OBTAINED FROM PRESENT EXPERIMENT, X - EXPERIMENTAL POINTS, 3 - CALCULATED FROM FURTH'S "HOLE" THEORY.



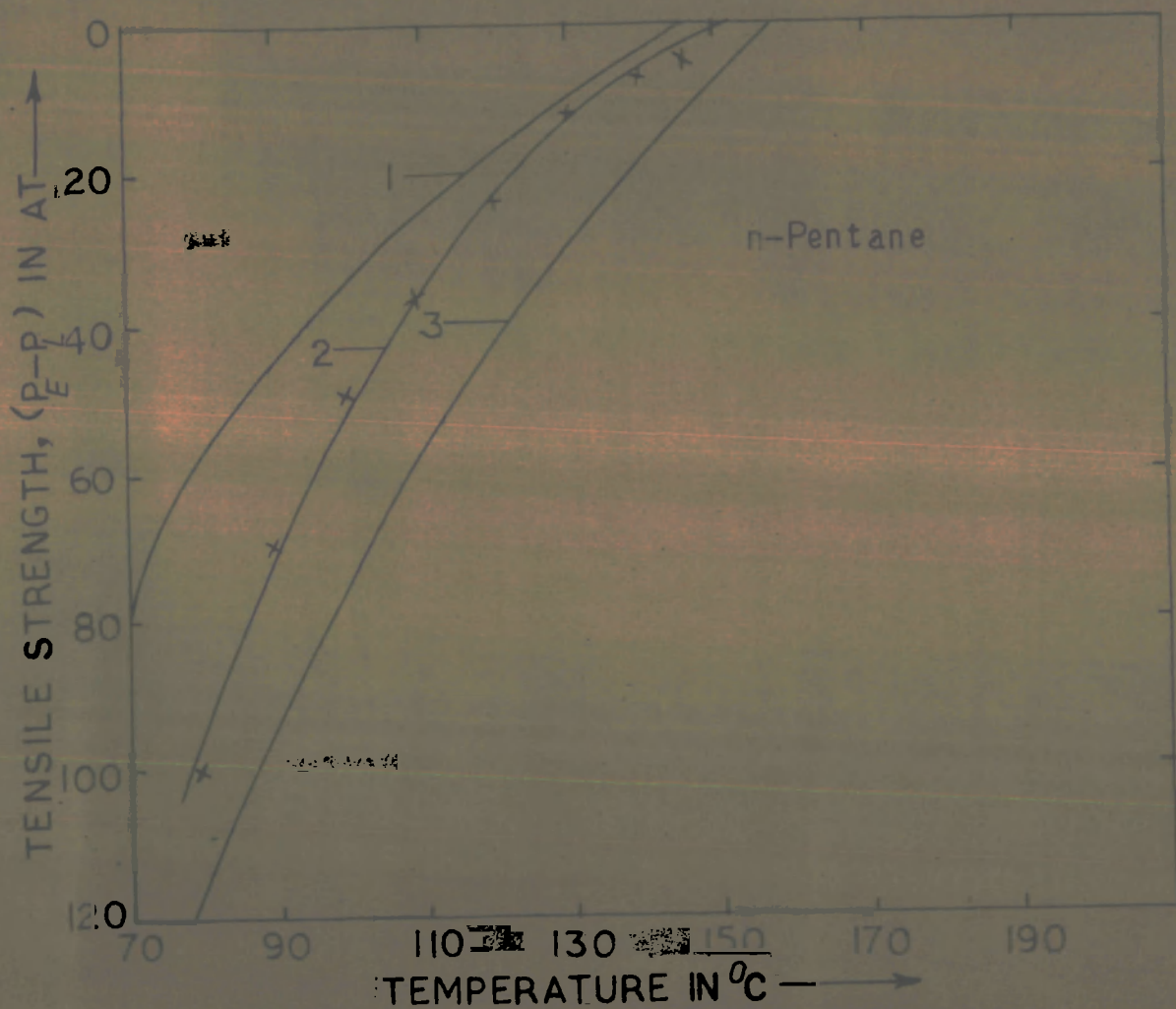


FIG. 5.8(i)

TENSILE STRENGTH OF n-PENTANE AT DIFFERENT TEMPERATURES. 1 - CALCULATED FROM KINETIC THEORY OF NUCLEATION, 2 - OBTAINED FROM THE PRESENT EXPERIMENT, x - EXPERIMENTAL POINTS, 3 - CALCULATED FROM FÜRTH'S "HOLE" THEORY.

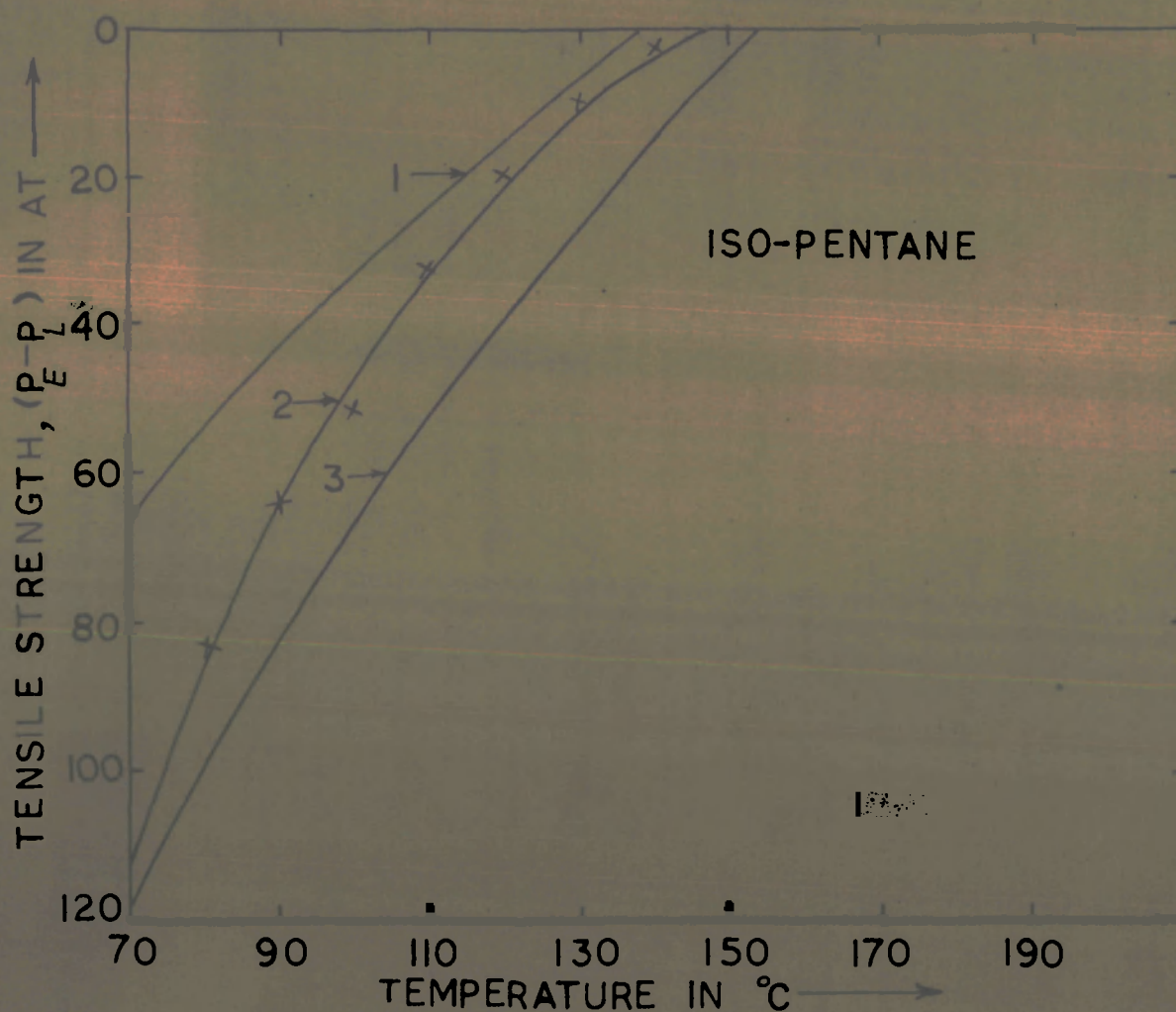


FIG. 5.8(C)

TENSILE STRENGTH OF ISO-PENTANE AT DIFFERENT TEMPERATURES. 1 - CALCULATED FROM KINETIC THEORY OF NUCLEATION, 2 - OBTAINED FROM THE PRESENT EXPERIMENT, X - EXPERIMENTAL POINTS, 3 - CALCULATED FROM FURTH'S "HOLE" THEORY.

$W_m^*$  is known as "energy barrier" to nucleation and is found by calculating the reversible isothermal work to form a vapour cavity of an arbitrary size, and then by calculating that value of the size variable that makes the work an extremum. A vapour cavity of such size which is called a critical cavity, is in unstable mechanical equilibrium and will grow to observable size if the temperature is infinitesimally increased or the pressure in the liquid is infinitesimally decreased. Although eq. 5.17 represents the work function for the formation of a vapour nucleus de novo in a liquid, the theoretical values of the limit of superheat calculated on the basis of this work function agree very well with the experimentally observed values in the case of some liquids.<sup>27</sup> This lends support to the contention that the above work function need not be modified to incorporate the contact angle between the test liquid and the glass container as shown in equation 2.20. This can also be supported by the fact that contact<sup>angle</sup> between most of the organic liquids with scrupulously cleaned glass surface is almost zero.

Thus, so far as the problem of nucleation in liquid due to the electric field is concerned one can compare the energy required for the formation of a critical nucleus

with the energy contributed by the electric field over the same volume and under similar conditions of temperature and pressure. The electrical energy contributed over the volume of radius  $r_c$  is given by

$$W_e^* = \frac{\epsilon(T) E^2}{8\pi} \times \frac{4\pi}{3} r_c^3 \quad \dots\dots (5.19)$$

The variation of  $W_m^*$  with temperature is shown in Table 5.4 for the three organic liquids used for the present study. The value of the critical voltage  $V_c$ , at the tin oxide coating required for inducing nucleation corresponding to the above temperatures are shown in the fifth column. The seventh column shows the values of electrical energy  $W_e^*$  contributed by the field. The agreement between the figures in the fourth and seventh columns may be considered as a fair one in view of the large number of assumptions involved in the calculations.

Exact agreement between the theoretical and the experimental values of energy given in columns 4 and 7 can not be expected because of a number of assumptions made in the calculations of electric field intensity.

TABLE - 5.4

$P_S$  = Saturated vapour pressure corresponding to given temperature.

n - Hexane

Temperature °C	$P_S$ ats.	$\sigma(T)$ dynes/Cm.	$W_m^* \times 10^9$ ergs.	$V_0$ Volts.	$W_g^* \times 10^9$ ergs.
120	4.0	11.2	2.80	900	46.70
130	4.9	10.0	1.10	750	9.80
140	6.0	8.9	0.50	600	1.40
150	7.4	7.9	0.20	500	0.30
160	9.0	7.0	0.09	375	0.08
170	10.7	5.9	0.04	300	0.02

n - Pentene

90	4.6	8.8	0.90	750	8.90
100	5.8	7.8	0.34	600	1.58
110	7.2	6.9	0.14	450	0.26
120	8.9	5.9	0.05	350	0.04
130	10.8	5.0	0.02	250	0.01

iso-Pentane

70	3.4	9.8	2.80	800	56.20
80	4.5	8.8	0.95	650	8.06
90	5.6	7.8	0.37	500	1.30
100	7.0	6.9	0.14	400	0.24
110	8.7	5.9	0.06	300	0.04

### 5.9 Determination of the limit of stability of liquids:

In order to determine the limit of stability of liquids used from the experimental results given in Tables 1-37 of Chapter IV, attempts were made to fit in the experimental values of the actual pressure,  $P$ , temperature  $T$  of the liquids at the instant of instantaneous nucleation, and the critical voltage of the external electric field required to induce nucleation. It has been found that for a given pressure,  $V_c$  and  $T$  are related through the following equation

$$V_c = A (T_m - T)^a + B (T_m - T)^b \quad \dots\dots\dots (5.20)$$

where  $A$  and  $B$  are constants and the powers ' $a$ ' and ' $b$ ' vary in the range ' $a = 0.5 \pm 0.5$ ,  $b = 2.5 \pm 1.5$ ' at different pressures.

$T_m$  in the above equation has the significance of the limit of the stability of the liquid at a given  $P$ . The quantities ' $a$ ' and ' $b$ ' are constants at a given pressure and the experimental data satisfy a family of curves (eq. 5.20) within 3% deviation. The equation 5.20 satisfies the boundary condition  $V_c = 0$  at  $T = T_m$  at a



given  $P$ . The family of such limiting points for a liquid can be joined by a curve terminating at the critical point. This curve happens to be the boundary of stability or the spinodal of the liquid. The  $P - T_m$  data thus obtained are compared with those calculated from the kinetic equation (5.16) and the F rth equation (eq. 2.6) in Table 5.5 and are plotted in Fig.5.9(a,b,c) for the three organic liquids used, namely n-Hexane, n-Pentane, and iso-Pentane.

The  $V_0 - T$  values at a given pressure were fitted in equation 5.20 by the method of least squares of curve fitting. The calculations were made with the help of IBM 1130 electronic digital computer using FORTRAN language. The powers 'a' and 'b' to  $(T_m - T)$  in equation 5.20 at different pressures for n-Hexane, n-Pentane and iso-Pentane are given in the tables 5.6 (i, ii, iii). The variation in 'a' and 'b' at different pressures are plotted in Fig.5.10 (i, ii) for the three liquids.

It is quite clear from these tables that 'a' decreases with pressure while 'b' increases. Thus the term  $A (T_m - T)^a$  in equation 5.20 is ineffective at higher pressures while much effective at lower pressures.

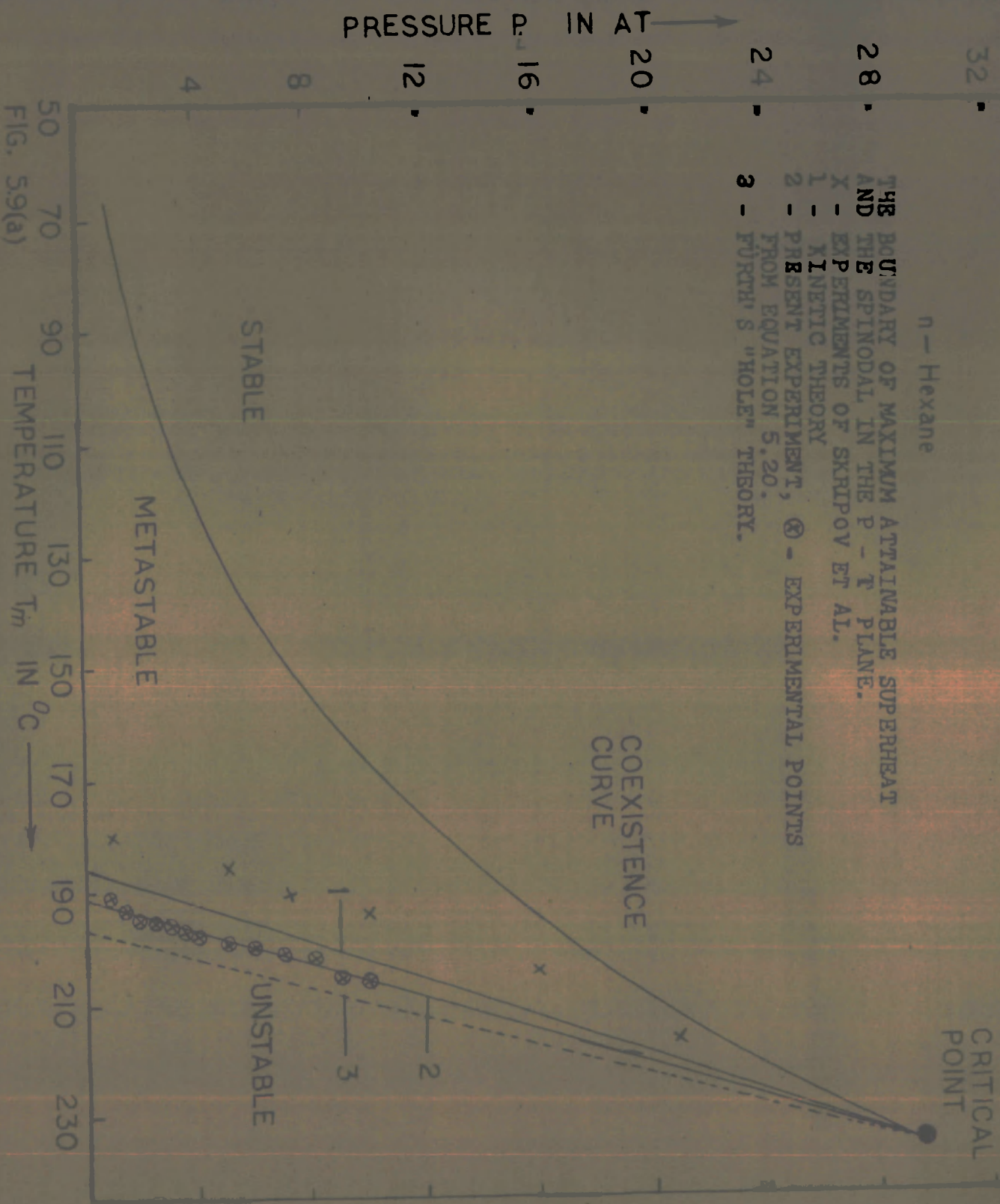


FIG. 5.9(a)



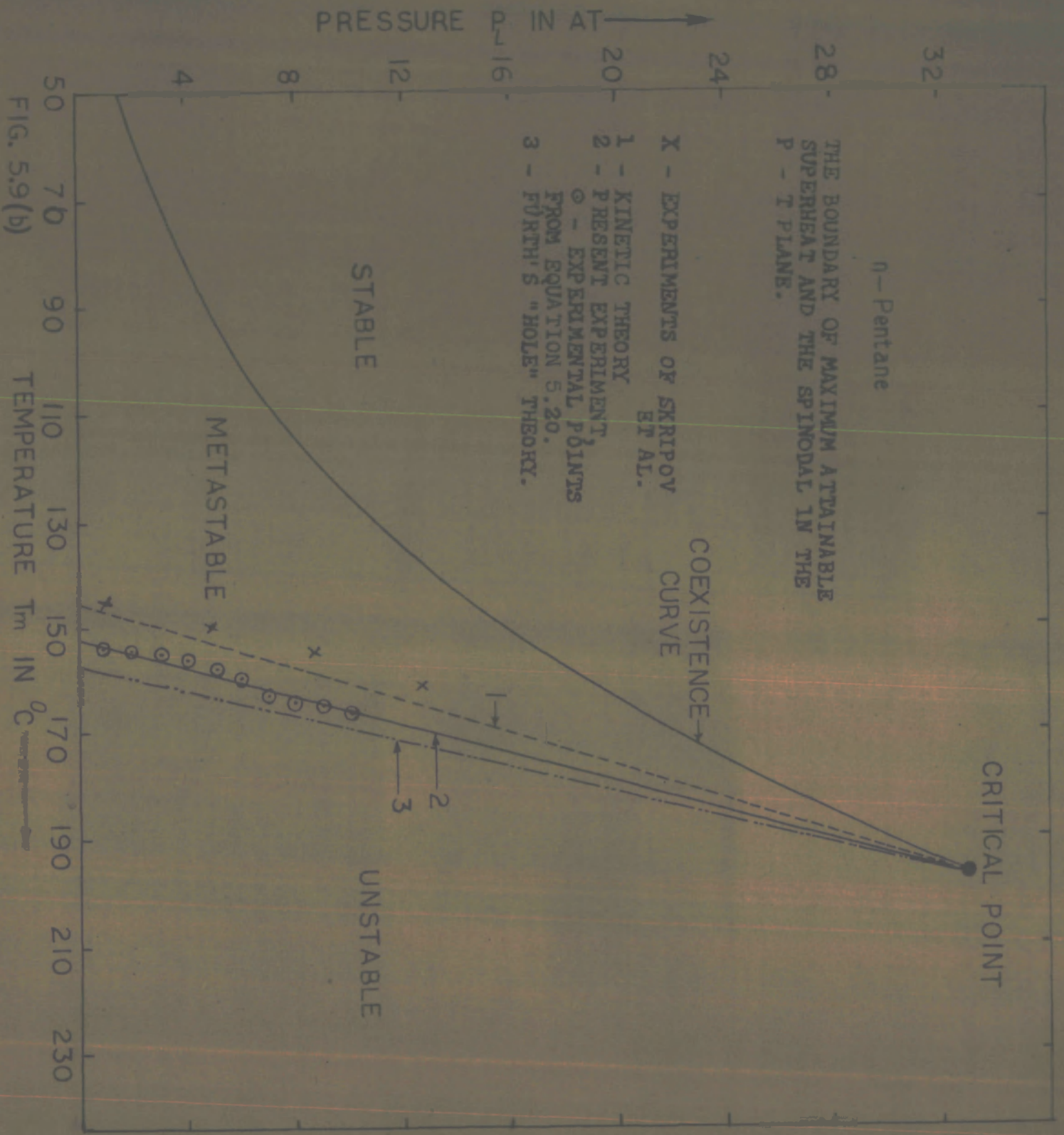


FIG. 5.9(b)

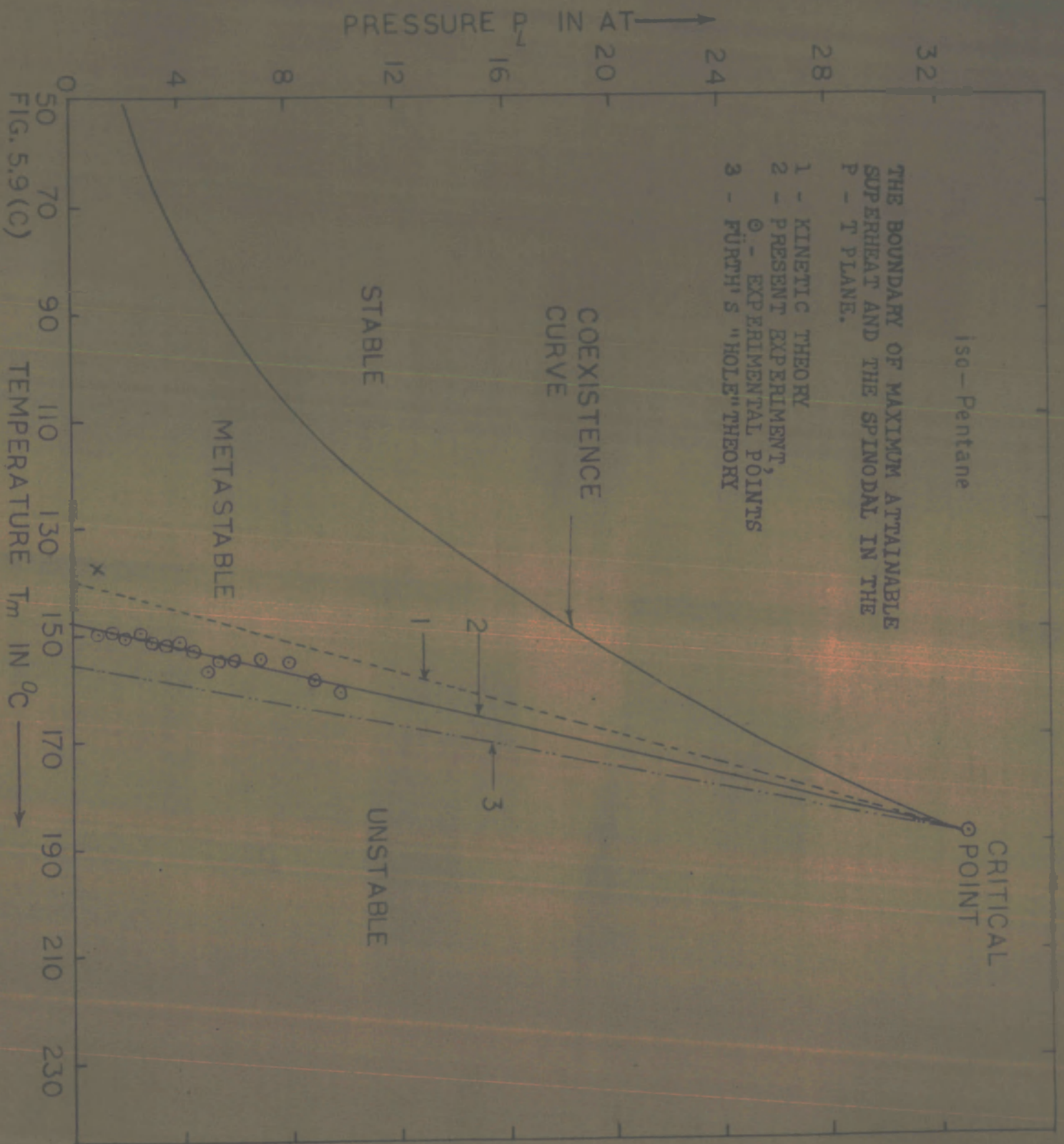


TABLE -5.5.

$P_S$  = Saturated vapour pressure at  $T_m$  obtained from the present experiment.

Liquid	$P_L$ ats.	$T_S$ °C	$P_S$ ats.	$T_m$ °C		
				Present Experi- ment	Kinetic Theory	Fürth's Theory
n-Hexane $T_c = 234.7^\circ\text{C}$ $P_c = 29.5$ ats.	1.0	68.7	15.4	193.1	187.5	198.0
	3.0	110.5	16.4	196.7	191.2	201.0
	4.0	122.0	16.8	198.2	192.5	202.0
	5.0	132.5	17.2	199.6	194.5	203.5
	6.0	141.0	17.4	200.2	196.0	204.5
	8.0	155.0	17.8	202.4	199.2	207.5
	10.0	167.0	19.2	205.7	202.2	210.0
n-Pentane $T_c = 196.6^\circ\text{C}$ $P_c = 33.8$ ats	1.0	36.1	17.0	155.3	148.0	159.1
	3.0	70.0	17.3	156.0	151.0	161.4
	5.0	93.0	18.2	159.1	154.0	164.0
	7.0	109.3	19.8	164.3	157.4	166.7
	9.0	121.1	20.4	166.2	160.0	168.8
	10.0	126.5	20.8	167.3	161.6	170.2
Iso-Pentane $T_c = 187.5^\circ\text{C}$ $P_c = 30.3$ ats.	1.0	27.8	18.6	150.2	141.0	156.2
	3.0	67.2	19.0	151.5	143.8	158.1
	5.0	86.2	19.8	154.0	146.7	160.3
	7.0	101.3	20.4	156.0	150.0	162.4
	8.0	107.5	21.0	157.5	151.3	163.5

# TABLE - 5.6 (1)

Values of various constants appearing in equation (5.20) for n- Hexane at different pressures.

P ats.	a	b	A	B	T <sub>m</sub> °C	Least Square value at a point
1.0	0.68	2.87	25.53	0.0019	193.5	$5.85 \times 10^{-3}$
2.0	0.63	2.93	29.13	0.0015	195.0	$3.55 \times 10^{-2}$
3.0	0.61	2.97	31.47	0.0013	197.0	$1.37 \times 10^{-3}$
4.0	0.57	3.12	34.69	0.0012	198.0	$5.76 \times 10^{-2}$
5.0	0.51	3.47	37.41	0.0012	199.5	$1.66 \times 10^{-3}$
6.0	0.46	3.53	41.79	0.0011	200.0	$7.97 \times 10^{-3}$
7.0	0.39	3.69	48.51	0.0009	201.5	$2.39 \times 10^{-2}$
8.0	0.33	3.81	56.73	0.0009	203.5	$1.09 \times 10^{-3}$

T A B L E - 5.6 (11)

Values of various constants appearing in equation (5.20) for n-Pentane at different pressures.

P ats.	a	b	A	B	T <sub>m</sub> °C	Least Square value at a point.
1.0	0.53	2.62	31.13	0.0062	155.3	$3.51 \times 10^{-3}$
2.0	0.52	2.64	33.37	0.0062	155.6	$4.51 \times 10^{-3}$
3.0	0.49	2.71	36.82	0.0059	156.1	$1.97 \times 10^{-3}$
4.0	0.45	2.87	41.57	0.0056	157.2	$5.62 \times 10^{-2}$
5.0	0.41	3.03	45.69	0.0055	159.2	$8.04 \times 10^{-4}$
6.0	0.39	3.17	47.51	0.0051	160.9	$2.17 \times 10^{-3}$
7.0	0.37	3.24	48.85	0.0049	164.4	$1.23 \times 10^{-3}$
8.0	0.36	3.53	53.71	0.0038	165.3	$7.89 \times 10^{-2}$
9.0	0.31	3.73	59.19	0.0031	166.2	$2.34 \times 10^{-3}$
10.0	0.27	3.85	71.34	0.0030	167.4	$3.01 \times 10^{-3}$



TABLE 5.6 (iii)

Values of various constants appearing in equation (5.20) for iso-Pentane at different pressures.

P ats.	a	b	A	B	T <sub>m</sub> °C	Least Square value at a point.
1.0	0.58	2.48	39.52	0.0140	150.2	$1.27 \times 10^{-2}$
2.0	0.56	2.58	42.23	0.0077	150.8	$4.88 \times 10^{-3}$
3.0	0.48	2.62	43.69	0.0075	151.5	$2.35 \times 10^{-2}$
4.0	0.47	2.77	44.13	0.0075	152.3	$1.73 \times 10^{-3}$
5.0	0.45	2.89	49.51	0.0062	154.0	$4.05 \times 10^{-3}$
6.0	0.44	3.13	52.63	0.0062	156.0	$3.79 \times 10^{-3}$
7.0	0.37	3.37	57.52	0.0057	156.5	$3.12 \times 10^{-3}$
8.0	0.31	3.48	60.17	0.0058	157.5	$1.25 \times 10^{-3}$
9.0	0.29	3.50	67.52	0.0041	159.0	$2.92 \times 10^{-3}$
10.0	0.21	3.62	75.43	0.0040	161.5	$4.72 \times 10^{-3}$

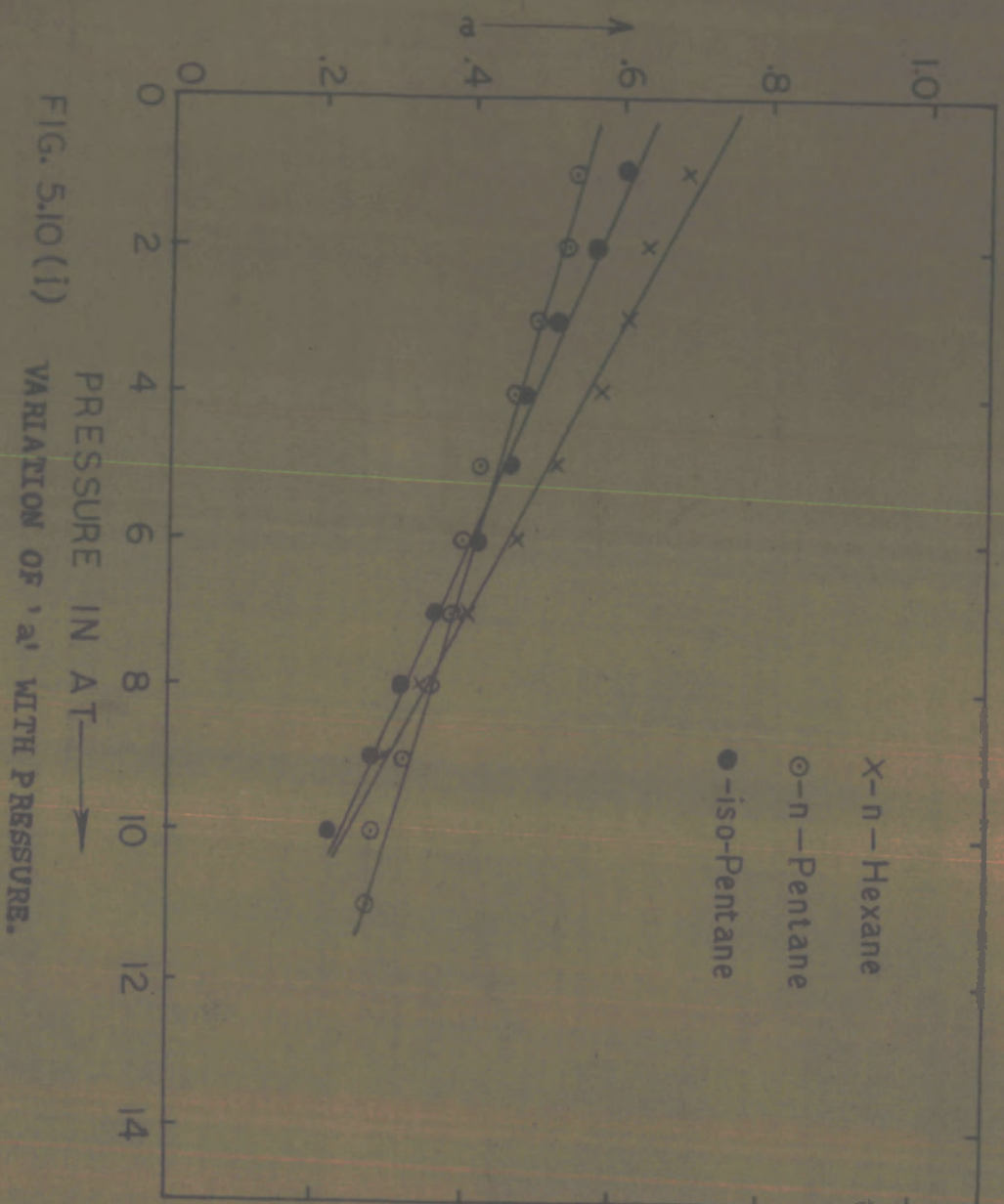


FIG. 5.10 (1)

PRESSURE IN AT →  
 VARIATION OF 'a' WITH PRESSURE.

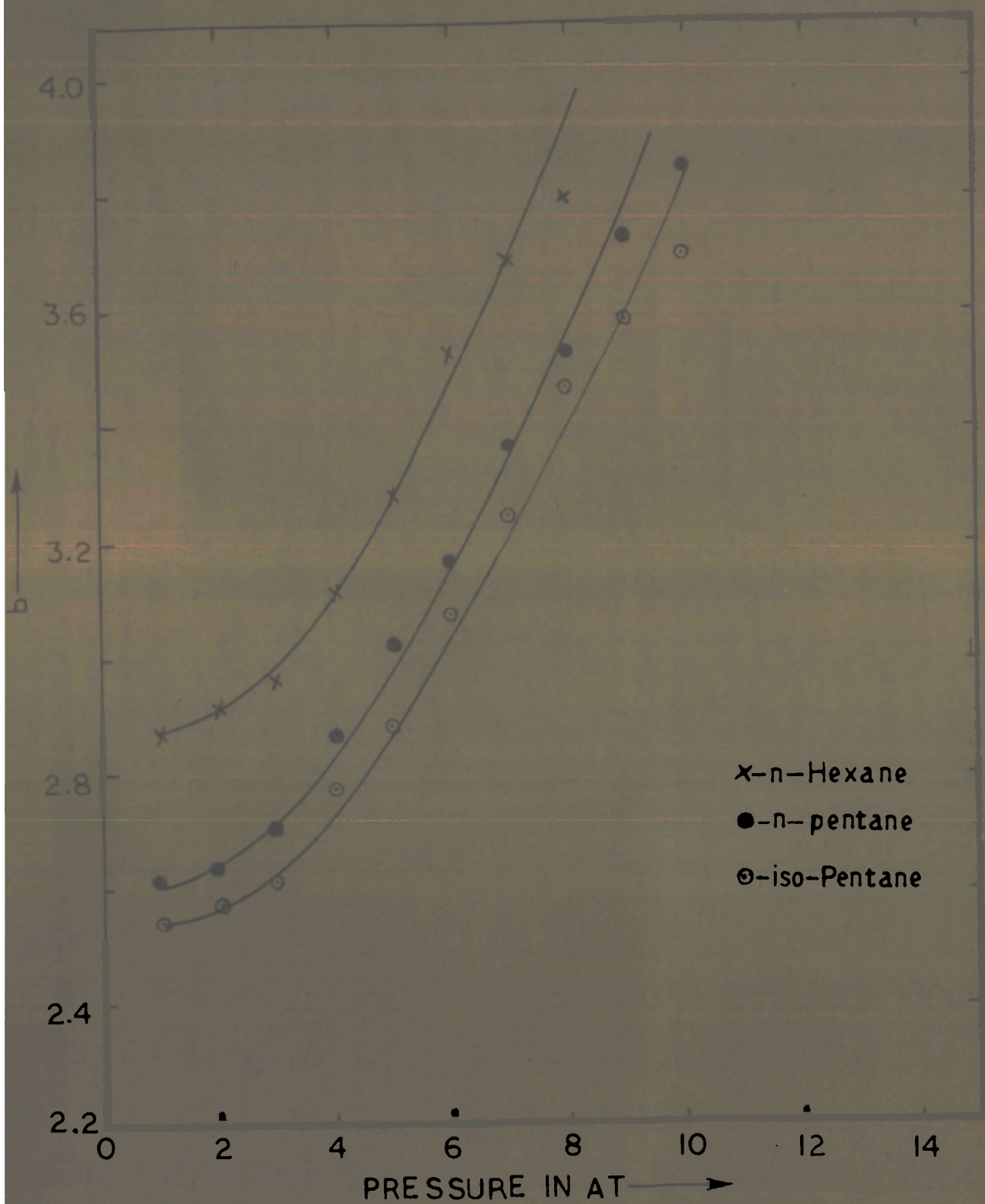


FIG. 5.10 (ii)

VARIATION OF "b" WITH PRESSURE.



The values of  $T_m$  calculated by us should in fact be higher than the values obtained by the other workers and the theoretical values calculated from the kinetic equation. In the experiments of Skripov et al.<sup>22</sup> Wakeshima and Takata<sup>23</sup> and Apfel<sup>24</sup> the minimum life times of the droplets of superheated liquids were of the order of 1 sec, whereas a limiting value obtained by extrapolation corresponds to an instantaneous phase transition. This may mean that the actual limiting value for the liquid should be a few degrees higher than the experimentally attainable superheat. Since the boundary of stability demarcates regions of the metastable and the completely unstable states of a liquid it is not realizable experimentally. It could be obtained as a result of extrapolation. The theoretical values calculated from the kinetic equation are also expected to be lower because of a lower value of  $J$ , the rate of nucleation usually assumed in calculating the limiting value of the superheat. At the limit of stability the whole liquid should virtually boil up which may mean a much higher rate for  $J$ . Sinitsin and Skripov<sup>25</sup> have already suggested that if  $J$  is put equal to  $10^{15} \text{ cm}^{-3} \text{ sec}^{-1}$  and not  $1 \text{ cm}^{-3} \text{ sec}^{-1}$ , it will mean a rise in the limiting temperature by  $3^\circ$ .

We now turn to the consideration of the accuracy of the results presented in Tables 5.2 - 5.6. The maximum possible error in the measurement of the temperature in the present experiment is of the order of  $0.5^{\circ}\text{C}$ . Errors in the voltage measurement are estimated to be not more than  $\pm 5\%$ . The maximum error in the measurement of pressure is  $10\%$ . This error arises from the calibration errors in the oscilloscope screen. Another source of error in the calculation of  $T_m$  lies in the  $T_m$  values but since the equation 5.20 satisfies the  $V_c$ - $T$ - $P$  data for a wider range of temperature and voltage, the error in the extrapolation can not be expected more than  $2\%$ .

The  $V_c$ - $\Delta P$  data could also have been represented by the equation of the form

$$V_c = A'(P-P_m)^{a'} + B'(P-P_m)^{b'}$$

where  $P$  is the external pressure on the liquid for which the  $V_c$  is the critical voltage at a specified temperature and  $P_m$  a parameter having the significance of the tensile strength of the liquid. But since we have to extrapolate the  $V_c$ - $\Delta P$  curves, as shown in Figs. 4.3 for a wider range of pressures to reach the condition  $V_c = 0$  for  $P = P_m$ .

This would have caused a larger error in the determination of the tensile strength due to the fact that the method of extrapolation leads to larger deviations when applied over <sup>a</sup> wide range.

Values of physical constants used in the calculations have been obtained from the "International Critical Tables", "Timmerman's Physico-Chemical constants of pure Organic Compounds", "Selected values of Physical and thermal properties of hydrocarbons and related compounds, Carnegie Press, 1953, Weissberger: "Organic solvents", "Technique of organic chemistry" Vol VII, Interscience Publishers Inc., N.Y. and K.A. Kobe and R.E. Lynn. Jr.: Chem Rev., 52(1953)117.

Specifically, values of surface tension for the test liquids in the temperature range near the explosion temperatures, which are most relevant to the limit and which are not given in any literature, were calculated using Katayama's formula<sup>26</sup> for the temperature dependence of surface tension.

The main significance of our work lies in the fact that the phenomenon of induced nucleation in liquids due to external electric fields is studied, most probably for the

first time, as a means for the determination of the limit of thermodynamic stability of the liquid state itself. The method for the investigation of the stability conditions under an intense electric field, enables us to correlate the state variables  $T$  and  $P$  of the system of a liquid with the external field parameter which consequently leads to the calculation of the limit of stability of the liquid. The significance of the present work lies also on the fact that the method for the simultaneous measurement of the tensile strength and the limit of thermodynamic boundary of stability (limit of transgression) of liquids has been devised most probably for the first time to produce liquid to vapour phase transition.

\*\*\*\*\*

# REFERENCES

1. Glaser, D.A., *Nuovo Cimento*, 11, 361 (1954).
2. Von Hippel, A.R., "Dielectrics and Waves", Wiley, p. 228 (1954).
3. Schneider, J.M. and Watson, P.K., *Physics of Fluids*, (USA), 13, 8, 1948 (1970).
4. Gross, M.J. and Porter, J.E., *Nature*, 212, 5068, 1343 (1966).
5. Sumoto, I., *Cyô Butsuri*, 25, 264 (1956).
6. Pohl, H.A., *J. Appl. Phys.*, 29, 1182 (1958).
7. Krasucki, Z., *Proc. Roy. Soc.*, 294, 393 (1966).
8. Pickard, W.F., "Progress in Dielectrics", (Temple Press, London, 1965), Vol.6, pp. 1-390.
9. Cretu, T., Macarie, Gh and Solomon, M., *J. Phys. D, Appl. Phys.*, 2, 999 (1969).
10. Daba, D., *Electrotehnica*, 8, 273 (1970).
11. Abraham, M. and Becker, R., "Theorie der Electricität", (Leipzig: Teubner, 1932).
12. Daba, D., *J. Phys. D, Appl. Phys.*, 5, 318 (1972).
13. Stratton, J.D., "Electromagnetic Theory", (McGraw Hill Co., N.Y., 1941).
14. Sumoto, I., *J. Appl. Phys. Japan*, 25, 264 (1956).

15. Garton, C.G. and Krasuski, Z., Proc. Royal Soc. London, 280, 1381, 211 (1964).
16. Cade, R., Proc. Phys. Soc., 83, 997 (1967).
17. Brown, W.F., Jr., Amer. J. Phys., 19, 290 (1951)
18. Adam, N.K., "Physics and Chemistry of Surfaces", (Oxford U.P., 1938).
19. Frenkel, J., "Kinetic Theory of Liquids", (Dover Publications, Inc., N.Y., 1946).
20. Volmer, M., "Kinetic der Phasenbildung", (Steinkopff, Dresden and Leipzig, 1939).
21. Fürth, R., Proc. Camb. Phil. Soc., 37, 252 (1941).
22. (a) Skripov, V.P. and Ermakov, G.V., Zur. Fisi. Khim., 30, 2, 396 (1964).
- (b) Sinitsin, E.N., "Issledovaniye Kinetiki Zarodishno-Obrazovaniya v peresagrevayemykh Zhidkostyakh", Ph.D. Dissertation, The Ural Polytechnical Institute, Sverdlovsk, USSR (1967).
23. Wakeshima, H. and Takata, K., J. Phys. Soc. Japan, 13, 1398 (1958).
24. Apfel, R.E., J. Acous. Soc. Amer., 42, 145 (1971).
25. Sinitsin, E.N., and Skripov, V.P., Priroda i Tekh. Nauch. No.4 (1966).
26. Katayama, M., Sci. Rep., Tohoku Univ. 4, 273 (1961)
27. Jaliluddin, A.K., "On the Superheat of Liquids", D. Phil. Dissertation, Calcutta Univ., 1962.

## P U B L I C A T I O N S

The following papers were prepared by the author  
in collaboration with Dr. A.K. Jalaluddin.

1. "DETERMINATION OF THE LIMIT OF ABSOLUTE THERMODYNAMIC  
STABILITY OF LIQUID USING EXTERNAL ELECTRIC FIELDS AS  
PERTURBATION"

Phys. Lett. A, 42A, 197-8 (1973)

2. "NUCLEATION IN SUPERHEATED LIQUIDS DUE TO ELECTRIC  
FIELDS"

J. Phys. D., Appl. Phys. 6, 10, 1287 (1973)

3. "DESIGN AND DEVELOPMENT OF A BUBBLE CHAMBER TECHNIQUE  
FOR THE STUDY OF ELECTRIC FIELD INDUCED NUCLEATION IN  
LIQUIDS"

J. Phys. E., Scientific <sup>fi</sup>Instruments,  
(to be published)

4. "DIELECTROPHORETIC FORCES IN LIQUIDS"

Jap. J. Appl. Phys. (to be published)

\*\*\*\*\*

## DETERMINATION OF THE LIMIT OF ABSOLUTE THERMODYNAMIC STABILITY OF LIQUID USING EXTERNAL ELECTRIC FIELDS AS PERTURBATION\*

D S PARMAR and A K JALALUDDIN

*Department of Physics Aligarh Muslim University Aligarh India*

Received 5 December 1972

A relationship between the pressure and temperature of superheated liquid n-hexane and the critical electrostatic field required for inducing nucleation in it is obtained experimentally. This relation is used for the determination of the limit of stability of the liquid.

The boundary of absolute thermodynamic stability, or the spinodal of a system in a given phase satisfies the equation  $(\partial p / \partial V)_T = 0$  [1]. In the  $p$ - $V$  plane, the critical point of a liquid-vapour system is situated at the apex of both the branches of the spinodal and the binodal (coexistence curve). The regions enclosed between the binodal and the spinodal represent the metastable states: superheat of the liquid and supersaturation of the vapour. Theoretically the description of metastable states is still an unsolved problem in statistical mechanics. Since the spinodal demarcates the metastable and the completely unstable states of a phase, it is not experimentally realisable.

Although most of the experimental results [2-4] on the maximum attainable superheat of liquids agree well with the predictions of the kinetic theory of nucleation [5], they do not correspond to the limit of stability of the liquid. One can, however, attempt to determine such limits only by extrapolating the above results provided one knows quantitatively the factors determining experimentally the maximum attainable values of the superheat of liquids.

In the present letter, we report an experimental method for the determination of the spinodal of liquids by extrapolating the maximum attainable superheat values of a liquid obtained under measured external perturbation (electric fields). The method is based on the phenomenon of nucleation in liquids induced by external electric fields as reported by one of the authors earlier [6].

\* The work has been done under a project sanctioned by the C S I R, India.

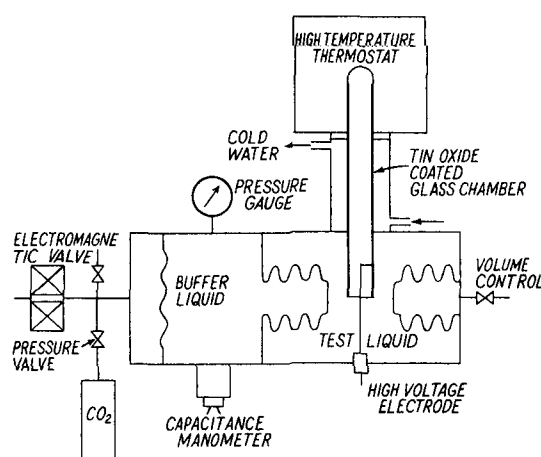


Fig. 1 Schematic diagram of the experimental setup.

The experimental set up is a miniature bubble chamber [7] shown in fig. 1. The upper portion of the test liquid (n-hexane) in the vertical glass tube is maintained at a temperature ( $100$ – $185^\circ\text{C}$ ) much higher than its boiling point ( $68.7^\circ\text{C}$ ). The inner surface of the glass tube is partially coated with a thin, transparent and highly conducting layer of tin oxide. The liquid is brought to a superheated state by releasing the external  $\text{CO}_2$  pressure from the chamber through the expansion mechanism and the nucleation is induced in it by applying a critical d.c. electric field at the region of discontinuity of the tin oxide layer at the upper end of the tube, the other electrode being inserted outside the glass chamber. At a given  $T$  and  $P$ , the critical voltage,  $V_c$ , required at the tin oxide surface for inducing instantaneous



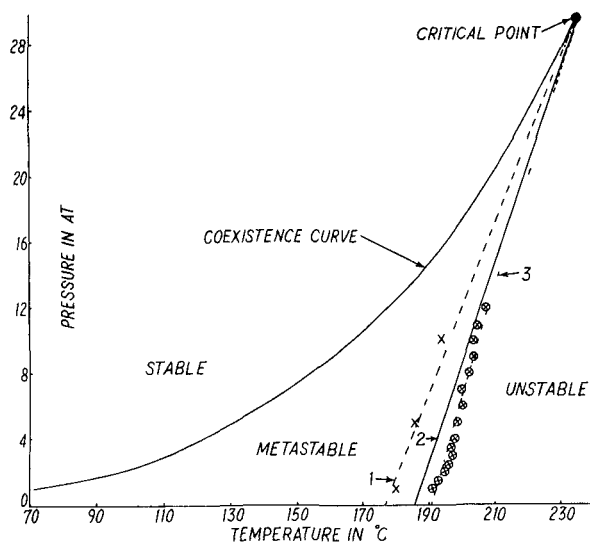


Fig. 2 The boundary of maximum attainable superheat and the spinodal of liquid n-hexane in the  $P$ - $T$  plane. Curve 1 maximum superheat attained experimentally,  $\times$  - experimental points [3]. Curve 2 - the boundary of maximum attainable superheat calculated from the kinetic theory of nucleation [5]. Curve 3 - the boundary of stability (spinodal) determined by the present method,  $\circ$  points obtained from the empirical  $V_c(T)$  relation reported in this paper.

nucleation is determined by successively increasing the value of the applied voltage (300–5000 V). The procedure is repeated for a set of values of  $P$  at each successively higher temperature.

The  $V_c(T)$  relation (in the  $V_c$  range 300–5 kV) has been found to fit in the equation of the form  $V_c = A(T_m - T)^2$ , where  $A$  is a constant and  $T_m$  a parameter having the significance of the maximum superheat temperature for a given  $P$  in the absence of the external electric field.  $T_m$  is calculated by successive approximation so as to satisfy the boundary condition  $V_c = 0$  for  $T = T_m$ . The value of  $T_m$  is thus determined for various values of the pressure. When plotted in the  $P$ - $T$  plane, the  $P(T_m)$  relation defines the boundary of stability (spinodal) of liquid n-hexane, as shown in fig. 2 (curve 3). As was expected the spinodal thus determined lies deeper in the metastable region of the liquid than the boundary of maximum attainable superheat of liquid n-hexane as observed by other authors (curve 1) and that calculated from the kinetic equation (curve 2).

Table 1

$T(^{\circ}\text{K})$	$\sigma(T)$	$W_m \times 10^9$	$V_c$	$\Gamma \times 10^{-6}$	$W_e \times 10^9$
413	11.2	2.75	900	5.7	46.7
443	5.9	0.04	300	1.9	0.02

One may analyse the role of the external electric field on the bubble formation in a superheated liquid by comparing, in table 1, the minimum energy  $W_m = 16\pi\sigma(T)^3/3\Delta p^2$  required [5] for the formation of a critical nucleus ( $r_c = 2\sigma(T)/\Delta p$ ,  $\sigma(T)$  = surface tension and  $\Delta p = P_s - P$ ,  $P_s$  being the saturated vapour pressure at  $T$ ) and the energy  $W_e = \frac{4}{3}\pi\gamma_c^3 \times \epsilon(T)E^2/8\pi$ , contributed by the electric field over the same volume, where  $\epsilon(T)$  is the dielectric constant and  $E$  is calculated, according to the geometry of the  $\text{SnO}_2$  layer, by the equation  $E = V_c/r_2 \log(r_2/r_1)$  with  $r_1 = 1.4 \times 10^{-4}$  cm the  $\text{SnO}_2$  layer thickness, and  $r_2$  the distance of the point of formation of the bubble from the layer ( $\approx 10^{-6}$  cm, the order of radius of the vapour bubble). The figures are tabulated in C.G.S. units. The surface tension is calculated from Katayama's formula [8] for the temperature dependence of surface tension.

The agreement may be taken as fair in view of the assumptions involved in the calculation of  $E$ .

## References

- [1] J. W. Gibbs, The scientific papers (Dover publications, Inc., N.Y. 1961) Vol. 1.
- [2] H. Wakeshima and K. Takata, J. Phys. Soc. Japan 13 (1958) 1398.
- [3] E. N. Sinitsin, Investigation of nucleation in superheated liquids, Dissertation, Ural Polytechnic Institute, Sverdlovsk (1967).
- [4] A. K. Jalaluddin, Study of the superheated state of liquids by the method of optical scattering, Dissertation, Moscow State University (1967).
- [5] W. Döring, Z. Phys. Chem. B36 (1937), B38 (1938).
- [6] A. K. Jalaluddin and D. B. Sinha, Nuovo Cimento (Suppl.) 26 Ser. X (1962) 234.
- [7] N. B. Delone, Puzirkovsk. Kameri, Gosatomizdat, Moscow (1963).
- [8] M. Katayama, Sci. Rep., Tohoku Univ. 4 (1961) 273.